THE DETECTION OF NEGATIVE IONS AND THEIR STABILITIES.

A thesis submitted for the degree of

DOCTOR OF PHILOSOPHY

By

ANTHONY THOMAS CHAMBERLAIN

In

THE UNIVERSITY OF ASTON IN BIRMINGHAM

JANUARY 1974.

SUMMARY

A description was given of the construction and operation of a quadrupole mass filter system. This was used to identify negative ions emitted from a hot polycrystalline tantalum surface.

The ionisation of various interhalogens and cyanogen halides were studied using the mass filter system. The kinetic methods of Page were applied to the results and the difference in electron affinity, of two radicals ionising simultaneously (halogens and cyanide) was evaluated. At pressures higher than 5×10^{-5} mm Hg., anomalous results were obtained and were explained quantitatively on the basis of positive ion formation, by negative ion collisions with the sample vapour, in the mass filter.

The ionisation of various substituted pyridines were studied. Only fragment negative ions were observed (m/e values 24, 25, 26, and 27) for these compounds. In the case of 2-6-dimethyl-pyridine, the observed ions, (m/e values, 24, 25 and 26) were shewn to be produced upon the tantalum surface. The appearance of intense positive ion peaks in the mass spectra of these compounds was again explained by negative ion collisions with the sample gas in the mass filter.

This thesis, "The detection of negative ions and their stabilities", is an account of the work done under the supervision of Professor F. M. Page, BA., Ph.D., Sc.D., at the University of Aston in Birmingham, during the period January 1970 to December 1973.

The work described is original, except where stated and has not been, or is being, submitted for any other degree or award.

A.T. Chamberlain.

January 1974.

Roads go ever ever on,
Over rock and under tree,
By caves where never sun has shone,
By streams that never find the sea;
Over snow by winter sown,
And through the merry flowers of June,
Over grass and over stone,
And under mountains in the moon.

Roads go ever ever on,
Under cloud and under star,
Yet feet that wandering have gone,
Turn at last to home afar.
Eyes that fire and sword have seen
And horror in the halls of stone,
Look at last on meadows green
And trees and hills they long have known.

J. R. R. Tolkien.

CONTENTS

LIST OF TABLES.

LIST OF FIGURES.

Following page.

* * *

ACKNOWLEDGEMENTS.

The author wishes to express his gratitude to Professor F. M. Page for his help and patience over the last three years, Dr. M.R. Painter for many helpful discussions and the technical staff of the University of Aston in Birmingham, especially Mr. M.J. Houghton, for their assistance during the construction of the Mass filter system.

The author also wishes to express his thanks to his father, Mr. C.M. Chamberlain, for the production of many of the complex items used in the Mass filter system.

Finally, thanks are due to the Hydrocarbon Research Group of the Institute of Petroleum and the University of Aston in Birmingham for their generous financial assistance.

1. INTRODUCTION

The study of negative ions, and their stabilities, have been overshadowed until recently, by the study of the more numerous and easily studied positive ions. The electron may be considered the simplest negative ion; however, the concept of a negatively charged atom or molecule is one of the basic assumptions of the theory of electrolysis. This theory assumes that a molecule AB will dissociate in solution to give A^- and B^+ ions, which may then move, under an applied potential difference, to the anode and cathode, respectively. The drift velocity through the solution is small and hence, solvated ion "clusters" were assumed to form.

The study of the passage of electricity through gases shewed that the charge carriers were not all electrons, but also ions of molecular mass. (1) Studies at pressures of about 10^{-1}mm. Hg. (2) shewed that ion clusters may also be formed in gas studies, as well as in electrolysis. Below about 10^{-3}mm Hg. however, relatively simple reactions predominate. JJ Thompson identified a number of simple ions having a negative charge (3); however, studies of the upper atmosphere, astrophysics, flame chemistry and recently, health physics, have greatly increased the interest in negative ions.

The discovery of negative ions in the ionised layers of the upper atmosphere has been followed by many experimental attempts to measure both the stability and rate of formation of these ions (4). The D and E layers have been found to contain simple ions, for example, O_2^- , O^- , NO_2^- , and NO_3^- .

It has been shewn that the absorption of light by hydrogen negative ions present in the solar photosphere determines the spectral distributions in the visible region(5) and hence, the apparent colour temperature of many other stars. In the atmosphere of certain cooler stars, there appears to be a rather greater proportion of carbon than in other stars and it is possible that CN^- and C_2^- might be important in determining certain features of the emission spectra of these stars. (6)

One of the fields where a knowledge of the stability of negative ions is important is that of flame ionisation. In addition to negative ions of the halogens, many negative ions have been detected in the natural ionisation of undoped hydrocarbon flames. Some of these ions are simple, such as, OH^- and CN^-, but the most striking feature of the negative ion mass spectrum, of a flame, is the large number of mass peaks which appear to be due to hydrocarbon negative ions. The technology of magneto-hydrodynamic generators and the control systems of rockets, have both benefitted from the study of negative ions in flames (7).

Lovelock et al (8). have studied the formation of negative ions by biologicaly active materials. The electron capture detector was used to determine the relative reduction, produced by various materials, in the electron concentration of a radio-actively generated plasma. The relative reduction in the electron concentration was found to depend upon the electronegativity of the material, with a few exceptions, where anomomously high reduction occured. This reduction almost always occured with compounds of high biological activity.

Although it was not implied that the ability to capture electrons was a direct cause of biological activity, the results suggest that there is a strong link between the two.

Most radio-active processes give rise to highly energetic species, which by collision with surrounding molecules may liberate secondary electrons and positive ions. The collision process may be continued until the energy of the electrons is such that capture by the surrounding molecules may occur to form negative ions. It may be seen that a single radio-active event will give rise to many negative ions in this manner. This type of process is of obvious interest in the study of the interaction of ionising radiation with living tissue. The work of L.G. Christophorou (9) has provided much information for this type of process.

A recent article (10) has presented evidence that the free negative ions in the air (about 20 ions per cm^3) have a profound psychological effect upon human beings. A reduction in the level of negative ion concentration in the air has been related to the alertness of human subjects who breath it. The implications of this discovery are wide ranging and further work is proceeding in this area of research.

The above brief survey of the processes in which negative ions play a significant part, indicates the importance of negative ions in all fields of science. The amount of knowledge available for negative ions is small compared to that for positive ions. The work described in this thesis is an attempt to extend the knowledge available for negative ions, especially those formed by a surface ionisation process.

2. THE EXPERIMENTAL DETERMINATION OF ELECTRON AFFINITIES.

The stability of a negative ion is usually given in terms of the electron affinity of the neutral molecule. This is defined as the work done in bringing an electron from infinity to the lowest lying vacant orbital of the isolated gas molecule. Experimentally, there are several techniques available for the measurement of the electron affinity of a species; those in which the energy threshold of the destruction, or formation, of the negative ion is determined, and the study of the equilibria between electrons, ions and molecules.

The accurate measurements of electron affinities of atomic negative ions occured as a result of the developement of the photodetachment techniques of Branscomb and co-workers (11). The technique consisted of determining the limiting frequency at which incident light, falling upon a mass filtered beam of negative ions, was sufficiently energetic to cause the detachment of an electron, thus allowing the activation energy of the detachment process to be evaluated. Berry (12) has studied the photodetachment of the halogen negative ions in a shock tube and Lineberger & Woodward (13) have obtained the electron affinity of sulphur as 2·0772 $\pm$ 0·0005 eV, which is believed to be the most accurate experimental determination for any negative ion. Unfortunately, the technique may only be used with species producing a large concentration of negative ions, which may then be detached.

Various studies of the equilibrium between ions, electrons and molecules have been carried out in flames and at heated surfaces.

The energy changes involved are computed either by the temperature dependence of the equilibrium constant (II law methods) or by the methods of Statistical Mechanics (III law methods).

The measurement of electron affinities by flame ionisation has been carried out by Rolla and Piccardi (14), who measured the attenuation of the electron concentration in a flame consequent upon the addition of an electron acceptor. This method was subject to considerable experimental difficulty and requires an extensive knowledge of the reactions occurring in flames. This limits the method to a study of thermally stable, strong acceptors only.

Of the procedures available for studying the equilibria at hot metal surfaces, the space-charge method of Glockler and Calvin (15) is the most simple. In brief, this method requires the determination of the current / voltage characteristics of a space charge limited diode, both with and without the presence of an electronegative gas. From this the contribution made to the total current by negative ions may be evaluated. Unfortunately this method has the limitation that the ions must constitute an appreciable fraction of the total current.

The magnetron method of Sutton and Meyer (16), in which the total negative ion current formed at a heated filament was compared with the thermionic electron current derived from the same source, provided information of the halogens. Page and co-workers (17) have extensively developed this technique and have measured the electron affinity of many organic radicals not easily studied by other techniques. The magnetron method is discussed in the following chapter.

In the method of Dukelskii and Ionov (18), a collimated beam of alkali halide molecules was allowed to impinge upon a heated tungsten filament and the ratio of positive ions to negative ions produced was measured by separation in a magnetic field of low resolution. Use of Statistical Mechanics allowed the electron affinity of the halogens to be computed, giving results which were in good agreement with the photo-detachment measurements. Ionov (19) later improved the method by mass analysing the various ions in a mass spectrometer. Recently, this variation of the method has been used to determine the electron affinity of antimony and bismuth (20). Scheer and Fine have obtained by this method, the electron affinities of tungsten and rhenium (21) and molybdenum (22), from the ratio of positive to negative ions derived from the self surface ionisation of these metals. Bakulina and Ionov (23) modified the method so that negative ions derived from two elements ionising simultaneously from the hot tungsten surface, were detected, allowing reliable values of the electron affinity to be calculated for one element, if the electron affinity of the other element was known. This improved method has been used to determine the electron affinity of atoms of the halogens (24,25), sulphur (26), gold, silver and copper (27). An attempt has also been made to determine the electron affinity of the CN radical by the surface ionisation of KCN and KCNS (28).

3. THE MAGNETRON TECHNIQUE FOR THE ESTIMATION OF ELECTRON AFFINITIES.

A thermionic vacuum tube provided with a uniform magnetic field at right-angles to its electric field is known as a magnetron.

In the magnetron technique, a hot, filamentary cathode in vacuo, emits electrons, which travel to the concentric anode, which is positively charged with respect to the cathode. When a magnetic field is applied at right-angles to the electric field the thermionic electrons are constrained to follow curved paths, and, if the field is strong enough, the electrons are prevented from reaching the anode. A concentric "squirrel cage" grid system held at intermediate potentials, is placed between the anode and cathode, which serves to prevent the build up of a large space charge, by removing the circulating electrons.

In the presence of a gas that can form negative ions at the filament, some of the emission current will be carried by the negative ions, which being vastly heavier than the electrons, will be virtually undeflected by the magnetic field. Thus, in the presence of a magnetic field, the anode current will be due to the negative ions alone, whilst if no magnetic field is present then the anode current is the sum of the electron current and the negative ion current. If the gas pressure and filament temperature are known, then the methods of Statistical Mechanics may be used to estimate the electron affinity of the negative ions, provided that certain assumptions regarding the mode of formation of the negative ions, are made.

FIG 1

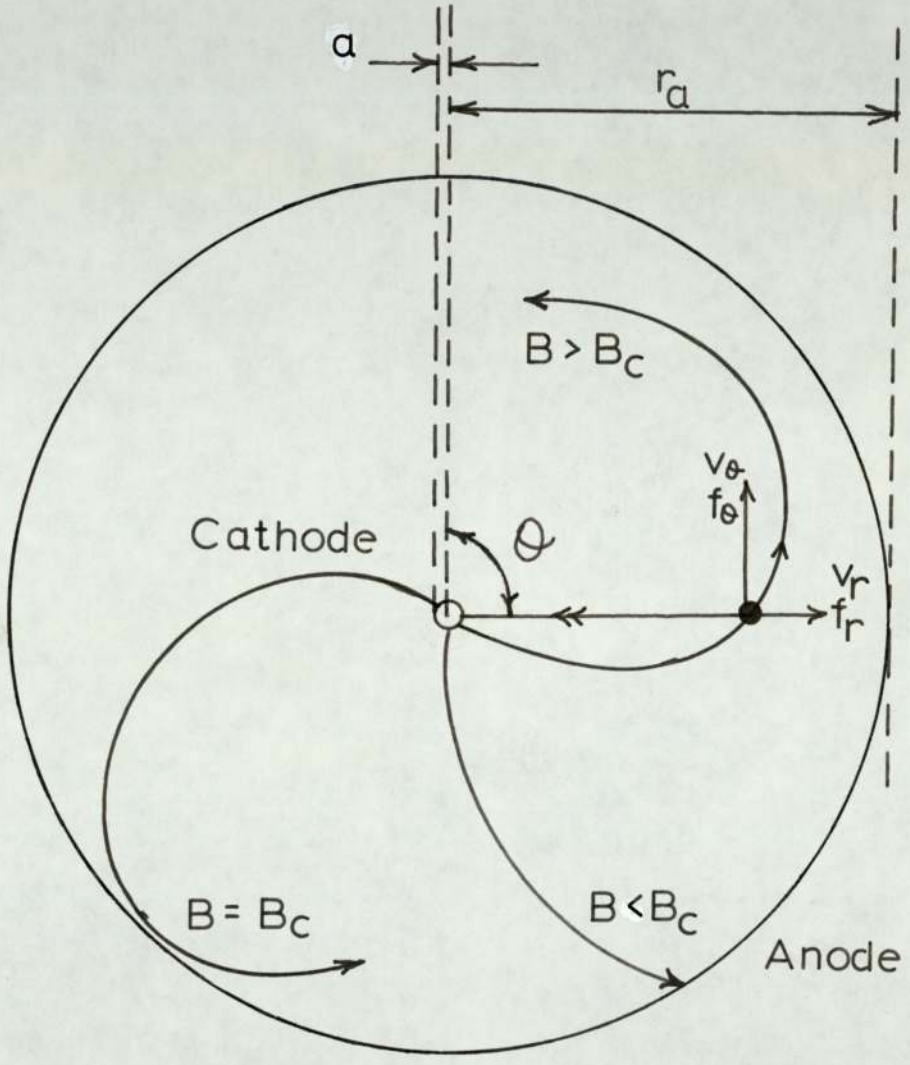

magnetic field perpendicular to paper.

The forces acting upon an electron in a cylindrical magnetron.

3·1 The Theory of the Method.

The original paper on the operation of the magnetron diode was published by Hull (29). The discussion given here illustrates the essential features of the apparatus (30).

The forces on an electron emitted from the central filament of a diode placed in a uniform magnetic field, of flux density, B, applied parallel to the length of the filament, is shewn in Fig. 1. The electrostatic force acting upon the electron is given by:

$$F = -e \cdot E$$
$$= -e \cdot dV/dr$$

where E is the electric field and V is the potential at a distance r from the filament.

The electromagnetic force is given by:

$$f = B \cdot e \cdot v$$

where v is the velocity of the electron at r.

If v is resolved into components v_r and v_θ, along and perpendicular to the radius vector, then the components of f will be:

$$f_r = B \cdot e \cdot v_\theta$$
$$f_\theta = B \cdot e \cdot v_r$$

If Θ is the angle between the radius vector and an arbitrary line in the azimuthal plane, the angular velocity, w, is given by:

$$w = d\Theta/dt$$
$$= v/r$$

The equation of radial motion is given by:

$$d/dt\,(m \cdot dr/dt)$$
$$= F - f_r$$
$$= e \cdot dV/dr - B \cdot e \cdot r \cdot d\theta/dt$$

where m is the electron mass.

The equation of azimuthal motion is found by equating the momentum of the impressed force to the rate of change of angular momentum:

$$r \cdot f_\theta = B \cdot e \cdot r \cdot dr/dt$$
$$= d/dt(m \cdot r^2 \cdot w)$$

Integrating both sides with respect to time and noting that $w = 0$ as the electron leaves the filament, gives:

$$w = \left((B \cdot e)/m\right)(1 - a^2/r^2) \qquad (1)$$

where a is the radius of the filament.

If the small thermal velocity with which the electron leaves the filament is ignored, its velocity at a point at which its potential is V will be given by:

$$v = (2 \cdot e \cdot V / m)^{\frac{1}{2}}$$
$$= \left[(dr/dt)^2 + r^2(d\Theta/dt)^2\right]^{\frac{1}{2}}$$

considering motion in the azimuthal plane.

At a certain value of the magnetic field strength, $B = B_c$, the electron will just fail to reach the anode. At this point:

$$V = V_a$$
$$r = r_a$$
$$dr/dt = 0$$
$$d\Theta/dt = w$$

whence:

$$w = v / r_a$$
$$= (1/r_a)\ (2 \cdot e \cdot V_a / m)^{\frac{1}{2}} \qquad (2)$$

Equating (1) and (2):

$$B_c = \left((8 \cdot V_a)^{\frac{1}{2}} / r_a\ (1 - (a^2/r_a^2))\right) \cdot (e / m)^{\frac{1}{2}}$$

whence, if $a \ll r_a$,

$$B_c = (8 \cdot m \cdot V_a / e \cdot r_a^2)^{\frac{1}{2}} \qquad (3)$$

Equation (3) shews the value of B_c to be independent of the potential distribution between the anode and cathode so that the presence of other electrodes or space charge effects should not alter the cut off conditions. In practice, the cut off is not so sharp when the grids are present, possibly due

to distortion of the magnetic and electric fields by the grid structures.

3·2 A Critique of the Method.

Since its introduction as a general technique for estimating electron affinities, two major criticisms have been levelled at the magnetron method.

1). The possibility of gas phase reactions occurring and being mistaken for a surface process. Positive and negative ions would be expected to be formed, and their relative magnitudes, as compared to the electron current is discussed below. However, the currents of all secondary ions formed in the gas phase will be proportional to the electron current. Hence, the ratio of these ion currents to the electron current are independent of the emitter temperature. Zandberg and Paleev (31) have shewn that a plot of log (I_e/I_i) against $1/T$, where I_i and I_e are the ion and electron currents, respectively, and T is the temperature of the cathode, will give a slope which is zero for gas phase produced ions, and a non-zero slope for ions produced by surface ionisation. In chapter 5 it will be shewn that, in the magnetron technique, it is usual to plot log (I_e/I_i) versus $1/T$ to determine the apparent electron affinity of the compound being investigated. In many cases, it has been found that such plots have a slope which is sensibly non zero. This is taken to indicate that, if several ions should in fact be formed, at least one has been produced by surface ionisation. In the cases where a zero slope has been obtained, (e.g.7) it does not automatically follow that the ions are not produced by surface ionisation;

however, this possibility must be remembered.

a) The magnitude of the positive ion current caused by gas phase reactions.

It will be appreciated that, in the magnetron, a flow of positive ions, formed in the gas phase by electron bombardment, to the cathode, cannot be distinguished from a flow of negative ions, formed by surface ionisation, to the anode. Thus, the measured current may be due to both positive and negative ions. Due to the small values of ionisation cross-sections, this effect will be of importance only when the path length of the electrons is large or the gas pressure is high.

The ratio of positive ions, I_+, to electrons, I_e, is given by:

$$I_+/I_e = N \cdot Q_i \cdot l$$

where N is the number of gas molecules per cm^3.

Q_i is the ionisation cross section (cm^2)

l is the electron path length.

For example, for nitrogen at 10^{-4} mm Hg. and 25°C, taking $Q_i = 2{\cdot}95 \times 10^{-16} cm^2$, (32):

$$I_+/I_e = \frac{(6{\cdot}023 \times 10^{23} \times 273 \times 10^{-4})}{(22{,}414 \times 298 \times 760)} \times 2{\cdot}95 \times 10^{-16} \times l$$

$$= 9{\cdot}6 \times 10^{-4} \times l$$

When no magnetic field is applied to the magnetron, l is approximately 3cm. Thus, I_+/I_e is about 3×10^{-3}. Therefore no significant error will be introduced by this effect into the total measured current, at pressures near to 10^{-4}mm Hg.

In the presence of a magnetic field, the exact value of l is subject to uncertainty, owing to the helical paths which the electrons follow. Usually, the magnetic and electric fields of the magnetron are arranged to produce an apogee in the electron path near to the first grid, which is usually spaced 1 cm from the cathode. Assuming that the electrons are captured by the grid upon their first approach, the path length of the electrons under these conditions is approximately 1·6 cm. Thus, I_+/I_e is about $1{\cdot}5 \times 10^{-3}$. Provided that the negative ion current, produced by surface ionisation, is not less than about 5×10^{-3} that of the electron current, the component of the measured ion current, due to positive ions will be negligible at about 10^{-4} mm Hg.

The "cut off" (33) produced by the magnetic field in the magnetron is not absolute; a small (about 10^{-4} that of the electron current) residual current always remains. Explanations of these residual currents have been sought in the alteration of the potential distribution by space charge (34), asymmetry in the electrode configurations (35) and in the initial velocity with which the electrons are emitted from the cathode (36).

An alternative explanation is that the residual current is due to gas phase formation of positive ions. It is shewn above that, under the conditions in the magnetron, at 10^{-4} mm Hg. the magnitude of the positive ion current was

similar to that of the residual current. Furthermore, Page (37) noticed that, in the presence of helium gas, the residual current was proportional to the gas pressure. Helium is not expected to form negative ions, but easily forms positive ions, under electron bombardment (32). These observations give support to the idea of gas phase detachment processes occurring in the magnetron.

b) The magnitude of negative ion currents produced by gas phase reactions.

In general, the production cross sections for the formation of negative ions by gas phase attachment, are of the order of 10^{-3} that for detachment processes (32). In many cases, the attachment cross sections are about 10^{-20} cm^2 (38). It was shewn in the preceding section that the formation of positive ions was negligible at 10^{-4} mm Hg. and small (about 3 cm) path lengths. Thus the formation of negative ions by gas phase attachment processes, under these conditions, will also be negligible.

2). The Indirect Identification of the Charge Carriers.

Experimentally, the magnetron technique can only resolve electrons from negative ions; no characterisation of the negative ions being possible. In consequence of this, the identification of the negative ions was performed by energetic considerations only. A substance which can give rise to negative ions in the magnetron may do so in several different ways.

Reaction schemes may be set up leading to different negative ions, or alternative routes devised to produce only one ion. Experimentally, a single substance may shew different apparent electron affinities in different temperature ranges, and if any useful deductions are to be made, the process giving rise to the negative ions in each range, must be identified. Usually, through lack of other information, several alternative processes must be considered.

The work of Herron, Rosenstock and Shields (39), has illuminated this aspect of the magnetron technique. Using a mass spectrometer, they were able to observe the negative ions produced in a surface ionisation source directly. Unfortunately, only a few compounds were studied and there is some uncertainty in these results due to insufficient cleaning of the filament. For example, they observed only WO_3^- from nitrogen dioxide over a tungsten filament, instead of NO_2^- as predicted by Farragher et al (40). However, the filament temperature in Herron et als work was, apparently, not raised above 1700°K, and Bakulina, Zandberg and Ionov (41) have shewn that the surface oxide layer of tungsten is only completely desorbed above 1700°K. Similarly, in Herron et als work with benzene, a mass peak attributed to CN^- was observed, which was explained on the basis of surface impurities.

However, the work of Herron et al may be broadly classified into three main divisions:

a) The ion predicted from the magnetron work was the ion observed by mass spectrometry. For example, tetracyanoethylene over platinum or tungsten, giving $C_2(CN)_4^-$

b) In a given temperature range, the magnetron method predicted a single negative ion, whereas, several ions were reported over the whole temperature range, by Herron et al.

For example, in the case of sulphur hexafluoride, Kay and Page (42) shewed that the surface ionisation was complex, but could be divided into three temperature regions in which the following main processes were deduced to occur:

i)

$$SF_6 + e = SF_6^- \qquad \text{below } 1320^\circ K$$

ii)

$$SF_5 + e = SF_5^- \qquad 1320 - 1540^\circ K$$

iii)

no feasible process above $1540^\circ K$

However, Herron et al report that SF_6^- , SF_5^- and F^- were observed as major peaks throughout the temperature range $1350 - 1700^\circ K$.

c) The ions predicted by the magnetron technique were not observed by mass spectrometry.

For example, Gaines and Page (43) deduced that the following process occured with benzene over tungsten carbide:

$$C_6H_6 + e = H_{ads} + C_6H_5^-$$

Herron et al observe C_2^- , C_2H^- and CN^- ions, but the latter is ascribed to surface impurities.

The work of Herron et al makes clear the difficulties encountered with the deduction of the reaction type occuring at the cathode of the magnetron. In those cases where the negative ions predicted by the magnetron technique are not observed, it should not be assumed that the magnetron method is invalid. The possibiltiy that the magnetron measurements refer to metastable negative ions must not be overlooked. If the negative ion which is first formed, and whose energetics are determined in the magnetron, is metastable, in that it changes to another negative ion before it is detected, the observed energy will depend on the primary ion, but the mass spectrometer will record only the secondary negative ion.

In conclusion, it might be stated that the magnetron technique for the estimation of electron affinities of atoms, radicals and molecules is valid experimentally, provided that the gas pressure remains near to 10^{-4} mm Hg.; the path length of the electrons is not more than about 3 cm and that the charge carriers have been directly identified.

4. THE QUADRUPOLE MASS FILTER SYSTEM.

INTRODUCTION.

A mass spectrometer system is usually composed of four distinct sections:

a) A source region.

b) A mass/charge analyser.

c) A detector.

and d) A vacuum system to enclose sections a), b) and c).

In brief, in the source region, the sample material is ionised by some means. In this study, a hot cathode was used. The ions produced in the source are passed into the analyser region, where the ions are characterised by their mass to charge ratio. Ions leaving the analyser are then detected. As the ions travel comparatively long distances in the system, a vacuum chamber is required to prevent an excessive number of collisions between the ions and gas molecules.

The following sections describe the various components and also the mode of operation, of the quadrupole mass filter system used in this work.

4·1 THE VACUUM SYSTEM.

A general review of vacuum techniques in conjunction with the requirements of mass spectrometry has been given by Tasman, Boerboom and Kistemaker (44). The principles expounded by these authors were used to design the vacuum system used in this work.

In seeking to obtain high vacuum (that is, pressures in the range 10^{-4} - 10^{-8} mm Hg.), one may either remove gas molecules from the vacuum chamber by expulsion to a higher pressure or trap the gas molecules in the system by physical or chemical means. In either case, the ultimate vacuum obtained will contain gas molecules liberated in the vessel by "outgassing" from the vacuum chamber components and "backstreaming" of vapours from the pumping system.

"Outgassing" of the components of the system may be reduced to negligible proportions in high vacua, by the use of metal gasket for joining the various components and a high temperature bake-out of the entire system. In the present system copper and lead gaskets were used, together with stainless steel components. The portion of the system above the diffusion pumps was enclosed by an oven, capable of reaching a temperature of about 200°C. Worrell (45) shewed that flushing the system with dry nitrogen was also beneficial in reducing "outgassing" and this technique was often used when dealing with compounds not easily removed by other means.

"Backstreaming" is a more serious problem. In the case of diffusion pumps reaching a maximum pressure of 10^{-7} mm Hg., Hengeross and Huber (46) state that back diffusion is negligible, but that significant contamination occurs from degraded pump fluids and vapours (in the case of oil diffusion pumps) and penetration of light vapours from the fore line. Holland (47) shewed that backstreaming rates increase temporarily, by over an order of magnitude, on switching on a diffusion pump, and to a lesser extent, on turning off. In order to avoid this type of contamination, the headgate valves above the diffusion pump were always closed for a few minutes before the pumps were switched on or off; the bypass line being used to maintain the fore-line pressure.

The main source of "backstreaming", however, is from the rotary pump producing the fore-line vacuum. Fulker, Baker and Laurenson (48) have shewn that backstreaming from a rotary pump is not only due to the volatility of the pump fluid, but also due to "cracking" of the fluid. This "cracking" is caused by hot spots at the vane-stator interface of the rotary pump (49).

"Backstreaming" may be reduced by including a suitable trap or baffle between the pump and the vacuum system. Water, or thermoelectrically, cooled baffles are often used to reduce backstreaming, but their efficiency is not so high as liquid nitrogen cooled traps, or molecular sieve traps.(50)

Liquid nitrogen traps, wherein the gas stream is made to pass over a liquid nitrogen cooled surface, are commonly used, but are not so efficient as molecular sieve traps, in

which the gas has to traverse a layer of molecular sieve, usually a zeolite or activated alumina.

Baker and Staniforth (51) have developed a molecular sieve fore-line trap of high efficiency and tests (52) shew that it behaves well in service. Craig (53) has shewn that, using alumina as trapping agent, the hydrocarbon partial pressure may be reduced by a factor of 10^5, together with a decrease in the water vapour partial pressure. Fulker (54) has shewn that activated alumina is a better trapping agent than zeolite as alumina continues to absorb hydrocarbons even when saturated with water, whereas zeolites tend to desorb hydrocarbons when saturated with water.

In view of its high efficiency, an activated alumina molecular sieve trap was placed between the rotary pump and the diffusion pumps. This trap was fabricated from stainless steel, to a design similar to that of Roepke and Pung (55), and incorporated a 5 cm diameter x 5 cm thick layer of 5 - 8 mm diameter alumina balls, as suggested by Baker and Staniforth (51). The alumina was regenerated by baking periodically.

Fig. 2 shews the schematic arrangement of the vacuum system components. The source, quadrupole mass filter and detector sections were enclosed by a stainless steel vacuum chamber, joined by copper or lead gaskets. The source and analyser/detector regions were separated by a diaphragm, containing a 1·0 mm hole, by which the ions entered the analyser. This arrangement enabled the source and analyser to be pumped differentially.

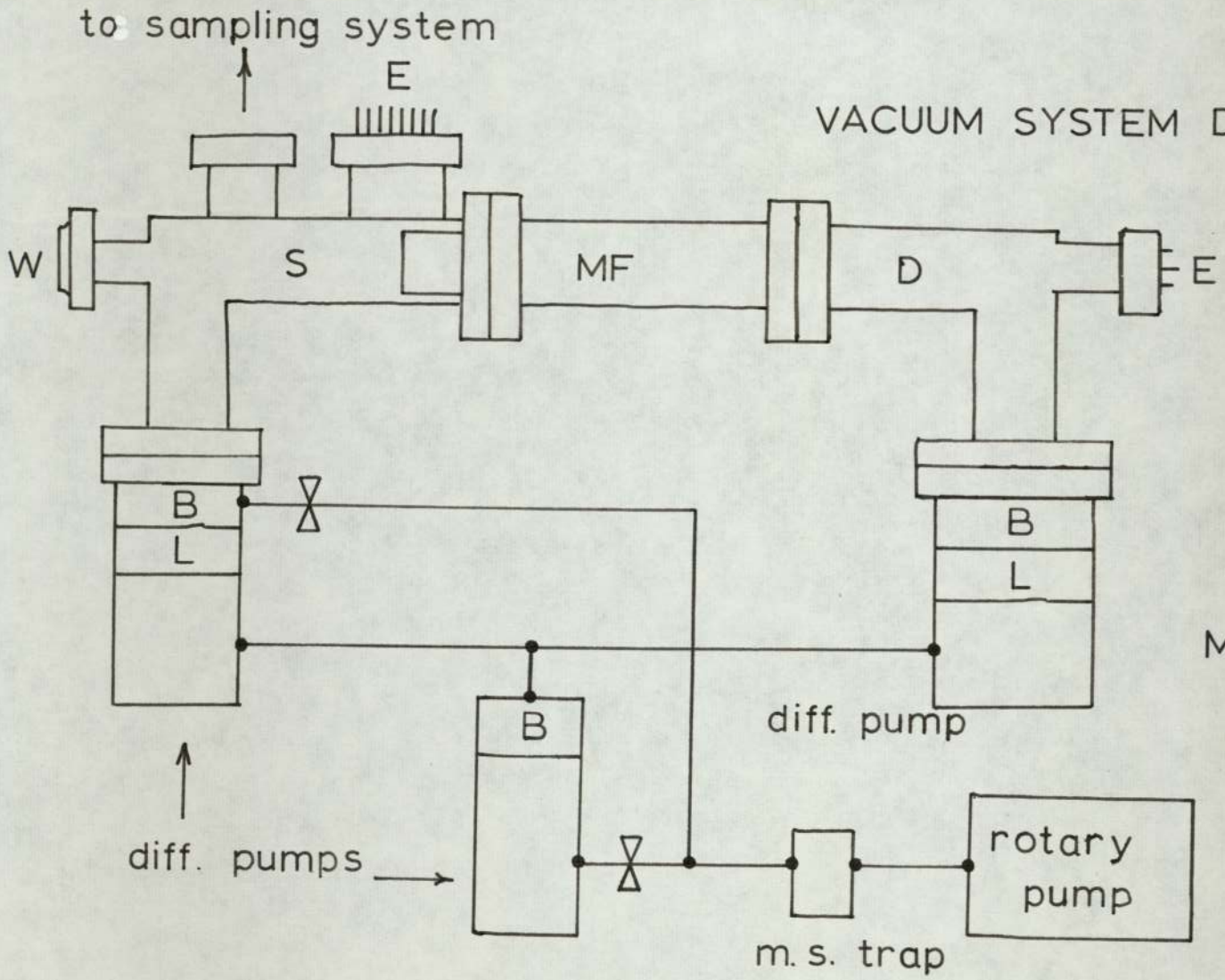

VACUUM SYSTEM DIAGRAM

FIG. 2

KEY :

B	baffle & cock
D	detector chamber
E	electrical leadout
MF	mass filter
S	source chamber
W	optical window

Liquid nitrogen traps, together with water cooled baffles, were used above the diffusion pumps. With this arrangement, after outgassing, by baking to about 150°C, pressures of less than 5×10^{-7} mm Hg were easily obtained.

A Varian leak valve was used to admit sample vapour to the source, from a gas sampling system, shewn in Fig. 3. The samples were always purified by trap to trap distillations followed by extensive "outgassing" by means of the usual freeze-thaw technique.

A very sensitive technique for the detection of incomplete degassing, is to study the spin-relaxation time (T_1) of an organic liquid, such as benzene, which contains dissolved oxygen from the air, in a N.M.R. spectrometer. Various authors have applied the freeze-thaw technique to study oxygen dissolved in benzene, and the longest spin-relaxation time obtained, which is a measure of the completeness of degassing, was 19·0 seconds (56). Dudley, Homer and M^{c}Whinnie (57) have shewn that, by using a chemical scavenger, a T_1 of about 24 seconds could be obtained, thus casting some doubt on the validity of the freeze-thaw degassing technique. Using a similar design of vacuum system to that described above, but with an ultimate vacuum of only about 10^{-4} mm Hg., a T_1 of about 23 seconds was obtained after only one cycle of the freeze-thaw technique. Further cycles gave results as shewn in Table 0.

FIG. 3

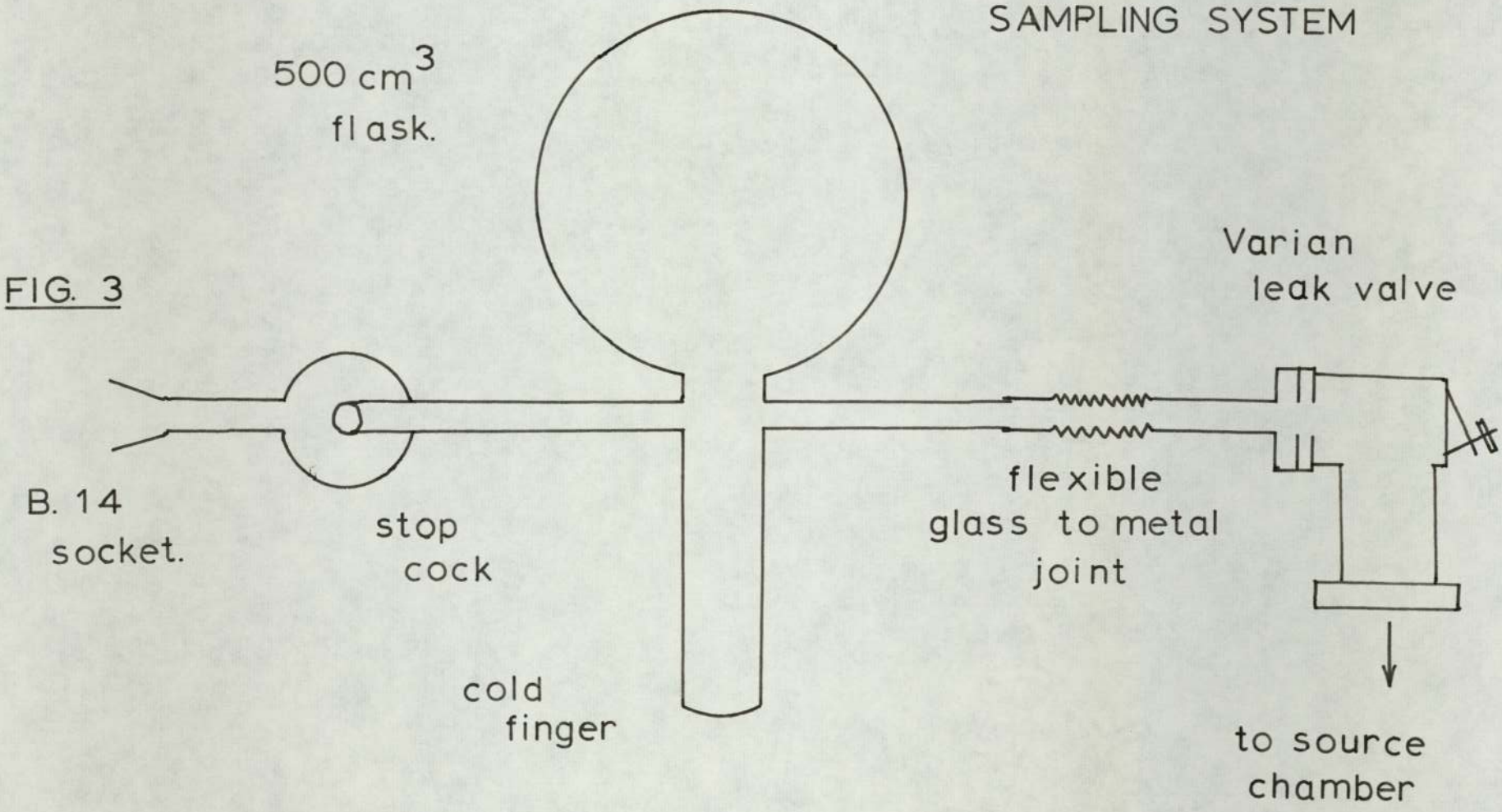
SAMPLING SYSTEM
500 cm3 flask.
Varian leak valve
B. 14 socket.
stop cock
flexible glass to metal joint
cold finger
to source chamber

TABLE 0

FREEZE-THAW DEGASSING DATA

No. of cycles.	Spin relaxation time, (secs.)
0	4•0
1	23•603
2	21•815
3	21•432
4	20•796
5	17•675
6	22•052

It may therefore be seen that the freeze-thaw technique, when properly applied, is a powerful tool in removing dissolved gases. The author wishes to extend his thanks to Mr. A.R. Dudley for determining the T_1's of the freeze-thaw degassed samples and for many discussions on this aspect of the work.

4·2 THE SOURCE SYSTEM.

For ease of fabrication, the stainless steel source region vacuum chamber was constructed so that a space of 5·5 cm diameter x 15 cm was available for the source itself. Many designs of surface ionisation source suitable to fit this space were constructed and tested, including a minature magnetron assembly. The most difficult obstacle to overcome, however, was that of maintaining accurate alignment of the cathode throughout its life, which was usually about 30 hrs. The design found most suitable was that of a planar diode with perforated anode; the perforating hole, 1 mm in diameter, being the entrance aperture of the quadrupole analyser.

The polycrystaline tantalum cathode, of dimensions, 3·3 x 0·2 x 0·003 cm, was supported by spot welding to stainless steel plates, which were insulated from the anode by means of pyrex spacers 1·0 cm thick, as in Fig. 4. The natural "springyness" of the supports was found to be sufficient to ensure that the cathode did not twist out of

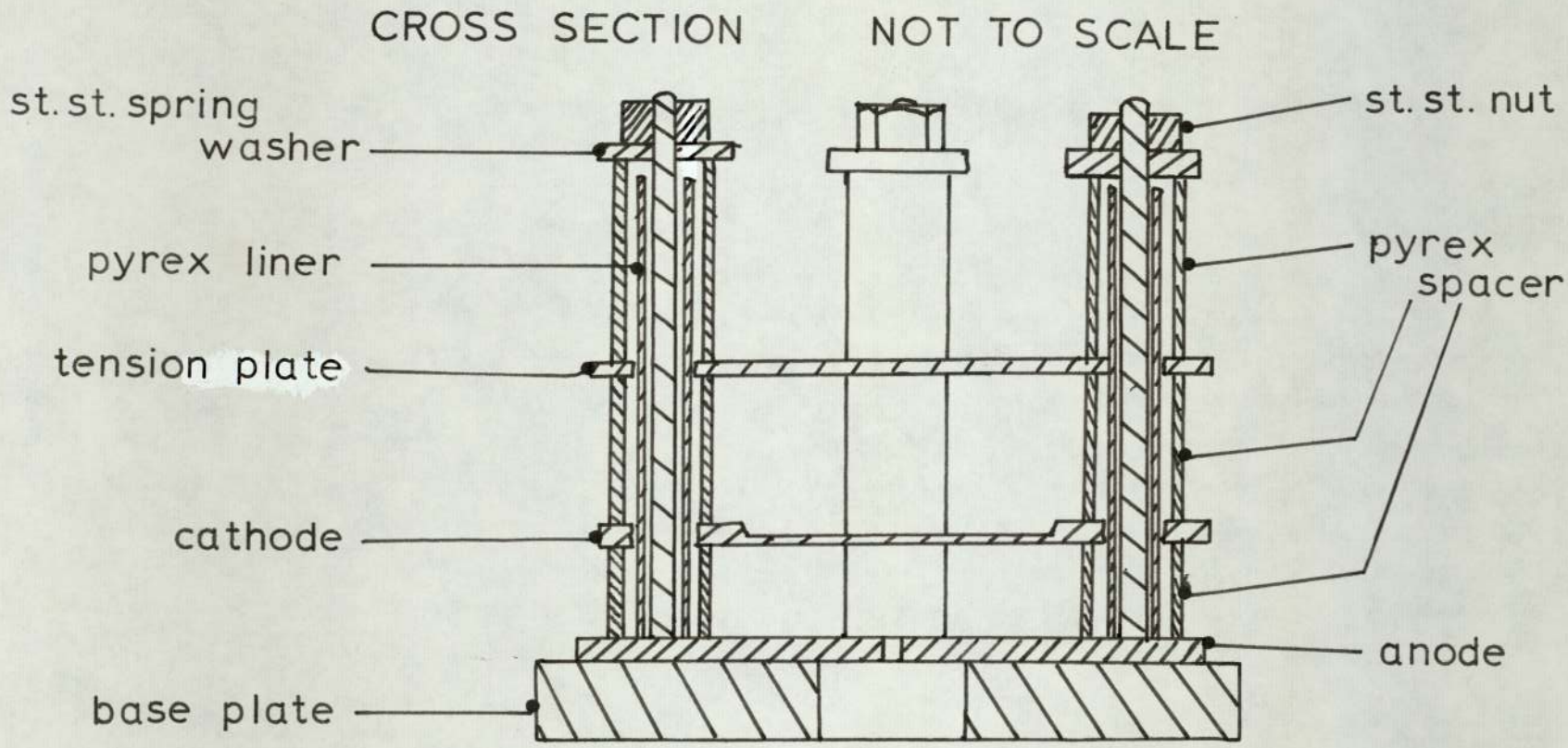

THE SURFACE IONISATION SOURCE FIG 4

alignment. By passing a current of 20 amps dc through the cathode, from a suitable power supply, temperatures in excess of 2400°K were easily obtained. A dc stabilised power supply variable between 0 - 300 volts, was constructed to supply the ion accelerating potential. The circuit diagram of the power supply is given in Fig. 5 and the overall circuit diagram of the system is given in Fig. 6.

The advantage of this type of source system was that a relatively large movement of the cathode, due to expansion, etc, could be tolerated during operation, without significant misalignment and subsequent loss of sensitivity. The main disadvantage of the planar diode was that, to ensure that the ion currents were field saturated, the emerging ions were of high (about 100 eV) energy, thus setting an upper limit on the resolution of the quadrupole mass filter.

A Leeds and Northrup disappearing filament optical pyrometer was used to determine the temperature of the cathode in use. The measurements made with the pyrometer were always found to be reproducible within 10°K for any temperature. Often, a reproducibility of better than 5°K could be obtained in the mid-part of the pyrometer's scale. The calibration of these types of pyrometer are reliable after several years of use (58).

The observed temperature must be corrected to allow for emissivity effects and also absorption by the glass window through which the cathode is observed.

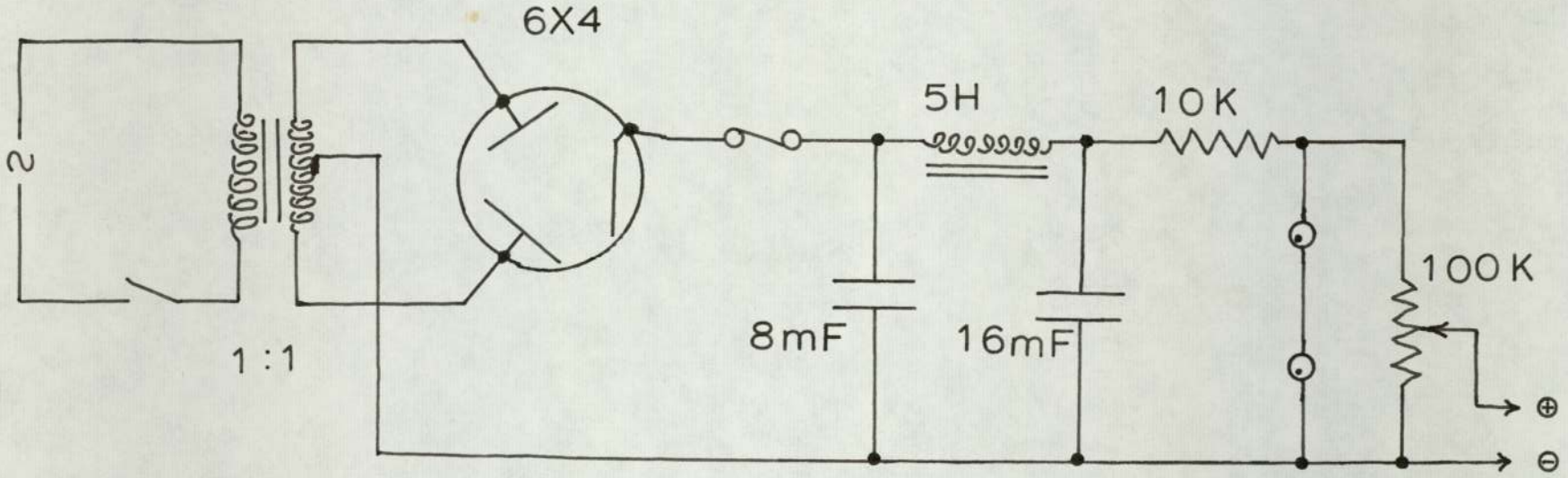

0-300 volt POWER SUPPLY FIG. 5

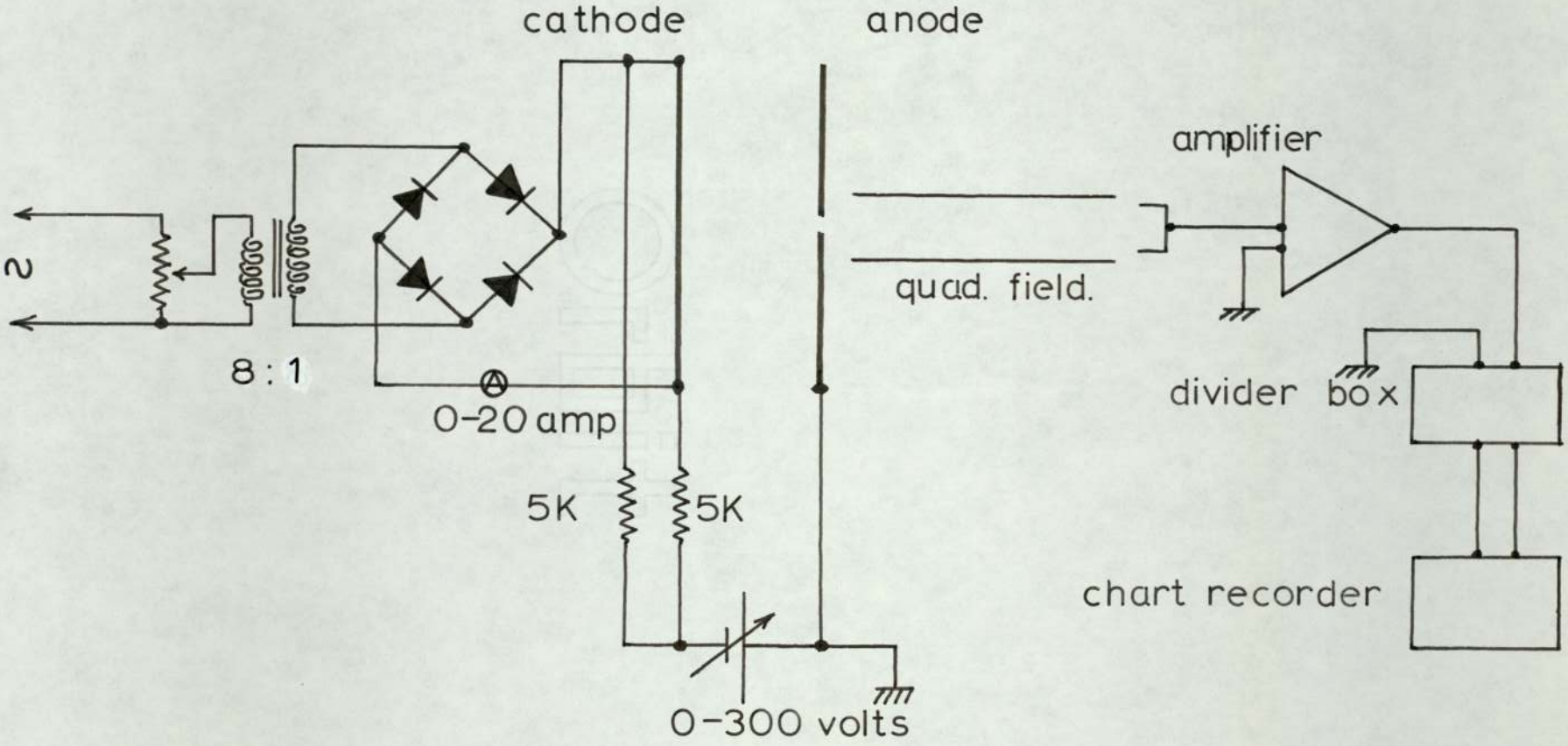

FIG. 6. Overall circuit diagram.

Malter and Langmuir (59) have given a relationship between the actual temperature T, and the observed temperature S, of a tantalum strip filament viewed through one thickness of glass as:

$$T = 0{\cdot}9919 \cdot S + 37{\cdot}14 \times 10^{-6} \cdot S^2 + 5{\cdot}74 \times 10^{-9} \cdot S^3$$

This expression was used to correct the observed temperatures.

Fig. 7, obtained from measurement on the cathode, using an optical pyrometer mounted upon a lathe top-slide, shows that there were no temperature gradients over the central part of the cathode.

4·3 THE MASS FILTER SECTION.

The mass analyser system employed to study negative surface ionisation phenomena was desired to possess the following main features:

i) Adequate resolving power.

A resolution of approximately 100 was deemed sufficient for the identification of simple ionic species.

ii) High sensitivity.

Negative ions, in general, are only about 10^{-4} the abundance of the corresponding positive ion.

iii) High ion source pressures.

Investigations in the magnetron were usually

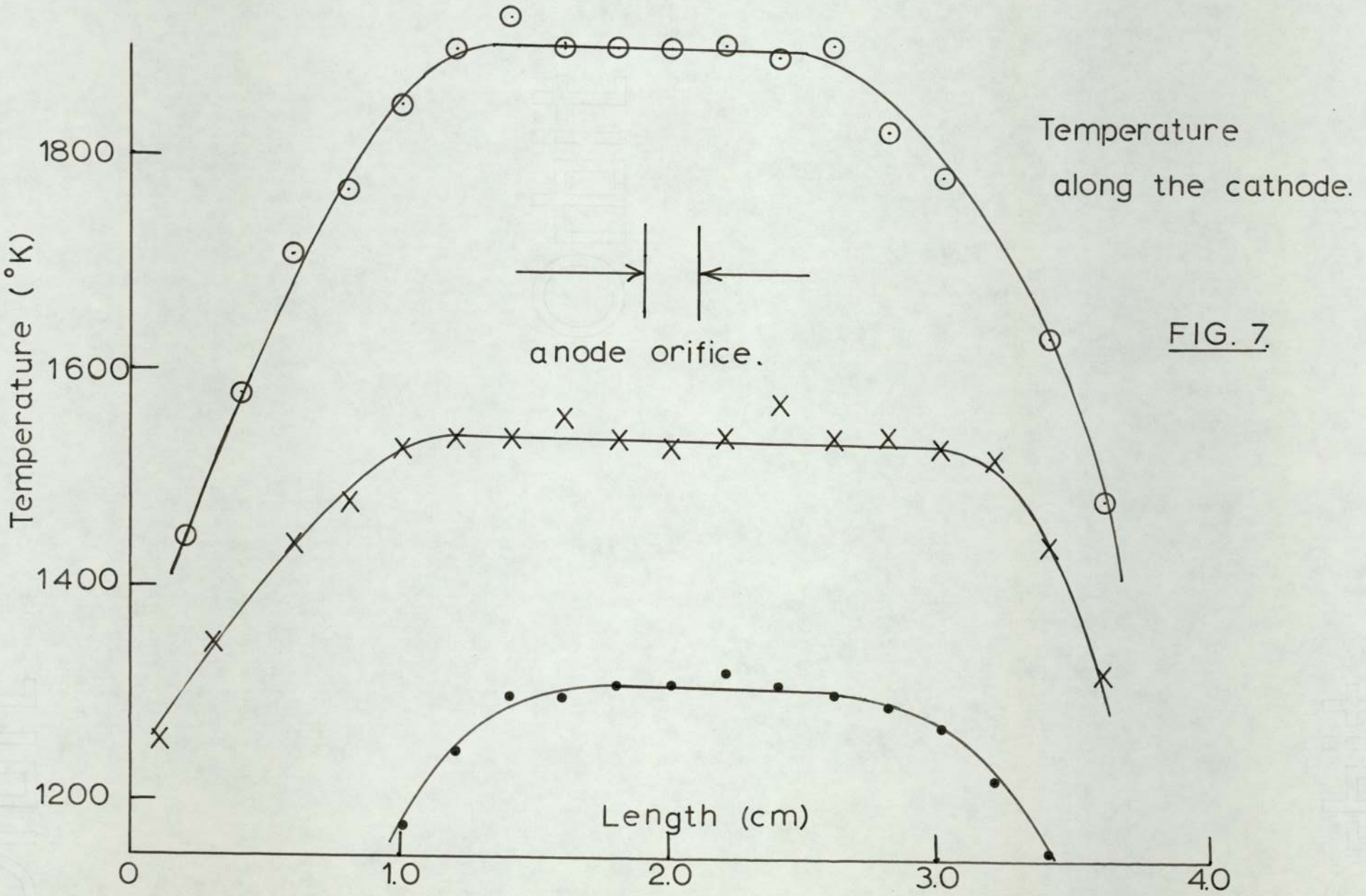
Temperature
along the cathode.
anode orifice.
Temperature (°K)
1800
1600
1400
1200
Length (cm)
0
1.0
2.0
3.0
4.0

FIG. 7.

performed over a range of 10^{-5} to 10^{-2} mm Hg., and it was desired to emulate the magnetron conditions as far as possible.

iv) Bakable system.

Highly electronegative materials, such as the halogens, must be removed from the system, if they are not to dominate the ion emission. Baking the system enables such materials to be easily expelled.

After a study of the different available types of spectrometer, the quadrupole mass filter was believed to be the most suitable type.

a) The mass filter has a very high transmission efficiency, especially at low resolving powers. The high transmission is maintained over high background pressures. This is due to the strong focusing action of the quadrupole field, which, with the exception of charge exchange reactions maintain transmission characteristics unchanged, to a first approximation, by collisions with residual gas molecules.

b) Ion beam injection conditions are not stringent for low resolutions, allowing simple modifications to the mass filter to be undertaken. The cylindrical symmetry of the analysing field enables the most practical method of extracting ions from the source to be used, namely, a small circular orifice.

The resulting ion beam is then of cylindrical symmetry, thereby maximising the coupling efficiency between the ion source and quadrupole field without the use of an ion lens.

Of the commercially available quadrupole mass filters the Atlas AMP 3 type was chosen as this instrument satisfies the criteria set above. In this work, only the quadrupole rods and housing, together with the associated electronics, were used.

Charged Particle motion in the Ideal Mass Filter.

Paul and his co-workers pioneered the construction and subsequent theoretical development of the quadrupole mass filter in the 1950's. The theoretical treatment of the ideal quadrupole mass filter given here, follows that of Dawson and Whetten (60).

The quadrupole field in an ideal mass filter may be obtained by using four parallel conducting electrodes ground accurately to a hyperbolic cross-section, located symmetrically about the instrument (z) axis, so as to correspond to the equipotential lines of a quadrupole field. Opposite electrodes are joined together electrically. Usually, a dc potential, U, and an rf potential V cos (wt), are impressed upon the electrodes. However, this is not the only possible

arrangment; a recent communication (61) shews that a rf square wave potential may be used, with some increase in performance.

Using the above potentials, the quadrupole potential, I, at any point, in rectangular coordinates, is given by:

$$I = (U - V\cos(wt))(\lambda x^2 + \sigma y^2 + \gamma z^2) \qquad (1)$$

where z is the instrument axis and the x direction is that through the centres of the pair of rods which have a negative dc potential with respect to the second pair of rods.

Electric fields, for each direction, may be obtained from the quadrupole potential at any point:

$$\begin{aligned} E_x &= -(U - V\cos(wt)) \cdot 2\cdot\lambda\cdot x \\ E_y &= -(U - V\cos(wt)) \cdot 2\cdot\sigma\cdot y \\ E_z &= -(U - V\cos(wt)) \cdot 2\cdot\gamma\cdot z \end{aligned} \qquad (2)$$

For the mass filter, it is usual to chose the values of the constants in eqn (1) so that:

$$\gamma = 0$$

$$\lambda = -\sigma = 1/2\cdot r_o^2$$

where r_o is the distance from the centre of the field to the nearest point of an electrode.

Provided there is no space charge within the electrode structure, the potential satisfies Laplaces' eqn.

$$d^2I/dx^2 + d^2I/dy^2 + d^2I/dz^2 = 0 \qquad (3)$$

as $\gamma + \sigma + \lambda = 0$

The equations of motion of a singly charged ion, at a point x,y are:

$$\begin{aligned} d^2x/dt^2 &+ (e/m \cdot r_o^2)(U - V\cos(wt)) \cdot x = 0 \\ d^2y/dt^2 &- (e/m \cdot r_o^2)(U - V\cos(wt)) \cdot y = 0 \\ d^2z/dt^2 &= 0 \end{aligned} \qquad (4)$$

The third equation expresses the fact that there is no acceleration in the z direction. These differential equations are of a type known as "Mathieu equations", whose properties are known.

Substituting:

$$wt = 2\xi$$

$$a_{\substack{x\\y}} = (8\,e\,U / m\,w^2) \qquad \{\lambda\}$$

$$q_{\substack{x\\y}} = (4\,e\,V / m\,w^2) \qquad \{\sigma\}$$

This enables the eqns (4) to be replaced by the canonical form of the Mathieu eqn:

$$d^2u/d\xi^2 + (a - 2q\cos(2\xi) \cdot u = 0 \qquad (5)$$

where u represents either x or y , and

$$a = a_x = -a_y$$

$$q = q_x = -q_y$$

Solutions to the Mathieu equation can be expressed in the form:

$$u = \alpha' e^{\mu\xi} \sum_{-\infty}^{\infty} C_{2s}\, e^{2is\xi} + \alpha'' e^{-\mu\xi} \sum_{-\infty}^{\infty} C_{2s}\, e^{-2is\xi} \qquad (6)$$

The integration constants α' and α'' depend on the initial conditions existing at introduction of the ions. The constants C_{2s} and μ depend only on a and q.

In terms of the transmission of ions through the filter, the solution of the Mathieu equations are of two distinct types in which:

i) x or y continues to increase with time, giving non-bounded, unstable, trajectories.

ii) x or y is periodic with time, giving stable, bounded trajectories, provided that the ions do not come into contact with the electrodes.

We are interested in solutions giving rise to stable ion motion. The constant μ in equation (6) determines the type of solution. Only if $\mu = i\beta$, where β is not a whole number, will the solutions be stable.

Since μ depends on the values of a and q, the regions of stable operation may be plotted in a - q space. In describing the mass filter, there are two sets of a - q diagrams, one for the x and y directions, respectively. For an ion to traverse the mass filter, it must have a stable trajectory in both the x and y directions. The combined stable region of operation for the x and y directions, used in the mass filter, is shewn in Fig. 8.

If the ratio of dc to rf potentials, that is, U/V, is fixed, then the ratio a/q is fixed and this defines the "mass scan line" on the stability diagram. For any chosen values of U, and therefore V, ions of differing values of e/m will be spread out along the mass scan line, according to their a,q values. Ions of large e/m values will be farthest from the origin.

By varying the magnitudes of U and V, keeping constant the ratio U/V, each ionic species may be brought in turn into the stable region, and can then be transmitted through the device. Thus, if a detector is placed at the exit of the mass filter, and the U and V potentials steadily swept over a given range, a plot of number of ions emerging from the filter versus the value of m/e, that is, a mass spectrum, may be obtained.

FIG. 8

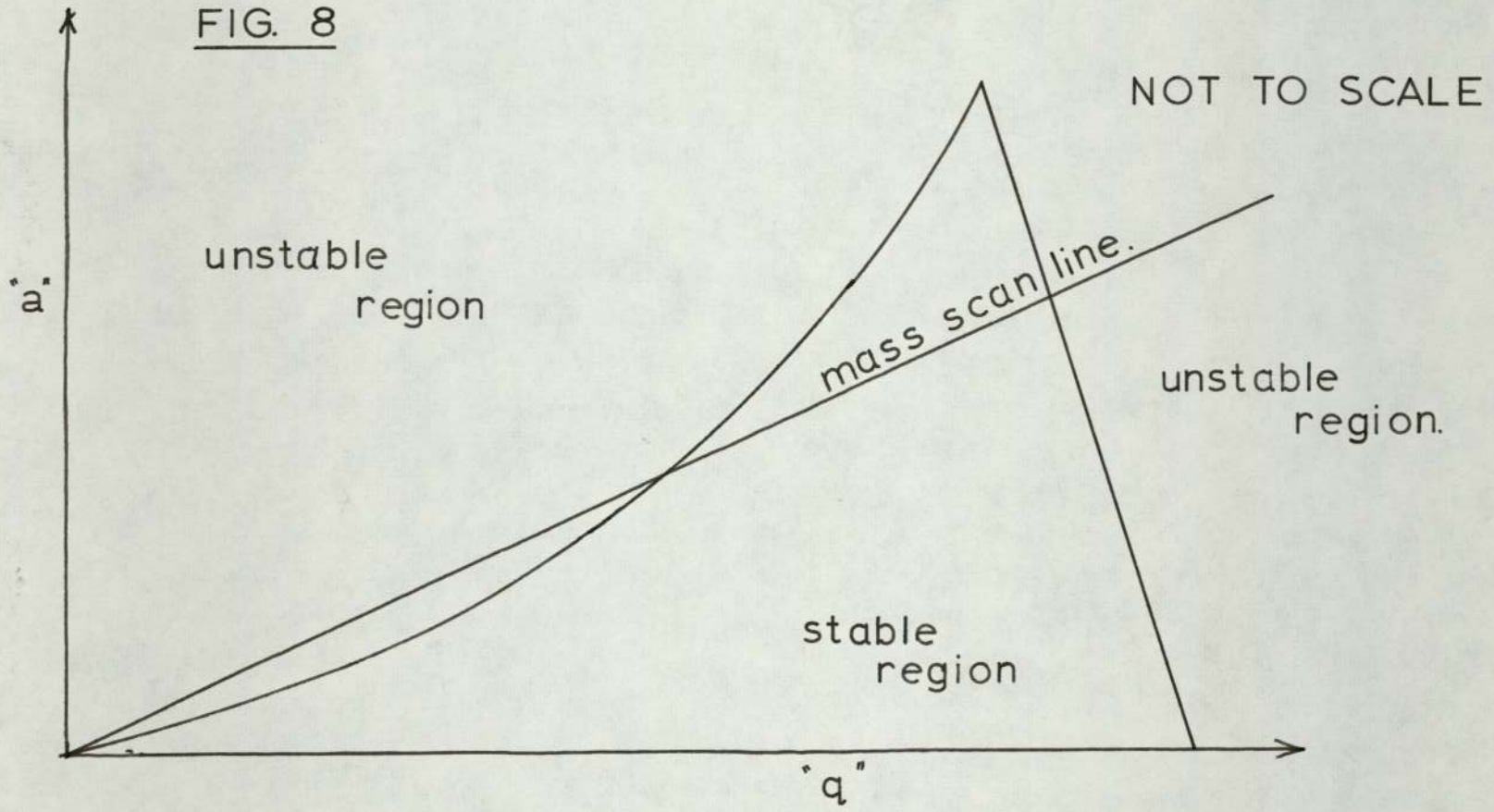

MASS FILTER STABILITY DIAGRAM.

The resolution of the mass spectrum is usually defined for mass filters, as $(M/\Delta M)$, where ΔM is the width, at half-height, of a peak appearing at mass M. Two resolution ranges may be distinguished:

i) The peaks are flat topped (trapezoidal) with 100% ion transmission. This is the low resolution range and is obtained when the mass scan line intersects the stable region below its tip.

ii) The peaks are triangular, with less than 100% ion transmission, and their intensity is inversely proportional to the resolution. This is the high resolution range and is obtained when the mass scan line intersects the tip of the stability diagram.

Compared with modern magnetic mass spectrometers, the mass filter's resolution is low, in general, below 500.

The Practical Quadrupole Mass Filter.

The previous section was concerned with the develop ment of the theoretical treatment of the quadrupole mass filter. This section deals with those aspects of the theoretical treatment which are only approximated to in practice.

It was previously noted that the quadrupole field forming surfaces should be of hyperbolic cross section, located so as to correspond to the equipotential lines of a quadrupole field . However, many mass filters, including the AMP 3, are constructed with rods of circular cross section. The best approximation to a hyperbolic field is to space the circular rods so that $r_{rod}/r_o = 1{\cdot}16$, where r_{rod} is the radius of the circular rod.

Brubaker and Chamberlin (62) have shewn that the resolving power of a given instrument, using hyperbolic rods was approximately twice that found when round rods were used. The performance of mass filters having imperfect fields has been treated by Dawson and Whetten (63). The use of round rods, and the occurence of mechanical imperfections, apart from causing loss of ions, was shewn to cause peak splitting. A comprehensive experimental study by Arnold (64) later shewed that mutual misalignment of the rods, or rods with source, caused peak splitting and loss of ions.

Quadrupole theory also assumes that the quadrupole field falls to zero potential at an infinite distance away from the rods. In practice, the rods are mounted near to a grounded metal housing. Denison (65) has shewn that the sensitivity of a given instrument may be significantly increased by optimising the rod spacing with respect to the position of the housing.

The analysis of the transmission of ions through a mass filter as a function of the angular entry of the ions, has given considerable insight into the effect of the entry and exit fringing fields. Though complex phenomena, the fringing fields have the effect of making ions passing through them unstable, thus causing loss of ions and hence, loss of sensitivity. Brubaker has shewn that, by using extra electrodes, the fringing fields may be modified to permit almost all the entering ions to pass through into the quadrupole field proper.

Modifications to the AMP 3 Mass Filter

The AMP 3 mass filter operates at a fixed frequency of 3 MHz, and the required resolution may be obtained with several combinations of aperture size, ion energy and a/q ratio. The smallest aperture provides greater resolution and greater transmission at high resolution. The largest aperture provides greater sensitivity at low resolutions (ie less than 10).

Experimentally, a value of 1mm was chosen for the diameter of the entrance orifice. For 100% ion transmission, the diameter of the input aperture, D, for high a/q ratios was:

$$D = r_o/(M/\Delta M)^{\frac{1}{2}} \qquad (7)$$

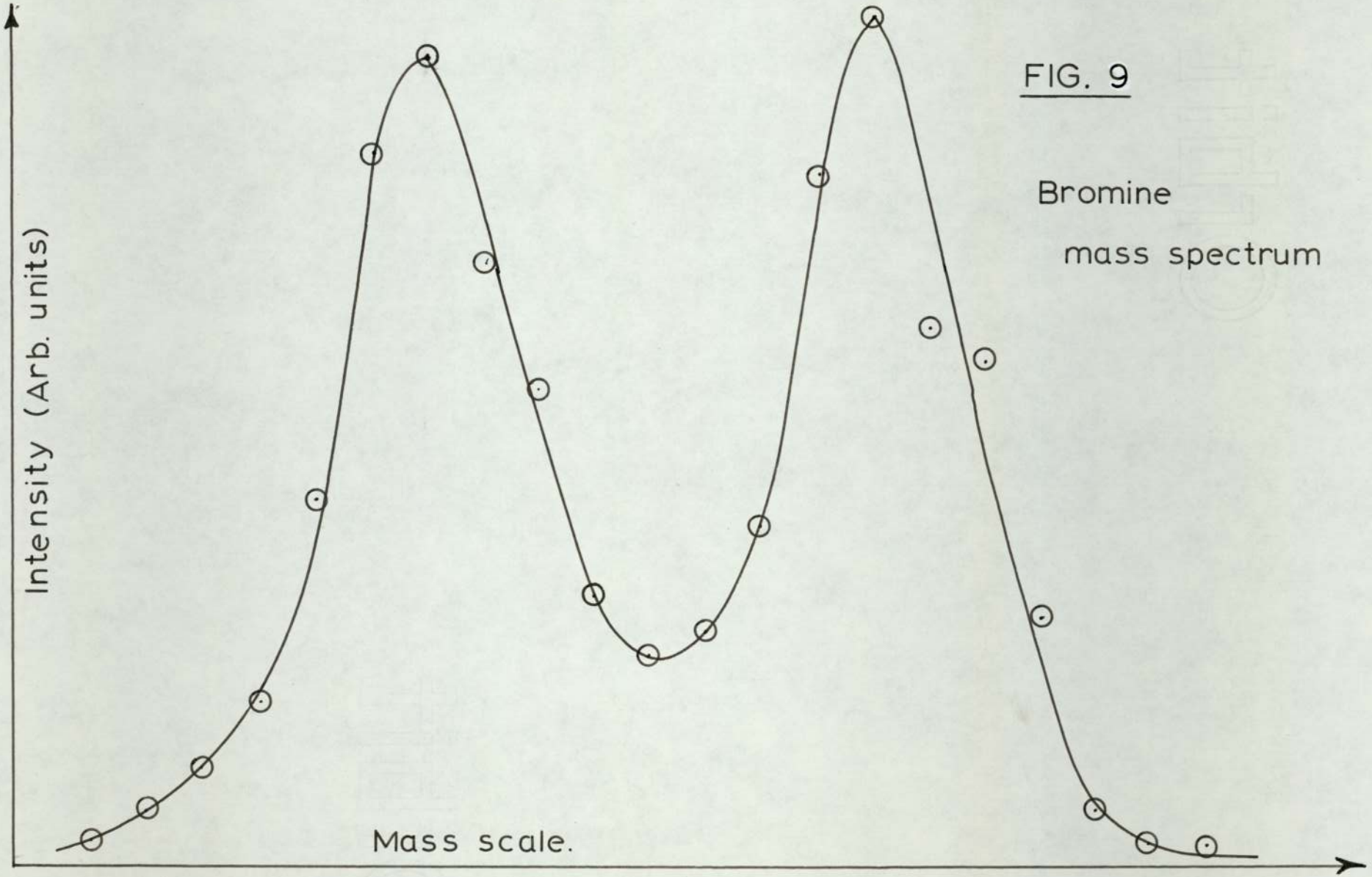

FIG. 9

Bromine

mass spectrum

Thus as r_o is 0•69 cm, the expected resolution would be approximately 48 at 100% ion transmission. The accelerating voltage is given by:

$$V = 4•2 \times 10^2 \times f^2 \times L^2 \times (M/\Delta M) \qquad (8)$$

where f is the frequency in MHz. (3•0MHz)

L is the length of the rods in m (0•2 m)

M is the ion mass.

For example, for mass 79 (Bromine), the accelerating potential, for a resolution of 48, would be approximately 249 volts. Experimentaly, using a channel electron multiplier as in the following sections on detectors, a mass spectrum of bromine was obtained, and is shewn in Fig. 9. The accelerating potential was 130 volts. For the ^{79}Br peak, the observed resolution was approximately 91. Inserting the accelerating potential and mass into equation (8) it may be seen that the expected approximate resolution is 92. This indicates that the system has been correctly set up and well aligned.

The electronic unit of the AMP 3 was designed for two modes of mass scanning operation:

i) by means of a helical potentiometer, the mass range could be manually scanned.

ii) by means of an internal electronic timing system the mass range could be scanned over a range of speeds and repetition rates.

In the study of negative surface ionisation, valuable information may be obtained by comparing the ion currents at various source temperatures and pressures. The automatic scanning system was unsuitable for this, as the slowest scan speed per amu corresponded to about 1/30 th of the detector's time constant, (using a Faraday cylinder detector). Manual scanning was extremely tedious. To obviate this difficulty, a simple "peak switching" circuit was constructed. This enabled three mass positions to be preselected. The peak switching circuit was composed simply of two extra 50K helical potentiometers wired in parallel with the existing helical potentiometer, and a three position, three way rotary switch enabled each potentiometer to be connected to the rf generator, as desired.

4·4 THE DETECTOR SYSTEM.

The quantity and charge of the ions leaving the mass filter must be measured. Commonly, an electron multiplier is used as a detector for low ion currents, although scintillation detectors and semi-conductor detectors are also in general use.

Although these detectors have a high sensitiv ty, their responce to different ions vary and their responce to a given ion changes with time (66). A study was therefore carried out, using a channel electron multiplier, to determine its suitability for use as a detector in the quadrupole system.

Study of the Channel Electron Multiplier.

A channel electron multiplier (CEM) consists of a narrow tube of insulating material, usually glass, the inside surface of which has been treated to produce a thin conducting layer. If a potential is applied between the ends of the tube, the thin conducting layer becomes a continuous dynode, electricaly analogous to the separate dynodes of a conventional photomultiplier, together with the resistor chain used to establish the separate dynode potentials. The resistance of the continuous dynode is about 10^9 ohms. The channel electron multiplier operates in vacuum, with an open window cathode, and an incident particle entering the cathode end of the multiplier generates secondary electrons on collision with the walls of the tube. These are accelerated along the tube until they strike the wall again, where they generate further secondary electrons. This avalanching process results in a large negative pulse arriving at the anode end of the multiplier.

CEM DETECTOR CIRCUIT DIAGRAM

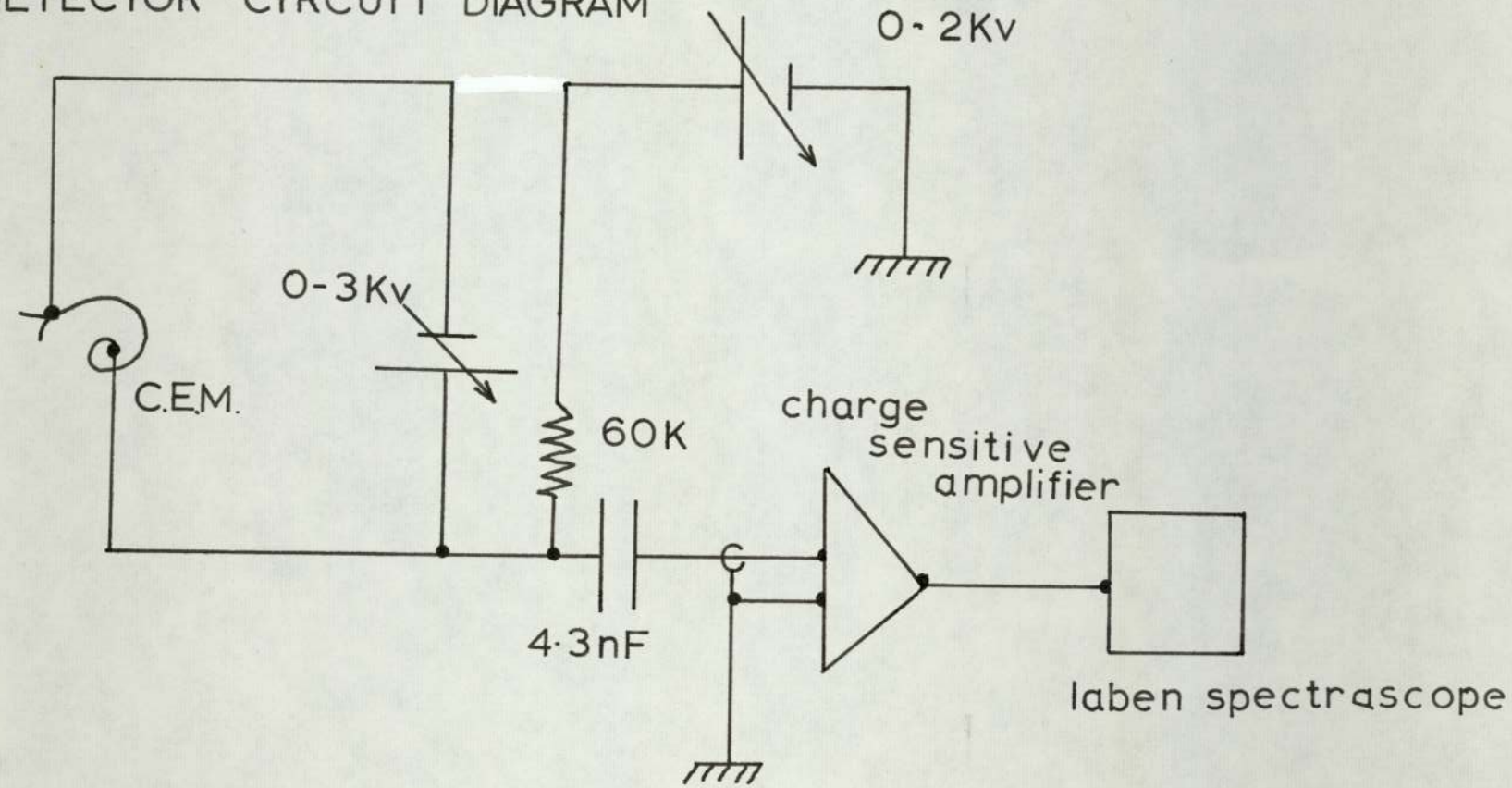

FIG 10

The gain of these multipliers, which is defined as the magnitude of the output pulse for a single input event, is high, often above 10^8. It is usual, with channel electron multipliers, to count the number of pulses appearing at the anode, rather than attempt to integrate them, to give a current measurement. The potential across the multiplier is approximately 3·5 kVolts, and some accelerating potential is usually applied between ground and the multiplier to ensure that the negative ions are accelerated into the cathode. This means that, in practice, the anode of the multiplier is about +4 kVolts above ground. Thus direct current measurements were impractical, as the amplifiers, etc., would have to be above ground by +4 kVolts also. However, in a pulse counting circuit a capacitor, which allows only the pulses from the multipliers anode to pass it, effectively separates the multiplier from the amplifiers, allowing them to operate at ground potential.

The channel electron multiplier used in this study was a Mullard B419BL, aligned with its funnel cathode in line with the axis of the quadrupole mass filter, and located about 3 cm from the quadrupole's exit aperture. The circuit used to detect the pulses is shewn in Fig. 10. The charge pulse at the anode of the channel electron multiplier is converted into a voltage pulse by the RC network. This voltage pulse is then amplified by a charge sensitive amplifier

instead of the more usual emitter-follower amplifier. The emitter-follower offers a simple solution, but it has the disadvantage that it must be placed as close as possible to the channel multiplier output in order to preserve the pulse information. In most cases it is necessary to place it inside the vacuum system. The charge sensitive amplifier can be used effectively here because its output voltage is almost independent of its input capacitance loading, consequently a long cable can be used to connect it to the output of the multiplier. The charge sensitive amplifier used was constructed according to the circuit given by Petley (67).

The resultant voltage pulse was detected by a "Laben mod 100 Spectroscope". The Laben Spectroscope is a versatile instrument which was used in these experiments in two ways:

i) As a simple scaler, in which the total number of pulses arriving per unit time, were counted.

ii) As a pulse height analyser. In this mode, the incoming voltage pulse is allocated to a particular scaler store, depending on the amplitude of the pulse. After a predetermined time, the number of pulses of a given amplitude could be determined, thus enabling a pulse height distribution diagram to be drawn.

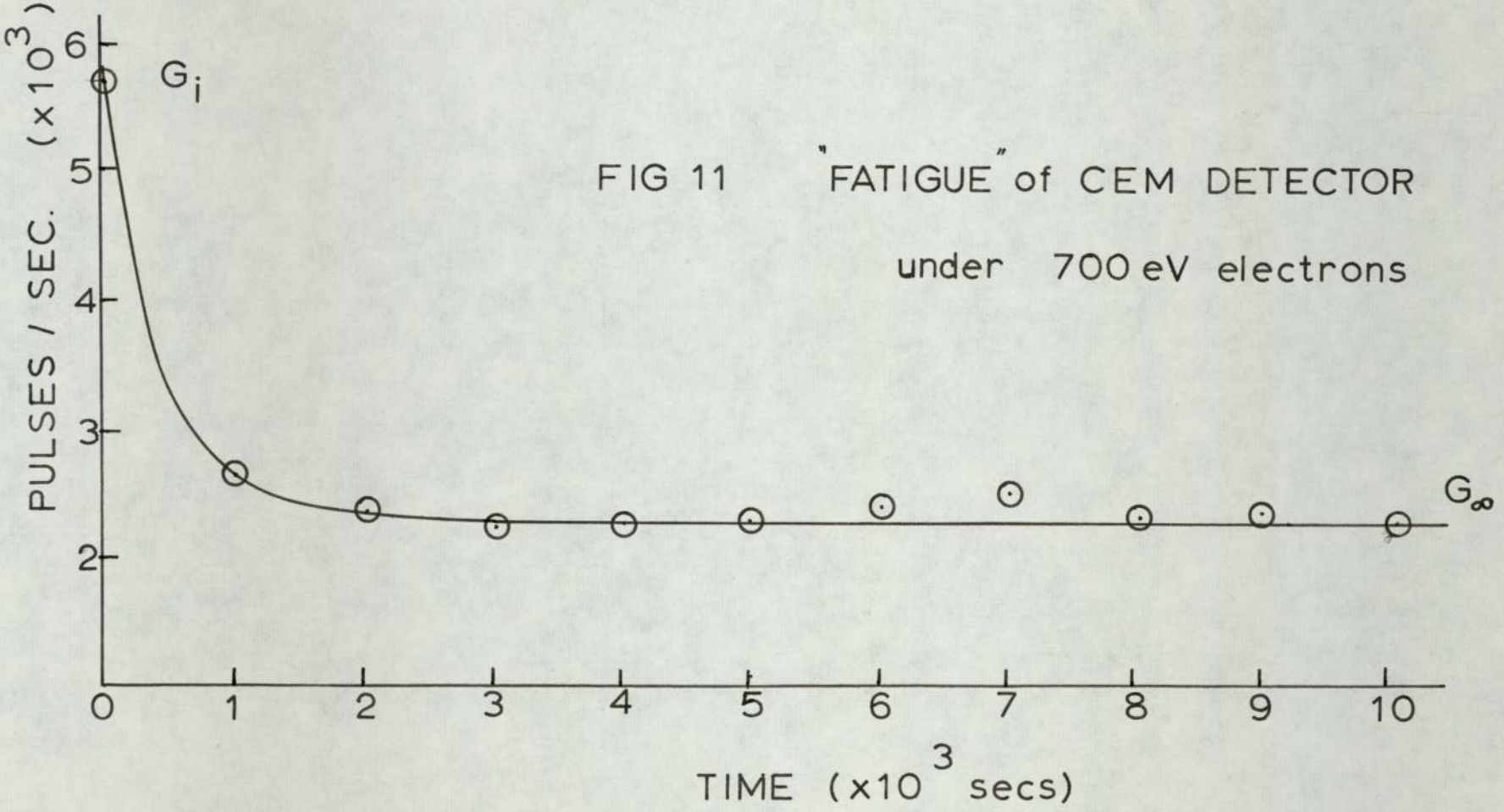

FIG 11 "FATIGUE" of CEM DETECTOR

under 700 eV electrons

The gain of channel electron multipliers tends to decrease when the number of incident ions is greater than about 100 per second. This effect is known as fatigue and is illustrated in Fig. 11. Many authors have studied the effect of channel electron multiplier fatigue due to high incident fluxes of positive ions and electrons. The work of Reed (68) is very comprehensive in this respect.

It may be seen from Fig. 11 that the number of detected ions falls to a limiting value, G_∞, for a given constant number of incident ions, G_i. Egidi et al (69) have shewn that G_∞ is inversely proportional to G_i for Bendix type channel electron multipliers. However, it is important to notice that the time taken for G_∞ to be reached is of the order of 0·5 hours. Thus this amount of time would have to be allocated to each measurement to ensure accurate results. Furthermore, Egidi et al have shewn that, for 5KeV electrons a time of approximately 10t when t is the measurement period, must be allowed between measurements to allow the gain to return to its original value. It may be seen that long periods of time must be devoted to any quantitative measurements made with channel electron multipliers, unless the incident ion rate is low.

The sensitivity and resolution of the quadrupole system, using a channel electron multiplier as detector, was considered sufficient. However, as sensitivity is inversely proportional to resolution, any negative ion of

low abundance would only be poorly resolved, due to the greater sensitivity required to detect it. A recent report by Van Gorkom et al (70) has shewn that it is possible to resolve isobaric positive ions by means of their differing secondary electron distributions when impinging on the first dynode of an electron multiplier. The method of Van Gorkom et al was to plot the position of the deconvoluted pulse height distribution maxima against the energy of the incident ion. By this means, isobaric krypton and cyclohexane positive ions could be easily distinguished. However, a recent paper published by Goodings et al (71) suggests that negative ions behave in a very different manner to positive ions on impact with the first dynode of an electron multiplier. This observation of Goodings et al is in direct disagreement with the work of Parilis and Kisinevskii (72) and Arifov and Khashimov (73).

A study was therefore made of the effect of impinging CN^- ions onto the cathode of the channel electron multiplier. By keeping the source temperature and pressure constant, a uniform beam of CN^- ions, derived from cyanogen bromide vapour, could be made to impinge on the cathode of the channel electron multiplier. The ions were accelerated after leaving the mass filter by a voltage of 0·5 - 2·0 KV applied between ground and the channel electron multipliers cathode. The Laben spectroscope recorded the pulse height distribution at a given accelerating potential, from which the position of the pulse height distribution maxima could be obtained.

The electron multiplier pulse distributions were not the true secondary electron energy distributions as would be observed when the CN^- ions impinged only on the cathode section. Instrumental broadening occurs in the channel electron multiplier and in the amplifier. However, it has been shewn that the position of the observed pulse height distribution maxima corresponds to the position of the most probable pulse height in the deconvoluted distributions. A plot was made of pulse height distribution maxima versus the ion energy, and is shewn in Fig. 12. These results are similar to those obtained for positive ions by Van Gorkom et al, having a marked linear dependence on the ion energy above about 1 KV.

Van Gorkom et al have shewn that this type of variation of the pulse height distribution maxima with ion energy is related to the structure, and not mass, of the impinging ion. For example, isobaric krypton ions and cyclohexane ions were easily distinguished. However, the charge upon the ion has no effect upon the dependence. Ar^+ and Ar^{++} were found to have the same dependence. This later observation is in agreement with the theoretical treatment of Parilis and Kisinevskii (72) who have shewn that the secondary electron emission is the same for a given ion, no matter what the magnitude and sign of the charge upon it.

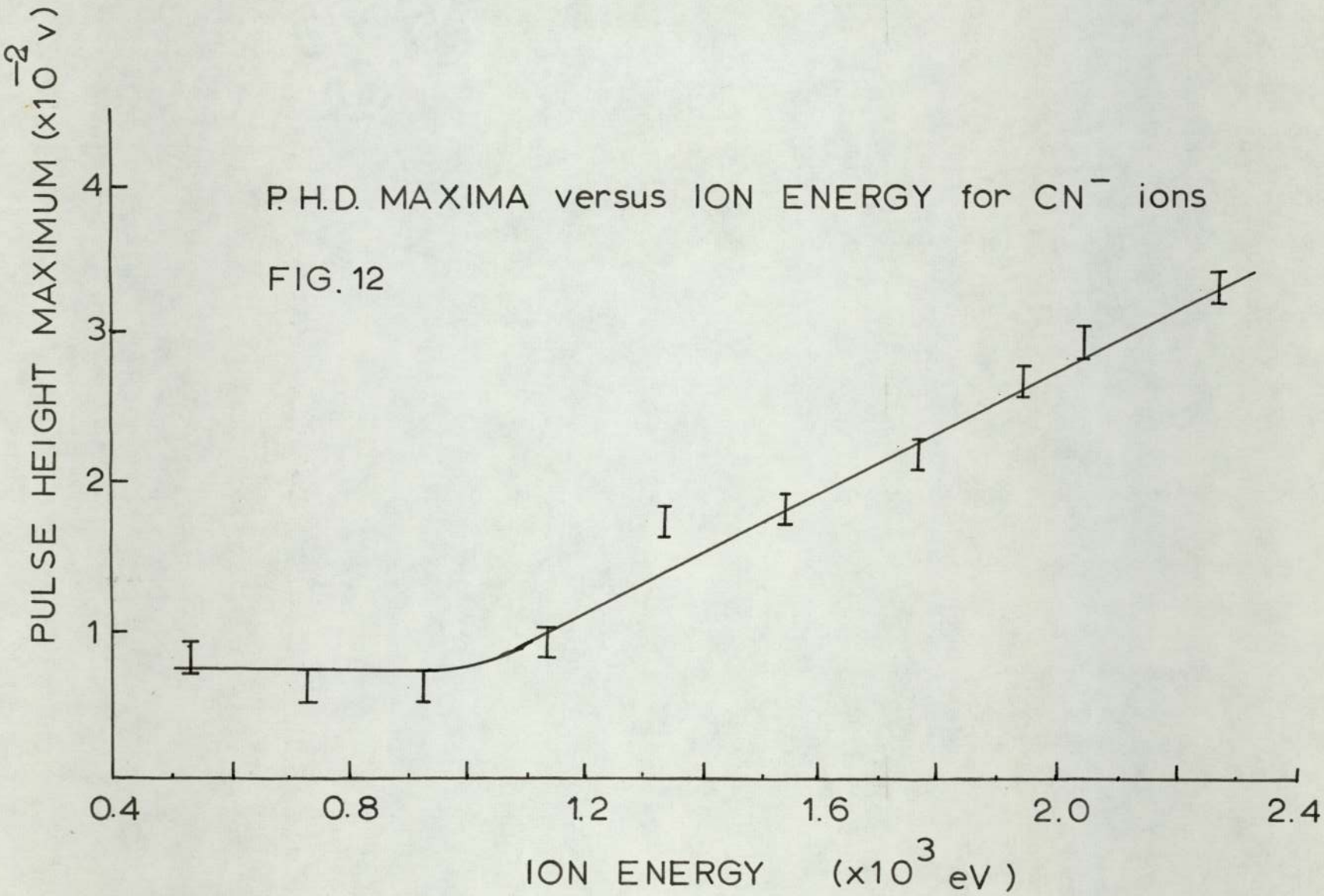
P.H.D. MAXIMA versus ION ENERGY for CN^- ions
FIG. 12
PULSE HEIGHT MAXIMUM ($x10^{-2}$ v)
4
3
2
1
0.4
0.8
1.2
1.6
2.0
2.4
ION ENERGY ($x10^3$ eV)

It is implicit in the results obtained for CN^- ions, that isobaric negative ions could be resolved by this technique, provided that the variation of their pulse height distribution maxima with ion energy, for a given multiplier, was known. This, however, was not verified experimentally.

The Faraday Cylinder Detector.

The Faraday cylinder, also known as a Faraday "cup" or"cage", consists of a partially screened electrode, at which ionic species may neutralise their charge and be detected. The Faraday cylinder is connected electrically to some current measuring device, so that the amount of charge neutralised in the cylinder per unit time, may be estimated.

The Faraday cylinder employed in this work had dimensions 2 cm diameter by 7 cm long. It was constructed from copper and was mounted on PTFE insulators. These insulators were bolted to a standard electrical leadthrough for vacuum chambers, supplied by Vacuum Generators Ltd. The external conductors were screened by a grounded metal box, and the Faraday cylinder itself was effectively screened by the grounded metal vacuum system.

Faraday cylinders usually have a partially closed entrance aperture, however, the beam of ions from a quadrupole mass filter is diffuse, and so a large aperture is required.

In use, the Faraday cylinder was located axially about 1 cm from the exit of the quadrupole mass filter. There is a possibility that secondary electron emission may occur at the Faraday cylinder, due to the energy (about 200 eV) of the bombarding ions. The secondary electrons may not be recaptured by the Faraday cylinder, thus causing an error in the measured current.

This effect may be detected by locating a bar magnet near the cylinder, outside the vacuum chamber. Any secondary electrons formed would then be deflected into the walls of the Faraday cylinder, causing a change in the measured current. This experiment was carried out, in the presence of the interhalogen vapours and no change in the currents was observed. In the case of cyanogen bromide vapour a difference in the measured currents, in the presence and absence of the bar magnet, was observed. These observations are discussed in the following chapter.

The ion current arriving at the Faraday cylinder was then measured by connecting the cylinder, by means of a screened cable, to a dc amplifier. Two types of amplifier were used:

i) An AVO 1388 B dc amplifier

This had a range of 10^{-7} to 10^{-14} Amps in decade steps and was used to obtain the ion currents in both the temperature and pressure dependence experiments. Unfortunately, the long time constant, approximately 30 seconds in the

lower current ranges, precluded its use in obtaining mass spectra by means of the AMP 3 automatic scanning system.

ii) A fast response integrated circuit amplifier. This amplifier was constructed using an Analog Devices varactor bridge operational amplifier and the circuit diagram is given in Fig. 13. The sensitivity of the amplifier in this mode of operation is calculated as 1 volt / pA and the manufacturer claims that the response time is of the order of 10^{-2} seconds. Great care was taken to ensure that the input leads were well screened, and PTFE insulators were used throughout. The whole amplifier was enclosed in a metal box efficiently grounded. This system was used solely to obtain mass spectra. The output of the amplifier was lead, via a voltage divider box to a chart recorder, which had a full scale deflection of 1, 5, or 10 millivolts in switched steps.

4·5 THE OPERATION OF THE APPARATUS.

Fig. 14 shews the variation of the measured ion and electron currents, derived from iodine bromide vapour, at constant source temperature and pressure, with anode accelerating voltage. Above about 80 volts, all the currents are field saturated, but in order that there was no possibility of space charge effects within the planar diode source, the anode voltage was usually set at 250 volts.

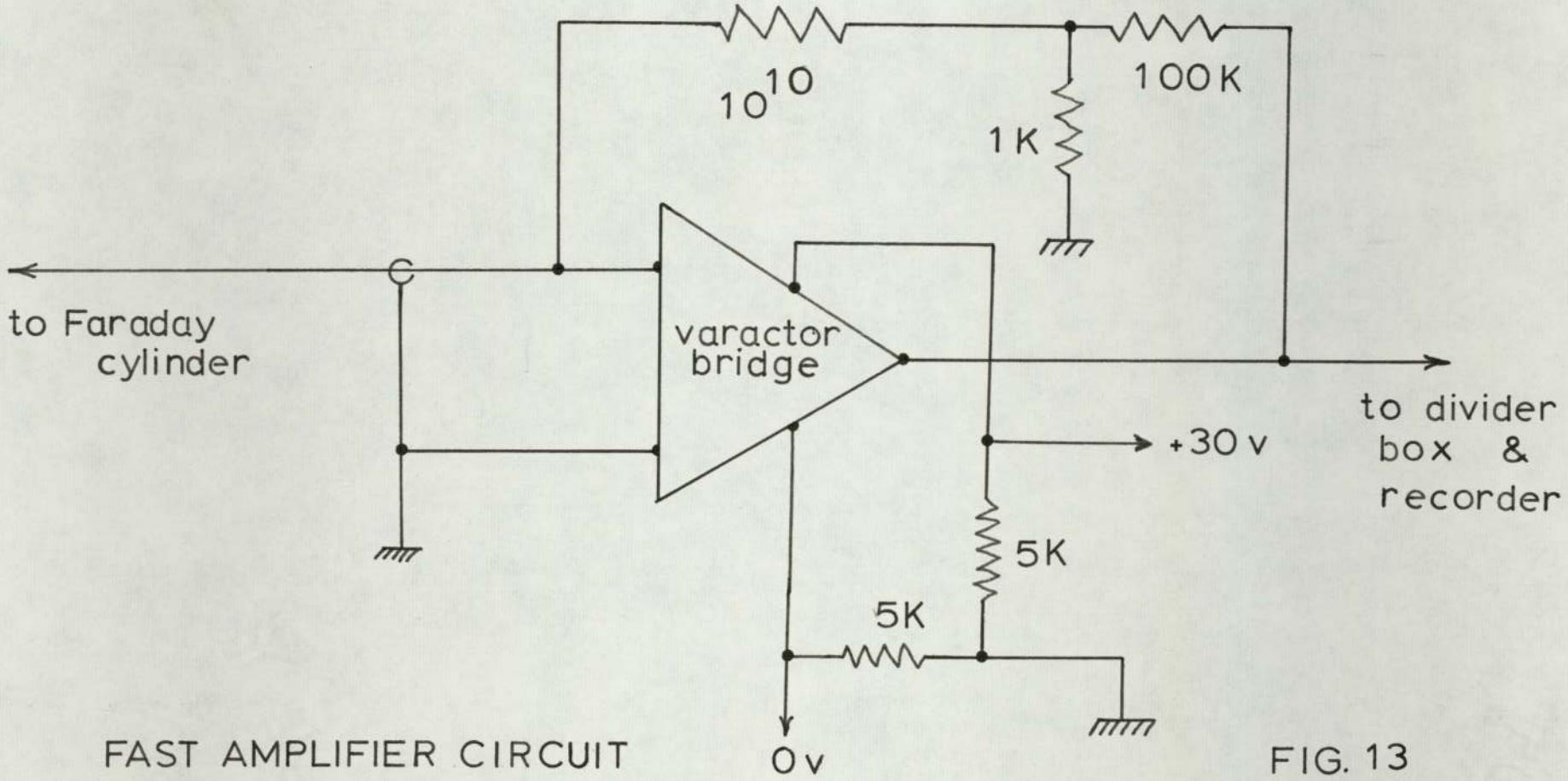

FAST AMPLIFIER CIRCUIT

FIG. 13

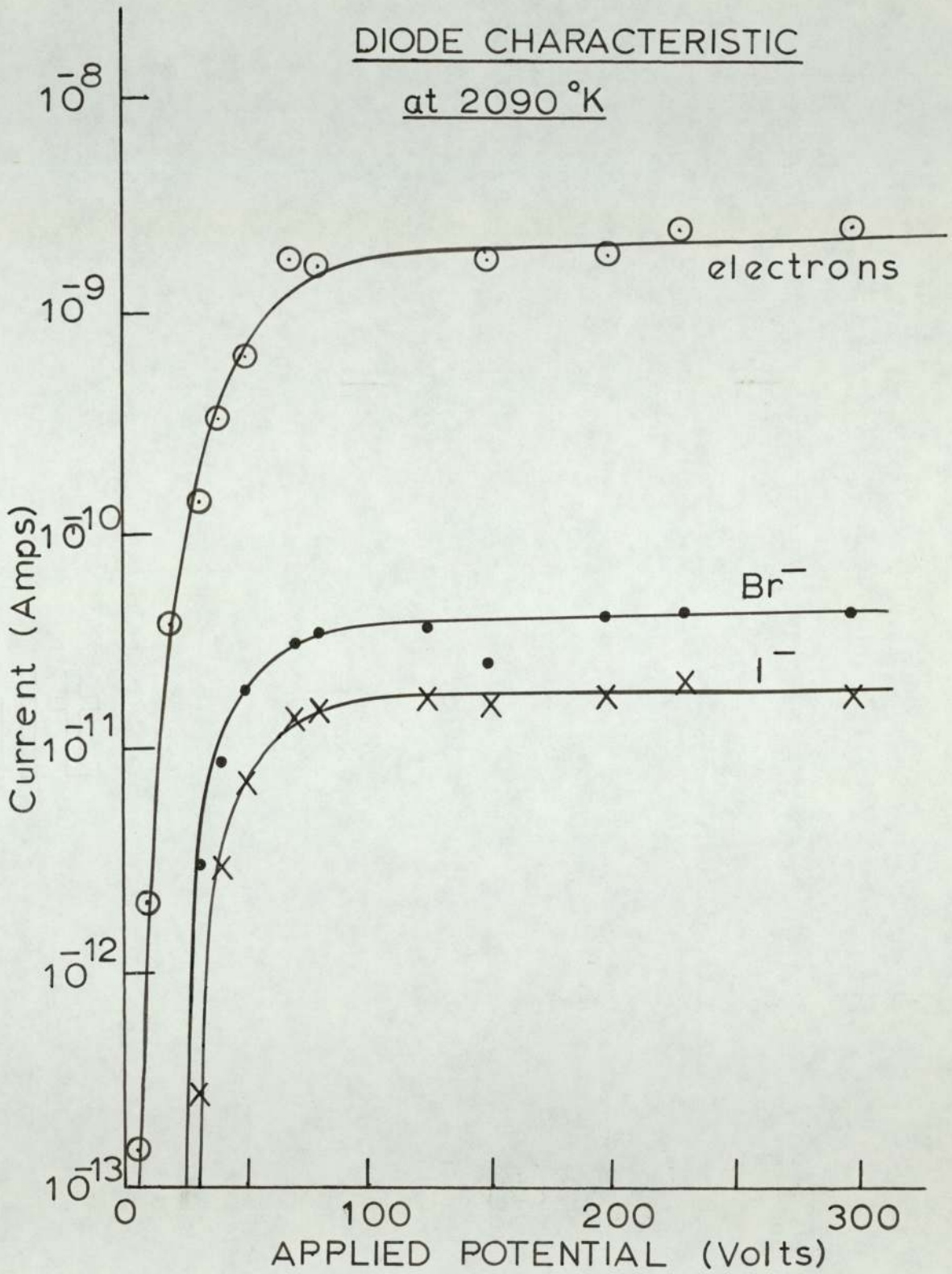
DIODE CHARACTERISTIC
at 2090 °K
electrons
Br⁻
I⁻
Current (Amps)
10⁻⁸
10⁻⁹
10⁻¹⁰
10⁻¹¹
10⁻¹²
10⁻¹³
0
100
200
300
APPLIED POTENTIAL (Volts)

FIG 14

In use, the hot cathode caused some outgassing of the glass and metal parts of the planar diode, and it was necessary to ensure that this process was carried out to completion before any measurements were made. The usual procedure adopted was to maintain the cathode above 2400°K with the anode accelerating voltage applied, for several hours, until the pressure dropped below 5×10^{-7} mm Hg. This procedure also ensured that cathode surface impurities, such as Ta_2O_5, were removed(41). After this treatment, the sample material was allowed to flow over the hot cathode, in vapour form, until measurements shewed that the system had become stable.

The measurement of the ion and electron currents at the detector may be undertaken in several different ways. Perhaps the best method would be to use a Faraday cylinder detector connected to a fast response logarithmic amplifier and to record mass spectra at various temperatures and pressures. Unfortunately, such an amplifier could not be obtained. The alternative was to obtain a mass spectrum of a given compound, using a slow, decade switched amplifier, or a fast uncalibrated decade amplifier, so that the position of every mass peak in the spectrum could be obtained. By use of the peak switching system, described previously the mass filter could then be pretuned to pass the observed

ions in sequence. In its lower ranges, the AVO amplifier had a time constant of about 30 seconds. This means that, in order to obtain an accurate measurement of a particular ion current, then that ion current must be measured continuously for a period of several minutes. It was therefore a pre-requisite to a set of measurements, that both the pressure and the temperature of the source were stable. A series of measurements could thus be obtained by setting the temperature and pressure to the approximate required values, allowing them to become stablised and then to make current measurements, for about three minutes, for each preselected mass position.

In obtaining a mass spectrum, using the automatic mass scan system of the AMP 3, it was often noticed that a long "tail" developed on the electron peak, which often extended up to about mass number 20. It was found possible to reduce this "tail" to negligible proportions by locating a small magnet near the quadrupole rods, outside the vacuum system. From Fig. 15, obtained using a large solenoid located half way along the quadrupole housing, it may be seen that the ion current is not affected by the external magnetic field, whilst the electron current is effectively reduced. The position of the magnet was found to be unimportant, provided that it was near to the quadrupole housing.

FIG 15.

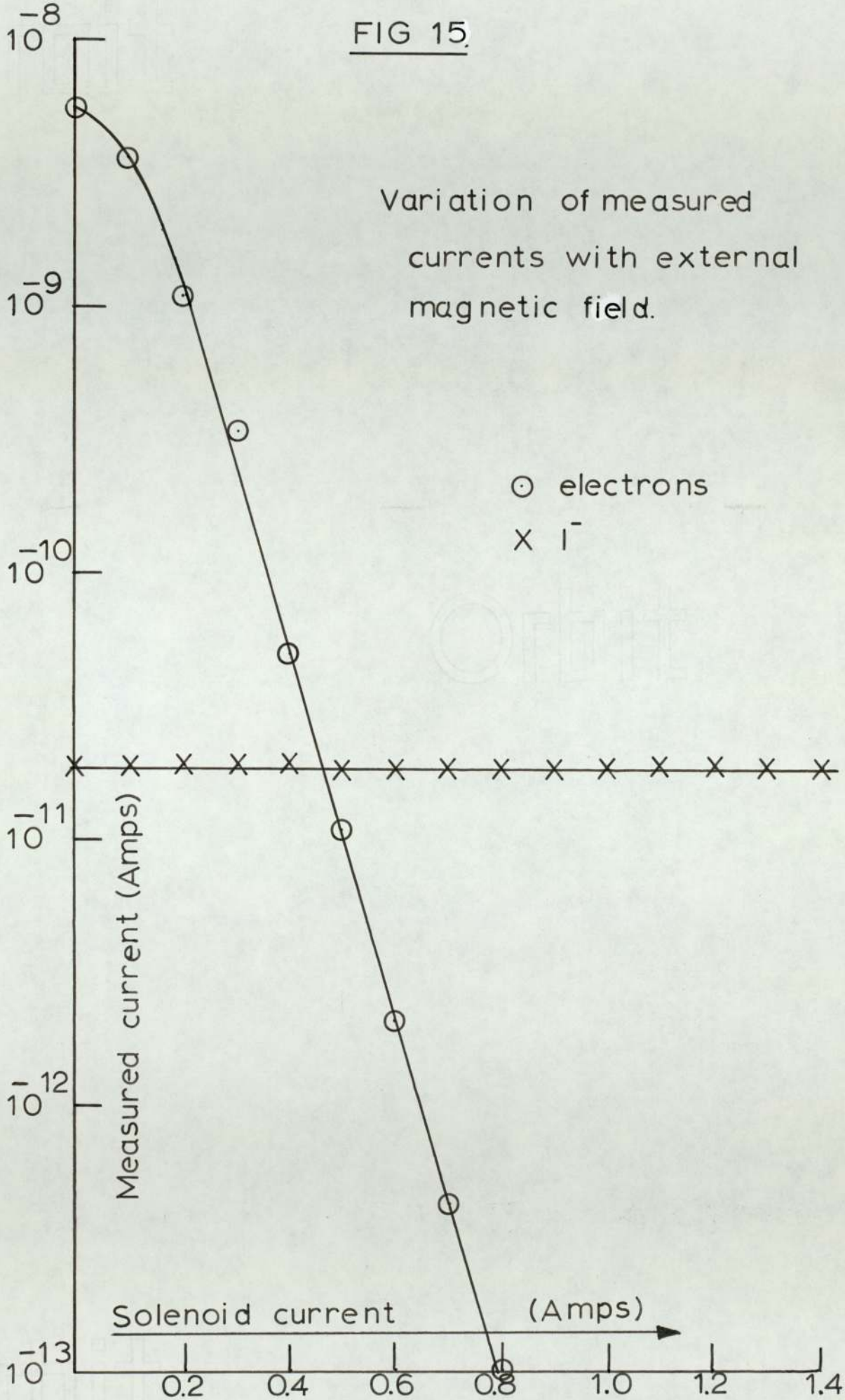
Variation of measured currents with external magnetic field.
⊙ electrons
X I⁻
10^{-8}
10^{-9}
10^{-10}
10^{-11}
10^{-12}
10^{-13}
Measured current (Amps)
Solenoid current (Amps)
0.2
0.4
0.6
0.8
1.0
1.2
1.4

5. THE ESTIMATION OF NEGATIVE ION STABILITIES USING THE QUADRUPOLE SYSTEM.

The early measurements of Mayer et al (74) were an attempt to measure directly the electron affinities of atoms derived from the dissociation of molecules at a hot metal surface. He assumed that atoms, electrons and ions were in both thermal and charge equilibrium with this surface and that it was therefore possible to compute the equilibrium constant and hence the energy change for the reaction:

$$A_{(g)} + e_{(g)} = A^-_{(g)}$$

By the use of statistical mechanics, Sutton and Meyer (74) estimated the electron affinity of the iodine atom as $302{\cdot}6 \pm 6{\cdot}3$ KJ mol^{-1}. Doty and Mayer (75) measured the electron affinity of the bromine atom, obtaining a value of $336{\cdot}5 \pm 1{\cdot}7$ kJ mol^{-1}, in good agreement with Weisblatts estimate of $334{\cdot}6$ kJ mol^{-1}, obtained using the same technique. The study of chlorine was hampered by the formation of tantalum pentachloride; however, using a silver coated apparatus, M^{c}Callum and Mayer (76) obtained a value of $358{\cdot}8 \pm 4{\cdot}2$ kJ mol^{-1}, using both chlorine gas and stannic chloride as substrates.

Bernstein and Metlay (77) obtained a value of $343{\cdot}7 \pm 16{\cdot}7$ kJ mol^{-1}, for the electron affinity of fluorine, using the magnetron technique.

These results obtained with the magnetron are in good agreement with the photodetachment studies (12) which give $347{\cdot}7$ kJ mol^{-1} for chlorine, $324{\cdot}0$ kJ mol^{-1} for bromine, $295{\cdot}1$ kJ mol^{-1} for iodine and $331{\cdot}9$ kJ mol^{-1} for fluorine.

The results obtained using the magnetron technique and interpreted by means of statistical mechanics, for oxygen (78) were found to be unsuccesful when compared to the values obtained for the electron affinity of oxygen by the spectroscopic technique (79). It is now well known that oxygen may interact with a hot tungsten filament, both to markedly raise the work function of the surface (80) and to produce WO_3^- negative ions under certain conditions (39). The manner in which the oxygen reacts with the filament will also affect the calculation of the degree of dissociation.

This failure to find suitable substrates caused interest in the magnetron method to decline until Page (81) made a further study of the halogens, using halogen hydrides as substrates.

Page noticed that the total current was inversely related to the gas pressure and interpreted this in terms

of some adsorption process which resulted in a raising of the work function of the surface. Apart from the demonstrable effect of adsorption, it may be shewn that both the ion current and the electron current are exponentially dependent on the reciprocal of the filament temperature, at constant pressure, and that the ion current is usually proportional to the pressure of gas in the magnetron. Page argued that the ratio $j_e\ p\ /\ j_i$, where j_e and j_i are the electron and ion currents, respectively, and p is the gas pressure, might be identified with some equilibrium constant, whose temperature coefficient leads to an energy term, which is the heat of some hypothetical reaction. This energy term may be identified with the overall enthalpy change between the gas-phase neutral species and the resultant negative ion.

The overall enthalpy change may be related to the electron affinity of a radical by considering the energetic process involved in chemisorption, ion formation on the surface and desorption of the negative ion, and in certain cases, desorption of uncharged fragments. A simple kinetic treatment of this process of ion formation was given by Page (81) and he deduced that:

$$j_e\ p\ /\ j_i\ =\ \text{const.} \times T^2 \exp\ (\ E'\ /\ R\ T\ )$$

where the pre-exponential constant is only slightly dependent on temperature and E' is the apparent electron affinity. Thus:

$$E' = d(\ln (j_e p / j_i)) / d(1/T) \qquad (1)$$

Page distinguished four types of mechanism of ion formation on the cathode surface, on the grounds of the energy terms which contributed to the apparent electron affinity.

i) Direct capture:-

Certain neutral species have been found to add an electron, to form a negative ion. Usually, the direct acceptor is a compound with many constituent electronegative elements, For example, sulphur hexafluoride.

$$SF_6 + e = SF_6^-$$

or containg a pi bond system, for example, tetracyanoethylene.

$$C_2(CN)_4 + e = C_2(CN)_4^-$$

Since the process of direct capture involves neither bond breaking nor adsorption of fragments, the apparent electron affinity must be equal to the true electron affinity, at the temperature of the measurement.

ii) Weak bond.

The transition between the direct capture process and a process wherein a strong bond has to be broken, is a gradual one and no sharp distinction may be made. Generally, if free radicals can capture an electron to form a negative ion, then, if the strength of the bond which has to be broken to form the free radical is less than about 290 K J mol^{-1}, the substance will behave as though it were composed of the free radical and the apparent electron affinity and the true electron affinity will be the same, at the temperature of the measurement. For example, this type of process occurs with hydrazine and dimethyl-mercury :

$$2e + N_2H_4 = 2NH_2 + 2e = 2NH_2^-$$

$$2e + Hg(CH_3)_2 = Hg + 2CH_3 + 2e = 2CH_3^- + Hg$$

iii) Strong bond.

This type of behaviour is observed when the bond energy is so high that only a small fraction of the material is dissociated at the filament temperature.

In this case, the apparent electron affinity will equal the true electron affinity minus the energy necessary to create the acceptor radicals. For example, in the case of oxygen:

$$2e + O_2 = 2O + 2e = 2O^-$$

This is a symmetrical fission of the O-O bond and:

$$E' = E_{true} - D / 2$$

where D is the dissociation energy of oxygen.

In the more general case of unsymmetrical fission, for example, carbon tetrachloride:

$$e + CCl_4 = Cl + CCl_3 + e = CCl_3 + Cl^-$$

$$E' = E_{true} - D$$

where D is the energy of the CCl_3-Cl bond.

iv) Dissociation with Adsorption.

This type of process is the most general case encountered. A bond energy term must be taken into account for the production of acceptor radicals, as in type iii) processes, together with a heat of adsorption term of

some fragment adsorbed onto the cathode. The apparent electron affinity is given as:

$$E' = E_{true} - D + Q$$

where Q is the heat of adsorption of the fragment.

Many examples may be quoted, shewing adsorption of different radicals. For example, carbon tetrachloride over platinum:

$$CCl_4 + e = CCl_3^- + Cl_{ads}$$

so $$E'_{CCl_3} = E_{CCl_3} - D + Q_{Cl/Pt}$$

where D is the bond energy of CCl_3-Cl bond.

The kinetic approach to the interpretation of results obtained from the magnetron, has allowed the estimation of the stabilities of a large number of negative ions, together with much information on the interaction of various compounds with hot metallic surfaces (17).

Farragher (82) has extended the kinetic approach by applying the theory of rate processes to the emission of ions and electrons. The extended kinetic treatment is shewn by Farragher to lead to exactly the same results as the statistical argu ments of Mayer in the simplest cases,

thus supporting Page's earlier argu ments in this respect.

The quadrupole system may be considered to be equivalent to the magnetron system in that the rate of formation of ions and electrons may be measured over a similar range of temperatures and pressures. However, the great advantage of the quadrupole system is that the identity of the charge carriers may be directly determined. As both electron and negative ion currents may be measured, it was proposed that the kinetic method of Page would be used to estimate stabiltities of various negative ions, using the quadrupole system.

The compounds chosen for initial study, over a polycrystalline tantalum cathode, were:

Iodine chloride
Iodine bromide
Cyanogen iodide
and Cyanogen bromide.

These compounds were chosen, as, apart from giving strong negative ion currents, much information is available on their thermodynamic properties (83) and therefore interpretation of the results should be clear.

Negative ion mass spectra were obtained in the temperature range 1250 - 2200^{o}K, for each compound.

Table 1 shews the ions detected. At the higher temperatures, the ion currents were about 1×10^{-9} Amps and as the detection limit was 1×10^{-14} Amps, any other ions which may have been produced must have an intensity of less than 10^{-5} that of the observed ions.

The dependence of the negative ion currents with gas pressure, at constant temperature, for these compounds, are discussed in the following section.

5·1 THE PRESSURE DEPENDENCE OF THE ION CURRENTS.

The variation of the total ion current with pressure, at constant temperature, in the magnetron, may in many cases, be divided into two portions. The high pressure portion, usually extending from 5×10^{-4} to 10^{-2} mm Hg., is characterised by the total ion current remaining constant with changes in the pressure. The low pressure portion, usually 1×10^{-6} to 5×10^{-4} mm Hg., is often linear, for simple compounds. The ion current, I_i, in this region, may be related to the pressure, p, at constant temperature, by an expression (17):

$$\log I_i = x \log p + \text{const.}$$

where x is an experimental constant.

In the presence of the vapour of bromine, iodine chloride iodine, bromide or cyanogen bromide, the variation

TABLE 1

Compound.	Ions observed.
Iodine chloride	I^- , Cl^-
Iodine bromide	I^- , Br^-
Cyanogen bromide	Br^-, CN^-
Cyanogen iodide	I^- , CN^-

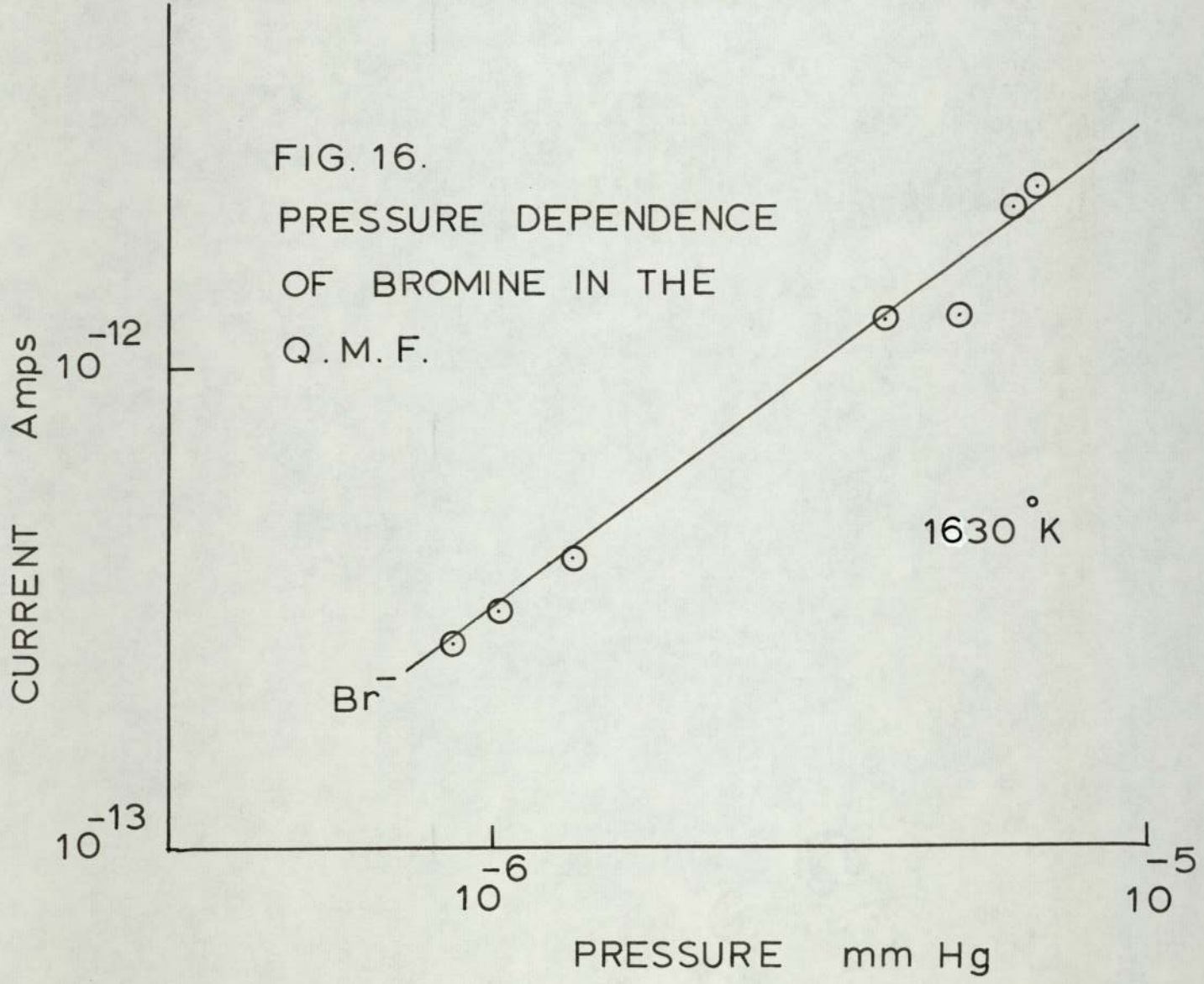
FIG. 16.
PRESSURE DEPENDENCE
OF BROMINE IN THE
Q.M.F.
1630 °K
Br⁻
CURRENT Amps
10⁻¹²
10⁻¹³
10⁻⁶
10⁻⁵
PRESSURE mm Hg

FIG 17.

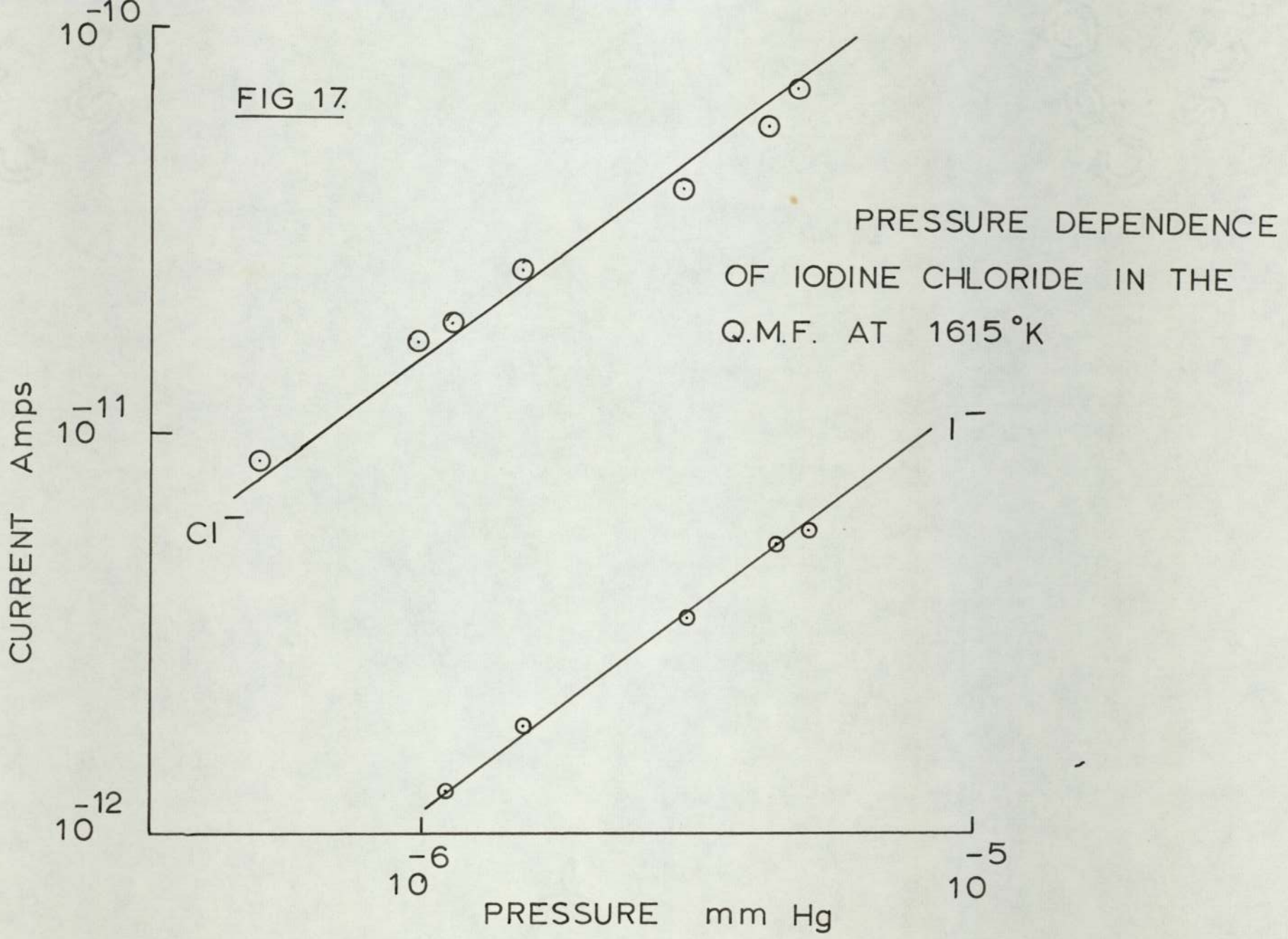
PRESSURE DEPENDENCE
OF IODINE CHLORIDE IN THE
Q.M.F. AT 1615 °K
CURRENT Amps
10^{-10}
10^{-11}
10^{-12}
Cl^-
I^-
10^{-6}
10^{-5}
PRESSURE mm Hg

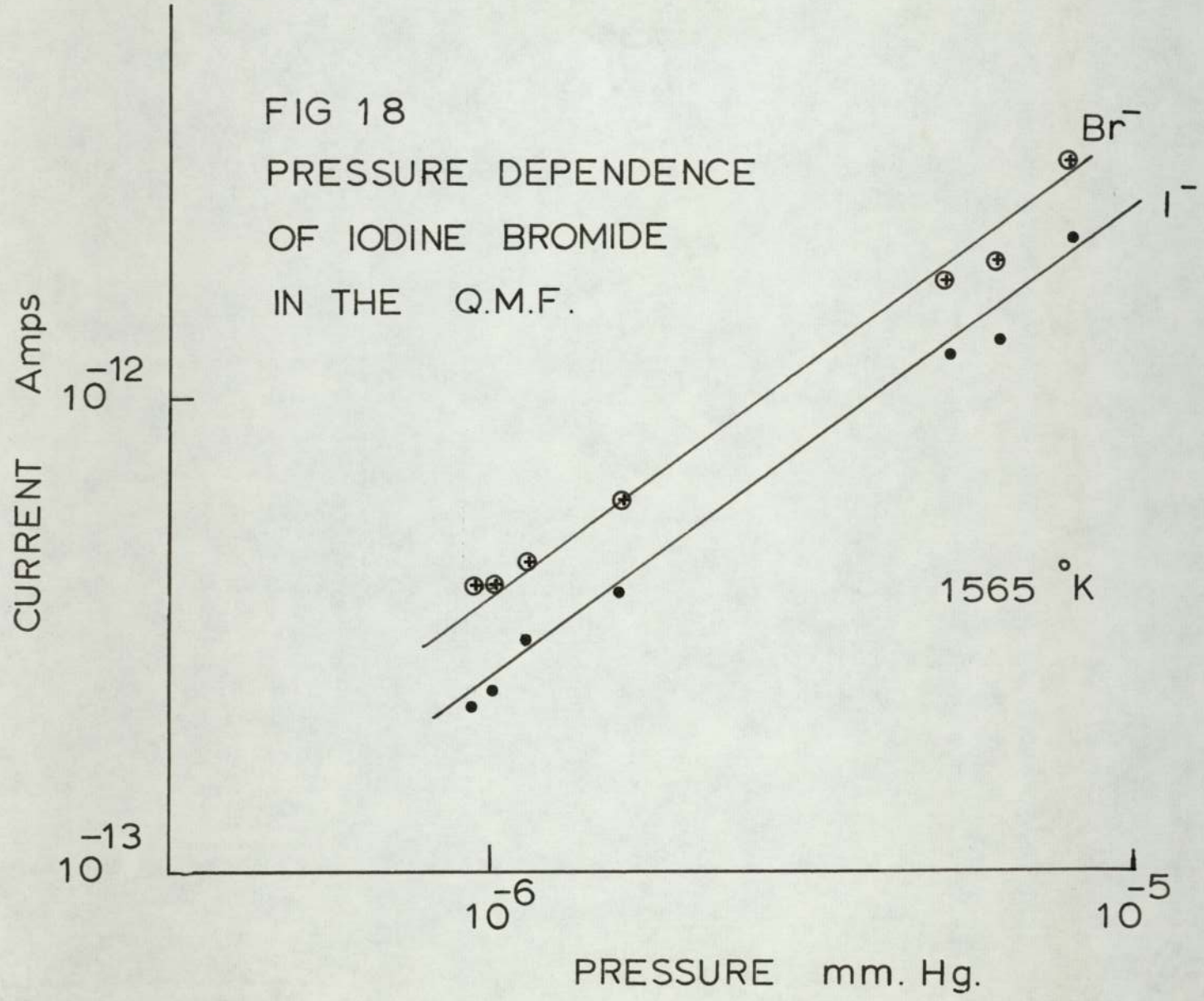
FIG 18
PRESSURE DEPENDENCE
OF IODINE BROMIDE
IN THE Q.M.F.
Br⁻
I⁻
1565 °K
CURRENT Amps
10⁻¹²
10⁻¹³
10⁻⁶
10⁻⁵
PRESSURE mm. Hg.

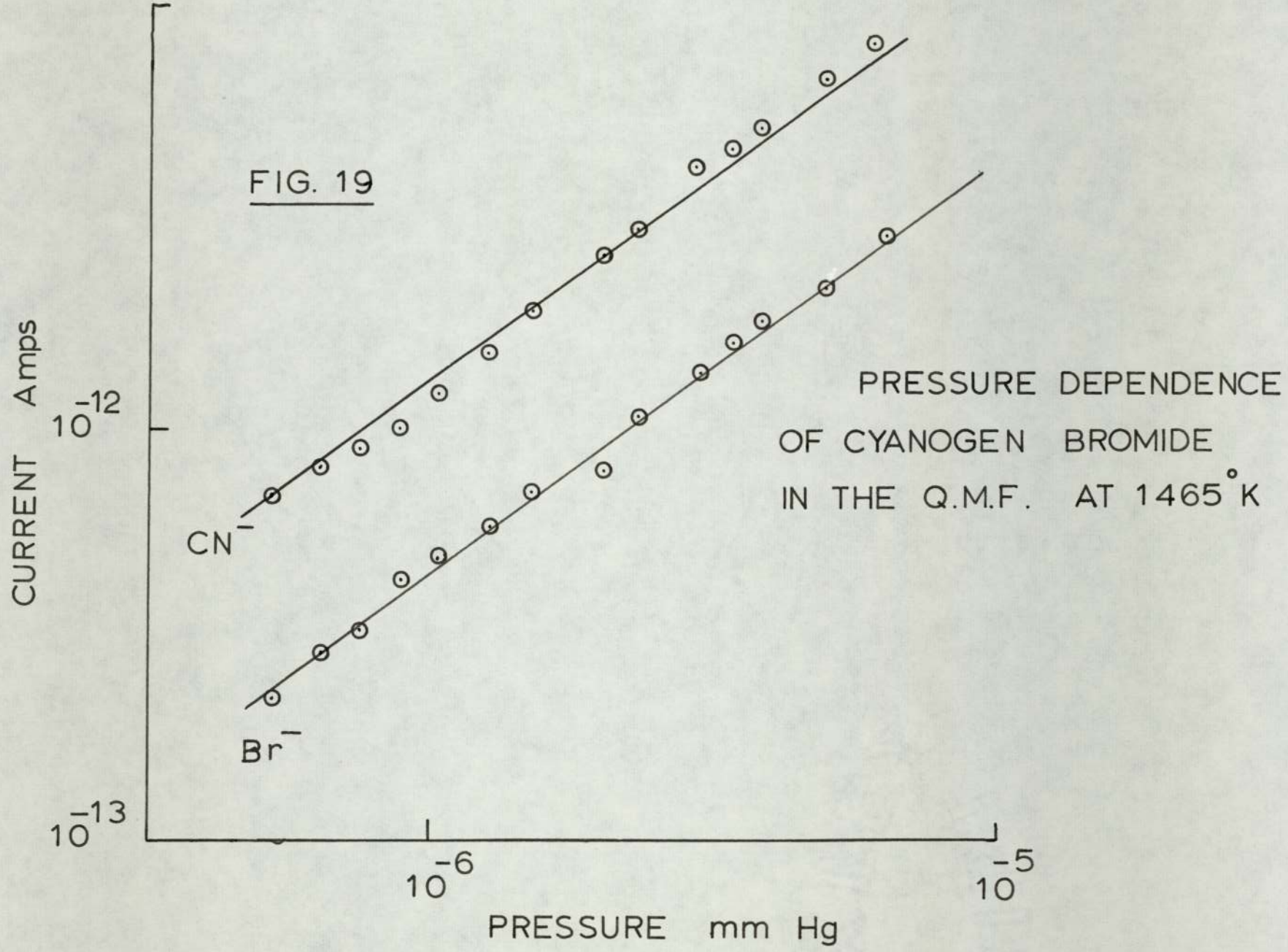
FIG. 19
CURRENT Amps
10^{-12}
10^{-13}
CN^-
Br^-
10^{-6}
10^{-5}
PRESSURE mm Hg
PRESSURE DEPENDENCE
OF CYANOGEN BROMIDE
IN THE Q.M.F. AT 1465°K

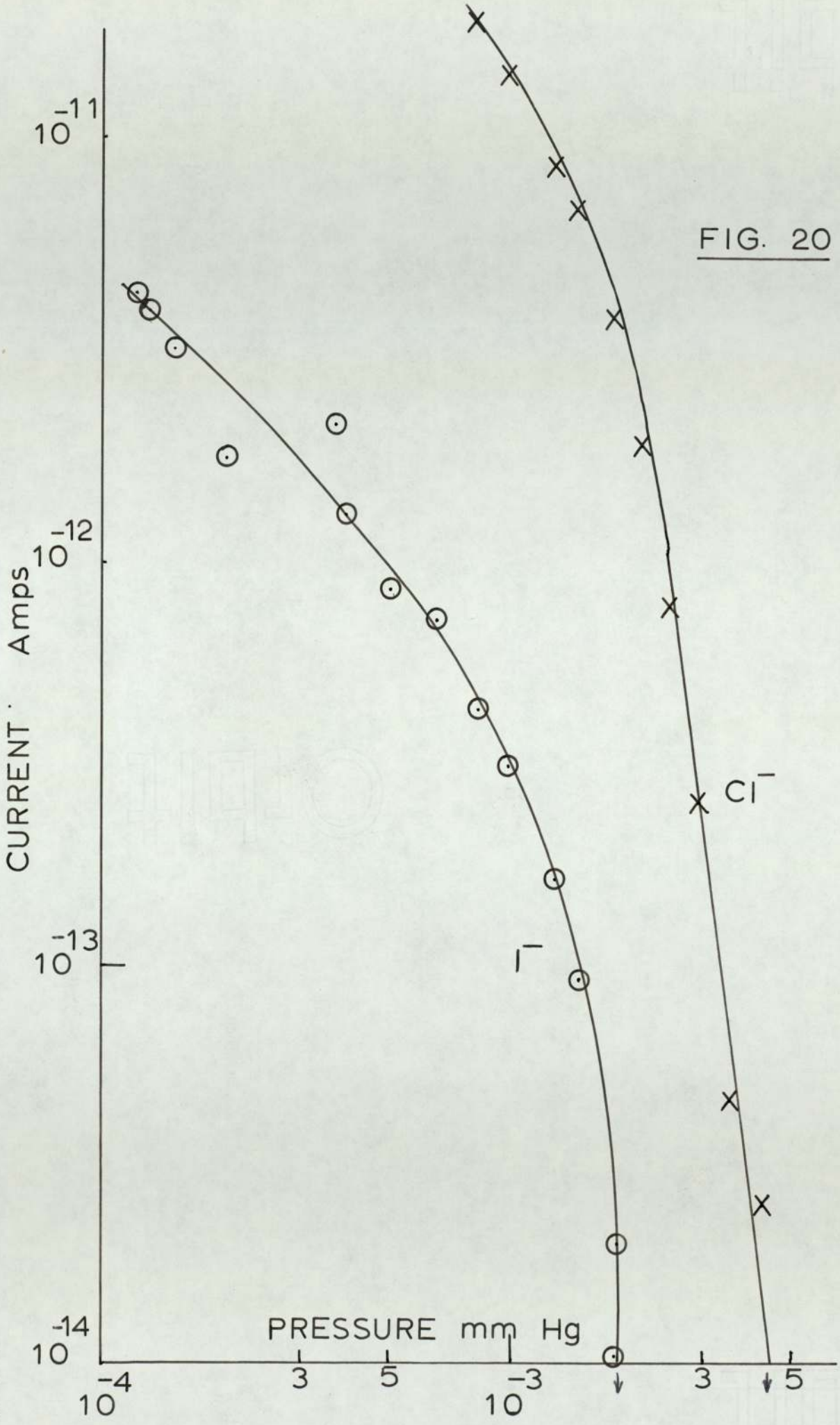
FIG. 20
CURRENT Amps
10^{-11}
10^{-12}
10^{-13}
10^{-14}
I^-
Cl^-
PRESSURE mm Hg
10^{-4}
3
5
10^{-3}
3
5

of the individual ion currents with pressure, at constant temperature, over the range 1×10^{-6} to 5×10^{-5} mm Hg., were obtained from the quadrupole system, and are shewn in Figs. 16 to 19. The source and the analyser regions were pumped differentially and a Penning discharge gauge, located in the source region, recorded the pressure. Each interhalogen gave rise to two negative ion currents and in each case, a plot of log I_i versus log p , at constant temperature, was linear and of unit slope. Plots of this type, indicate that the rate determining step of the negative ion formation process is first order with respect to the parent gas phase molecule concentration.

Using the quadrupole system, it was found that, when the source region and the analyser were differentially pumped, the measurement of the variation of the individual ion currents with pressure, at constant temperature, was difficult above pressures of 5×10^{-5} mm Hg., as the ion currents became erratic. However, by closing off one pump, the ion currents became steady and measurements could be made over the range 5×10^{-5} to 5×10^{-3} mm Hg. The pump that was usually closed off was that which pumped the analyser section. Measurements of the ion current were made about ten minutes after a change in pressure, to allow the pressure in each region to equalise.

Iodine chloride, the only compound to be examined in the quadrupole system in the range 5×10^{-5} to 5×10^{-3} mm Hg., gave plots of log I_{I^-} versus log p , and log I_{Cl^-} versus log p, at constant temperature, which were entirely unexpected. The pressure was measured by a Baratron diaphragm gauge and the plots are shewn in Fig. 20, and were very reproducible. The unusual nature of these plots suggested that further information was required and so the variation of the total current with pressure, at constant temperature, from iodine chloride, iodine bromide and bromine, were obtained, using the magnetron technique. These are shewn in Figs. 21, 22 and 23. The plots of log (total ion current) versus log pressure, at constant temperature, shew a direct dependence below about 5×10^{-4} mm Hg., and a constant ion current at higher pressures. Clearly, the processes occuring in both the magnetron and the quadrupole systems at low pressures, are the same.

The fact that, at high pressures, positive currents are observed, using the quadrupole system to obtain plots of log I_i versus log p, at constant temperature, indicates that some other ionisation process may be occuring. Secondary electron emission from the Faraday cylinder was discounted, as a bar magnet placed near to the cylinder produced no change in the observed currents.

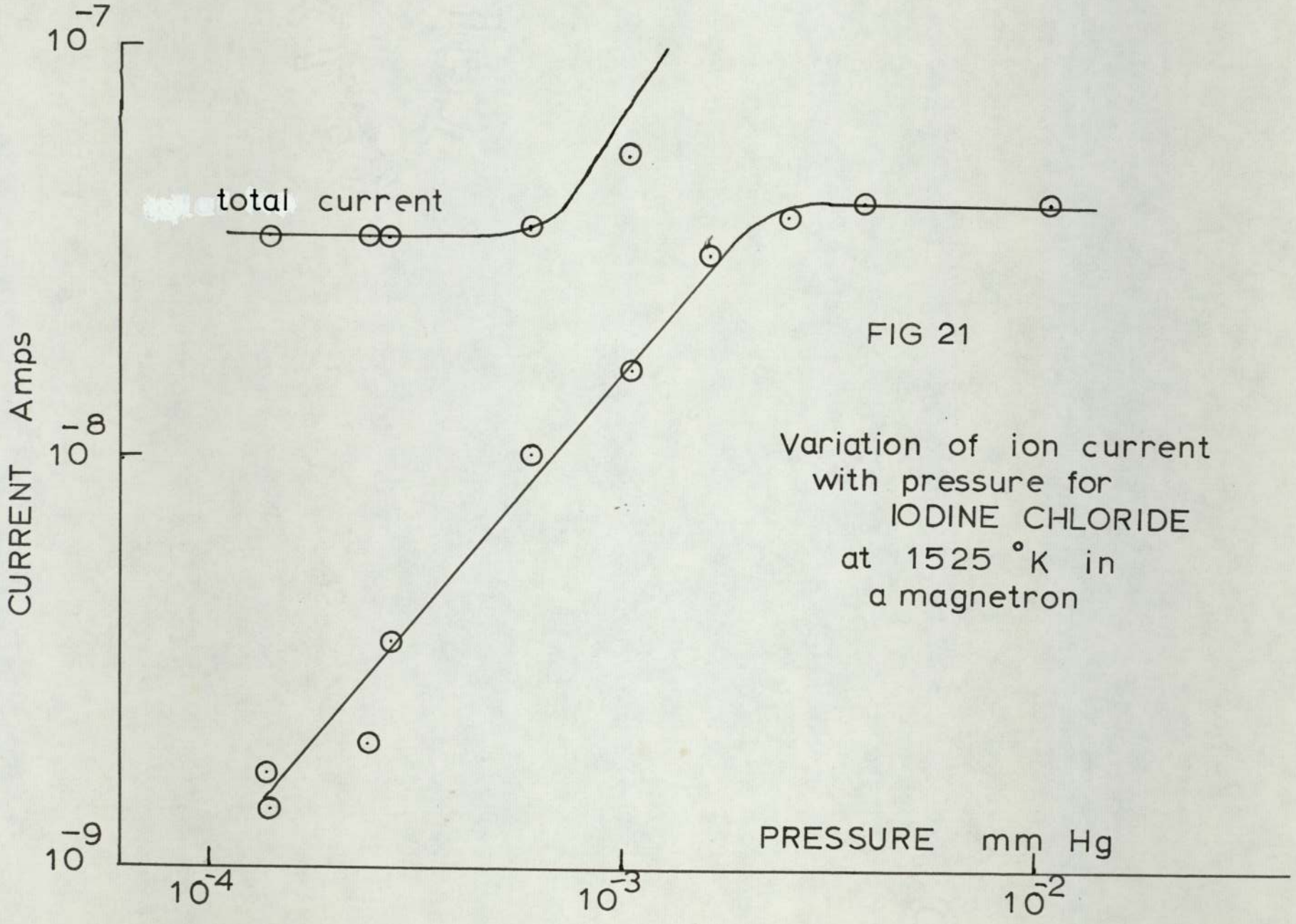

FIG 21

Variation of ion current with pressure for IODINE CHLORIDE at 1525 °K in a magnetron

FIG 22.

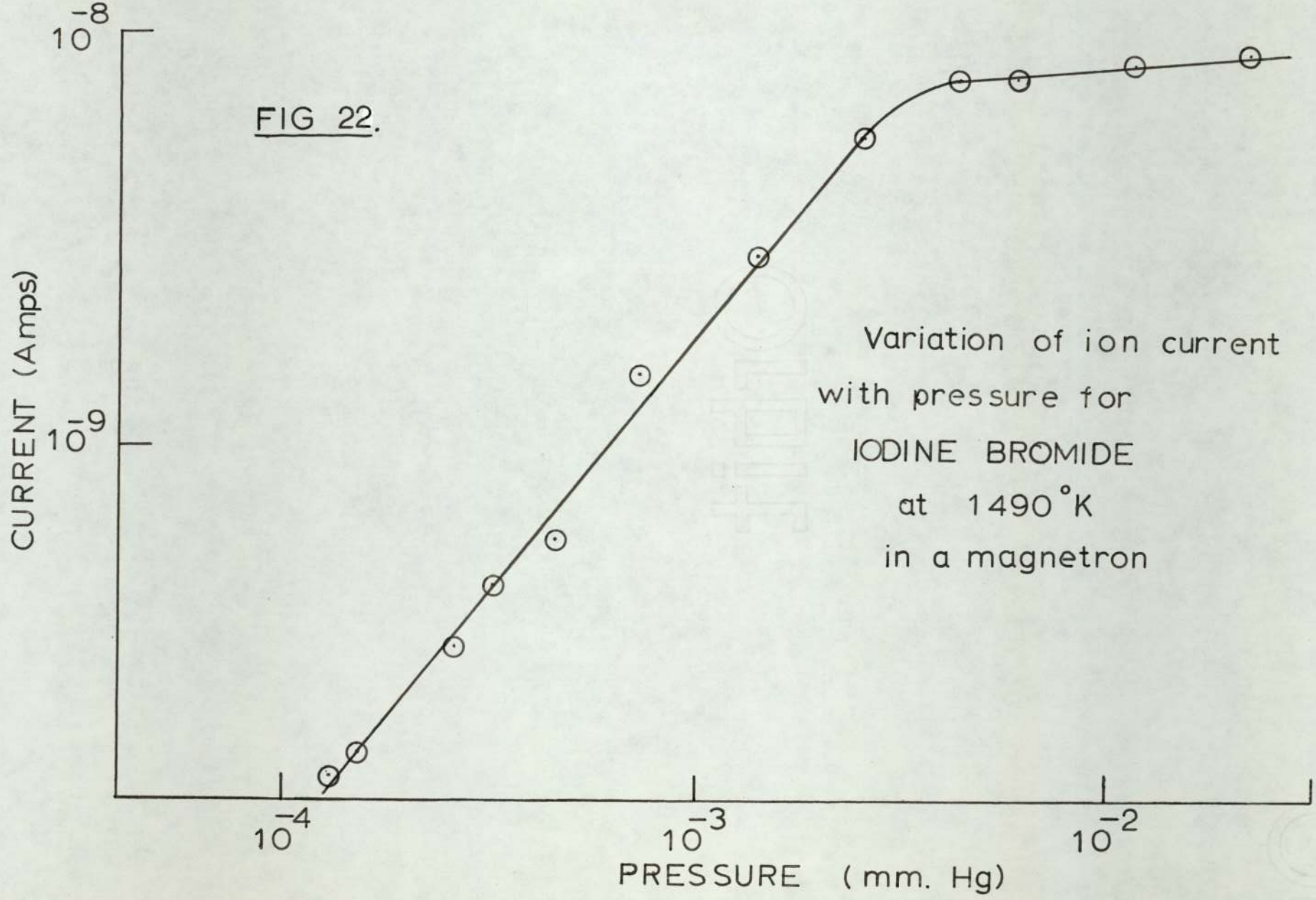
10^{-8}
10^{-9}
CURRENT (Amps)
10^{-4}
10^{-3}
10^{-2}
PRESSURE (mm. Hg)
Variation of ion current
with pressure for
IODINE BROMIDE
at 1490°K
in a magnetron

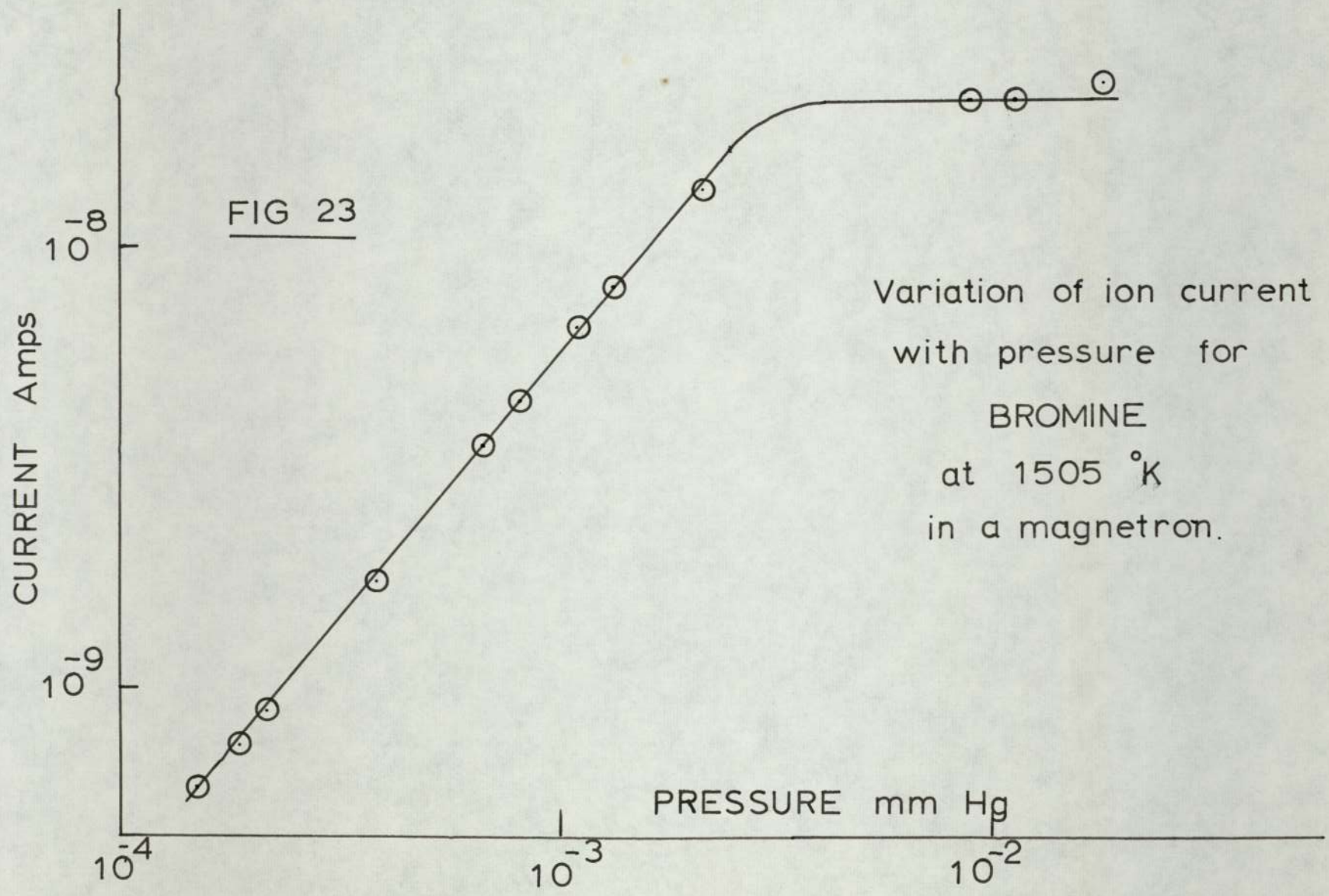
FIG 23
Variation of ion current with pressure for BROMINE at 1505 °K in a magnetron.
CURRENT Amps
10^{-8}
10^{-9}
PRESSURE mm Hg
10^{-4}
10^{-3}
10^{-2}

Consideration of the various ionisation processes which might occur, suggested that gas phase positive ionisation by electron or negative ion impact, was most likely. The magnetron and the quadrupole systems were therefore carefully considered, in order that, should gas phase positive ion formation be occurring, its effect on the measured ion currents might be calculated.

In the magnetron, if a positive ion is formed in the gas between the cathode and the anode, then the electrons resulting from the collision:

$$M + e = M^{+} + 2e.$$

will be accelerated towards the anode, whilst the positive ion will be accelerated towards the cathode; a simple electrical charge balance shews that for every positive ion formed, two electrons will flow from the anode to the cathode via the external galvanometer circuit, provided that the grids do not capture any charges. In other words, a "negative" current flows in the external circuit for both negative surface ionisation processes and gas phase detachment processes. However, the path length in the magnetron is small, and it was shewn in chapter 3, that, provided the pressure is less than about 10^{-4} mm Hg gas phase processes have a negligible contribution to the measured currents.

In the mass filter, a positive ion produced by the collision of a gas molecule with an electron or negative ion, will not be acted upon by any AXIAL electric field, analogous to the radial field of the magnetron. However, the RADIAL fields of the mass filter will act in a manner analogous to negative ions. In the collision, a transfer of momentum would ensure the positive ion drifting towards the detector.

In general, the positive ion would be formed some distance from the entrance apertureof the mass filter; thus the positive ion would not be greatly resolved relative to a negative ion which had traversed the entire length of the field. This point is exemplified in the following chapter, where it is shewn that positive ion fragments could cause "positive" peaks in a negative ion mass spectrum.

The strong focussing action of the quadrupole field (84) ensures that a large proportion of positive ions formed would traverse the field and be detected, provided that the ion was stable in the quadrupole field. This type of process would only be of importance, however, at very high pressures or very long path lengths. The following calculations provide an estimate of the path length of various ions in the mass filter.

The number of cycles, n , which an ion performs in the quadrupole field may be calculated as follows:

In the planar diode source, ions of mass, m , fall through a potential of E volts, to gain a velocity, v. Now:

$$e E = \tfrac{1}{2} m v^2$$

or $$v = (2 e E / m)^{\frac{1}{2}}$$

Hence;

$$n = L f (m / 2 e E)^{\frac{1}{2}}$$

where L is the length and f is the frequency, of the quadrupole field.

Setting

$L = 0{\cdot}2$ m

$f = 3{\cdot}0$ MHz.

$E = 250$ volts.

It may be calculated that:

Electrons perform 0·65 cycles in the field.

Chlorine ions " 16·2 " " " "

Iodine " " 30·9 " " " "

Numerical integration of the equations of motion of an ion in the quadrupole field, under given entry conditions enable the trajectories of the ions to be calculated (85). However, a given ion performs a variety of trajectories, depending on the phase angle of the field as the ion enters. Thus an accurate value for the path length is difficult to calculate.

An estimate of the path length of an ion in the quadrupole field may be made by considering the trajectory of a stable ion to approximate to a regular triangular wave. It may easily be shewn that the length of such a wave, C , characterised by an amplitude, A , and a wavelength D , for a single cycle, is given by:

$$C = 4(A^2 + D^2/16)^{\frac{1}{2}}$$

The path length, S , through the field for a stable ion, will thus be:

$$S = 4 n (A^2 + D^2/16)^{\frac{1}{2}}$$

but $$D = L / n$$

therefore $$S = 4 n (A^2 + L^2/16 n^2)^{\frac{1}{2}}$$

The amplitude of any stable ion trajectory cannot exceed r_o, the distance between the axis of the quadrupole field and the nearest electrode. Brubaker (86) has shewn that ions having excursions in excess of 70% of r_o are lost in an experimental system.

In the AMP 3 quadrupole, r_o has the value 0·0069 m. Thus setting A = 0·0048 m and L = 0·2 m, it may be calculated that:

Stable electrons have a path length of 0·2 m

" chlorine ions " " " " " 0·37 m

" iodine ions " " " " " 0·65 m

Unstable ions and electrons will also be present within the quadrupole field, near to the entrance aperture. There is no method for estimating the path lengths for unstable species, however, it is assumed that they are of the order of 10^{-2} that of the stable species path length.

Using these estimates of the path lengths of ions traversing the mass filter, the number of positive ions, I_+, resulting from collisions in the mass filter, may now be calculated.

The number of positive ions, derived from gas phase impact ionisation processes, in general, is given by:

$$I_+ = I_- \; Q \; N \; l$$

where I_- is the number of bombarding ions, Q is the cross section for ionisation, N is the number of gas molecules per unit volume and l is the path length.

Thus, in the mass filter:

$$I_+ = I_e \, Q_e \, N \, l_e + I_u \, Q_u \, N \, l_u + I_s \, Q_s \, N \, l_s$$

where the subscripts refer to unstable electrons, unstable ions and stable ions, respectively.

It may be seen from Fig. 21, that at these pressures, the magnitudes of the ion currents are similar to that of the electron current. Therefore:

$$I_e = I_u = I_s$$

No data are available for the cross section for ionisation of iodine chloride by negative ions. However, the ionisation cross section of Xenon, for 500 volt electrons is $2{\cdot}65 \times 10^{-16}$ cm^2 (32). Hence, assuming that the cross section for ionisation for electrons and negative ions at 250 volts is about 3×10^{-16} cm^2:

$$Q_e = Q_u = Q_s$$

As

$$I_e = I_u < I_s$$

The approximate number of positive ions will therefore be given by:

$$I_+ = I_s Q_s N I_s$$

Thus it may be seen that the positive ion current depends mainly on the stable negative ion current.

The positive ions once formed, would move towards the detector, due to the momentum transferred during the collision. Thus the Faraday cylinder will collect both positive and negative ions. When an equal number of negative and positive ions reach the cylinder, no current will flow in the external circuit. The pressure, P_c at which this occurs may now be calculated:

At 20°C,

$$I_+ = I_s \times 3{\cdot}535 \times 10^{-16} \times P_c \times 273/293 \times Q_s \times l_s.$$

For Cl^-,

$$P_c^{Cl^-} = 293 / (273 \times 3 \times 10^{-16} \times 3{\cdot}535 \times 10^{16} \times 37)$$
$$= 2{\cdot}7 \times 10^{-3} \text{ mm Hg.}$$

For I^-,

$$P_c^{I^-} = 293 / (273 \times 3 \times 10^{-16} \times 3{\cdot}535 \times 10^{16} \times 65)$$
$$= 1{\cdot}1 \times 10^{-3} \text{ mm Hg.}$$

It may be seen from Fig 20 that the values for the calculated pressure at which cross-over is assumed to occur, corresponds to the pressure at which cross-over from positive to negative currents is observed to take place, bearing in mind the approximate nature of the calculation.

This is taken to indicate that, in the case of iodine chloride, at pressures higher than 5×10^{-5} mm Hg.,

the variation of the individual ion currents with pressure, at constant temperature, may be explained as a result of gas phase ionisation processes occuring within the mass filter section.

It follows from these results that other compounds would behave in a similar fashion. Thus, to eliminate such effects, studies of the emission of negative ions from hot surfaces should be carried out in the quadrupole system at pressures of 5×10^{-5} mm Hg., or less.

5·2 THE TEMPERATURE DEPENDENCE OF THE ION CURRENTS.

The variation of the two ion currents and the electron current, with temperature, at constant pressure of 1×10^{-5} mm Hg., was studied for each of the compounds using the quadrupole system.

The measurements were straightforward in the case of iodine bromide. The results from iodine chloride tended to be more difficult to obtain due, apparently, to two mechanisms giving rise to the chlorine ions; this is discussed later. In the case of cyanogen bromide, very erratic results were initially obtained. Both the electron and ion currents apparently changed sign from negative to positive and back to negative, in a few seconds.

This behaviour was found over the whole temperature range. The erratic nature of the currents did not alter even after allowing the cathode to be heated to about 1900°K in the presence of the vapour for over 25 hours. It was found, however, that if a bar magnet was placed near the Faraday cylinder detector, the currents became steady, with negative values. Examination of the Faraday cylinder, which was of copper construction, shewed that a light green deposit had formed over its entire surface. A gold plated Faraday cylinder was substituted and it was found that the currents were steady in the absence of the bar magnet. It is assumed from this that, under bombardment of ions and electrons, the light green surface coating of the Faraday cylinder emitted large numbers of secondary electrons, thus causing the apparent reversal of sign of the measured currents.

Cyanogen iodide was studied using a stainless steel Faraday cylinder at an early stage in the development of the apparatus and unfortunately, only one run was performed.

The kinetic approach of Page, discussed earlier, enabled the apparent electron affinity, E', to be evaluated.

Page shewed:

$$E' / R = d (\log (j_e p / j_i)) / d (1/T)$$

where p is the pressure of the gas, j_e and j_i are the electron current and ion current, respectively and T is the cathode temperature. R is the gas constant. At constant pressure:

$$E' / R = d (\log_e j_e) / d (1/T) - d (\log_e j_i) / d (1/T)$$

Table 2 shews the values of $R.d (\ln j_e) / d (1/T)$ and $R \cdot d (\ln j_i) / d (1/T)$ obtained for iodine bromide in the quadrupole system.

The bond energy of iodine bromide is 177·6 kJ mol^{-1} and hence, using Pagès criteria for type of ion formation, the apparent electron affinity, E', is expected to be equal, for iodine and bromine, to the true electron affinity at the temperature of the measurement. Page has also shewn that, in this type of process, the true electron affinity at $0^{\circ}K$ may be obtained by taking a factor of 2RT from the apparent electron affinity value.

It may be seen from table 2 that the values of the apparent electron affinities for iodine and bromine are not in agreement with the literature values and that correction to $0^{\circ}K$ increases the discrepancy.

There may be several reasons for this; the most likely appeared to be that the measured currents were not

TABLE 2

IODINE BROMIDE

Number of runs = 9

The values in this Table are expressed in kJ mol^{-1}.

$d(\ln j_e)/d(1/T)$	$d(\ln j_I-)/d(1/T)$	$d(\ln j_{Br}-)/d(1/T)$	E'_I-	$E'_{Br}-$
--485·0	- 241·0	- 228·2	- 244·0	- 256·8
- 542·0	- 245·8	- 219·6	- 296·2	- 322·4
- 522·6	- 240·6	- 220·0	- 282·0	- 302·6
- 542·0	- 239·6	- 220·8	- 302·4	- 321·2
- 510·0	- 244·6	- 209·4	- 265·4	- 300·6
- 491·4	- 214·0	- 206·6	- 277·4	- 284·8
- 536·0	- 235·6	- 207·4	- 300·4	- 328·6
- 542·4	- 245·8	- 230·8	- 296·6	- 311·6
- 511·4	- 235·0	- 201·8	- 276·4	- 309·6
		Mean =	- 279·8	- 301·8
		Std. Dev. =	19·6	19·6

directly proportional to the emission currents. There was no reliable way in which this could be ascertained for negative ions. The measured electron current could, however, be compared to the electron current emitted from the cathode, as described below.

Transmission of electrons through the Mass Filter.

When the pressure was reduced to less than 5×10^{-7} mm Hg in both the source and the analyser regions, the number of negative ions passing into the mass filter was negligible, compared to the electron current. At a given temperature, with the mass filter tuned to pass only electrons, the electron current arriving at the Faraday cylinder could be measured, j_{far}. The electron current passing into the mass filter at this temperature could be estimated by disconnecting the quadrupole rods from the rf generator and instead, connecting them to a galvanometer. A bar magnet, placed near to the rods, enabled the electrons entering the mass filter to be deflected into the rods, giving j_{rod}. Measurements were carried out at several temperatures.

Suppose that the measured current was related to the emission current by an equation:

$$j_{rod} = A \times j_{far} \times \exp (B / R T)$$

where A and B are experimental constants.

Fig. 24 shews a plot of log (j_{rod} / j_{far}) versus 10^4 / T. A straight line is obtained, but deviation occurs at high measured currents. From the straight portion, B may be evaluated as about 80 kJ mol^{-1}.

The deviation from a linear behaviour may be accounted for by the presence of a space charge within the quadrupole field. Dawson and Whetten (60) have calculated the maximum ion current which may pass through a quadrupole field. From their results, the maximum electron current expected to pass through the mass filter is about 5×10^{-8} Amps. Deviation occurs at measured currents higher than $1{\cdot}5 \times 10^{-8}$ amps, which is in agreement with the expected value.

The Difference Method for determining Electron Affinities.

It was apparent, therefore, that the measured electron currents were in error and that the apparent electron affinities, evaluated by measuring the electron and ion currents as a function of temperature and pressure, would be incorrect.

However, if two species, A and B, were ionising on the cathode surface simultaneously, having been derived from a common precursor, it may be written:

$$j_{eA}\, p_A / j_{iA} = C_A\, T^2 \exp (E'_A / R\, T)$$

$$j_{eB}\, p_B / j_{iB} = C_B\, T^2 \exp (E'_B / R\, T)$$

At any temperature:

$$j_{eA} = j_{eB}$$

and $$p_A = p_B$$

Thus:

$$C_A\, T^2\, j_{iA} \exp (E'_A / R\, T) = C_B\, T^2\, j_{iB} \exp (E'_B / R\, T)$$

or

$$j_{iA} / j_{iB} = C' \exp (E'_A - E'_B / R\, T)$$

Hence, taking logs and differentiating with respect to $1/T$:

$$d (\ln (j_{iA}/j_{iB})) / d (1/T) = (E'_A - E'_B / R)$$

or

$$d (\ln j_{iA}) / d (1/T) - d (\ln j_{iB}) / d (1/T)$$

$$= (E'_A - E'_B / R)$$

TRANSMISSION CHARACTERISTIC PLOT

FIG. 24

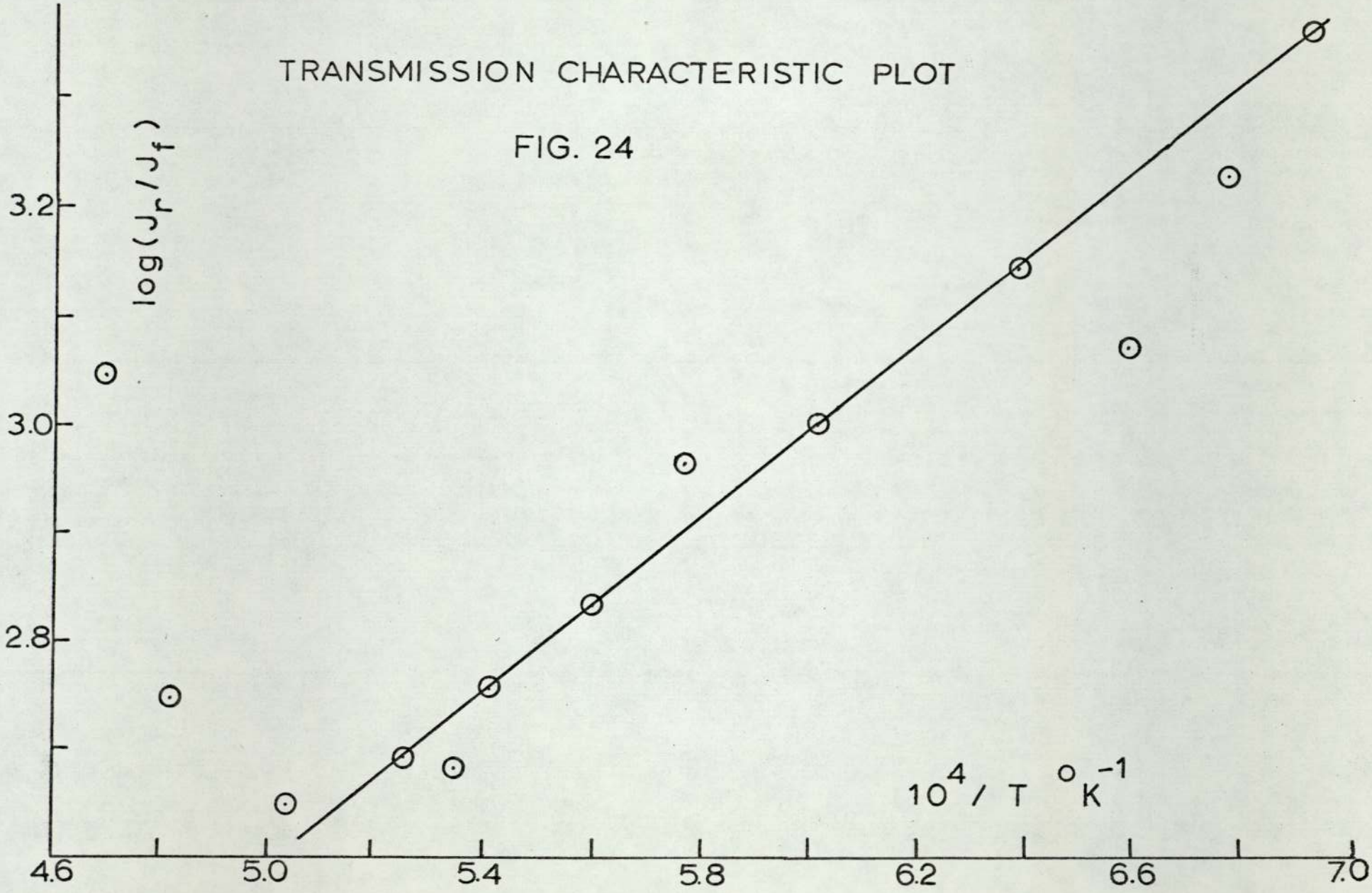

Thus, in the quadrupole system, provided that the negative ions of A and B pass through the mass filter with the same transmission dependence, the values of the difference in their electron affinities may be evaluated.

A typical plot of log Br^- versus $10^4 / T$ and log I^- versus $10^4 / T$ is shewn in Fig. 25 , derived from iodine bromide. Least squares determinations of $R\, d(\log j_i) / d(1/T)$ were carried out and the results are shewn in table 2. From this table, the difference in the apparent electron affinities and therefore, the true electron affinity difference, of bromine and iodine, was evaluated as:

$$E_{Br} - E_I = + 22{\cdot}2 \text{ kJ mol}^{-1}$$

$$\text{Standard Deviation} = 8{\cdot}8 \text{ kJ mol}^{-1}.$$

From Meyers results, $E_{Br} - E_I = + 33{\cdot}9 \pm 7{\cdot}9$ kJ mol^{-1}, and from Berrys results, $E_{Br} - E_I = + 28{\cdot}8$ kJ mol^{-1}. Bailey (58) found that $E_{Br} - E_I = + 32{\cdot}1 \pm 0{\cdot}8$ kJ mol^{-1}. Therefore, the measured value of $E_{Br} - E_I$ was in good agreement with the literature values, giving support to the assumption that the transmission dependencies of each negative ion through the mass filter were equal.

Tables 3 and 4 give the values of $d(\log j_i) / d(1/T)$ for cyanogen iodide and cyanogen bromide, respectively. These values were obtained by a least squares treatment of the experimental plots. Typical plots are shewn in Fig. 26 and Fig. 27.

The difference in the electron affinities of bromine and cyanide was found to be + 35·1 kJ mol^{-1} with a standard deviation of 13·8 kJ mol^{-1}. For the difference between iodine and cyanide ($E_I - E_{CN}$) a value of - 13·0 kJ mol^{-1} was obtained. As only one run was performed, the error was estimated from Fig. 26 to be $\pm$ 25 kJ mol^{-1}.

Page (87) has evaluated the stability of cyanide to be 305·2 $\pm$ 4·2 kJ mol^{-1}. With Mayers values of the electron affinity of bromine and iodine, the values of $E_I - E_{CN}$ and $E_{Br} - E_{CN}$ were calculated as - 2·5 $\pm$ 10·5 kJ mol^{-1} and + 31·4 $\pm$ 5·9 kJ mol^{-1}, respectively.

Again, it may be seen that there is good agreement between the experimental determinations and the literature values.

In the case of iodine chloride, the results obtained were complex. A typical plot of log ion currents versus $10^4 / T$ is shewn in Fig 28. It may be seen that the iodine negative ion current behaves as expected, that is, linear over the whole range. However, the chlorine negative ion currents shew two linear portions, the change over occuring

FIG. 25.

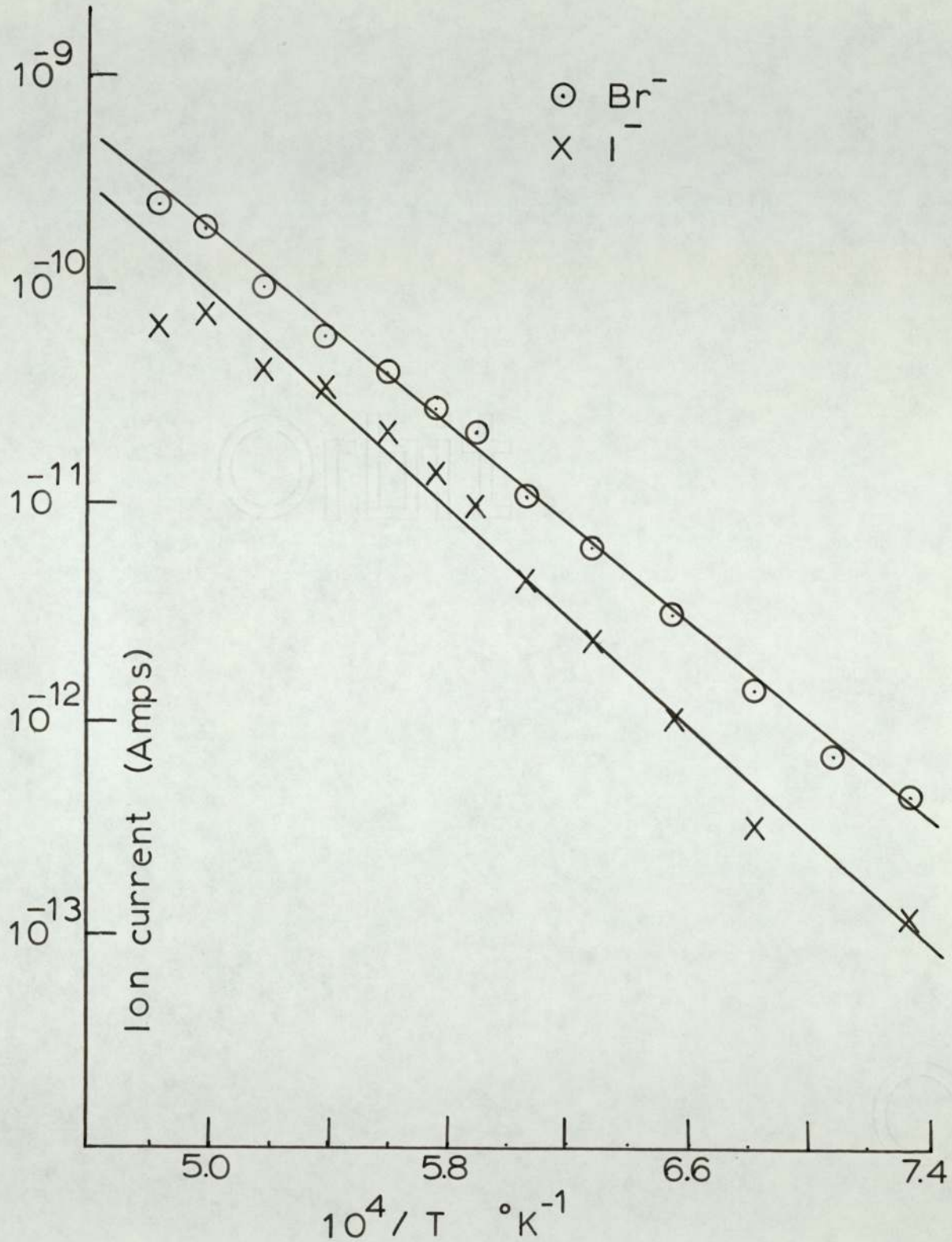

Variation of ion currents with 1/temp.
for IODINE BROMIDE.
at 1×10^{-5} mm. Hg.

TABLE 3

CYANOGEN IODIDE

Number of runs = 1

$d(\ln j_{I^-})/d(1/T) = -272{\cdot}2 \pm 11$ kJ mol^{-1}.

$d(\ln j_{CN^-})/d(1/T) = -259{\cdot}2 \pm 14{\cdot}6$ kJ mol^{-1}.

$E'_{CN^-} - E'_{I^-} = +13{\cdot}0 \pm 25{\cdot}6$ kJ mol^{-1}.

TABLE 4

CYANOGEN BROMIDE

Number of runs = 5

$d(\ln j_{Br^-})/d(1/T)$	$d(\ln j_{CN^-})/d(1/T)$	$E'_{Br} - E'_{CN}$
- 300·6	- 342·8	+ 42·2
- 285·2	- 338·6	+ 53·4
- 283·4	- 299·8	+ 16·4
- 280·8	- 303·4	+ 22·6
- 276·4	- 318·4	+ 42·0
	Mean =	+ 35·4
	Std. Dev. =	14·8

The values in this Table are in kJ mol^{-1}.

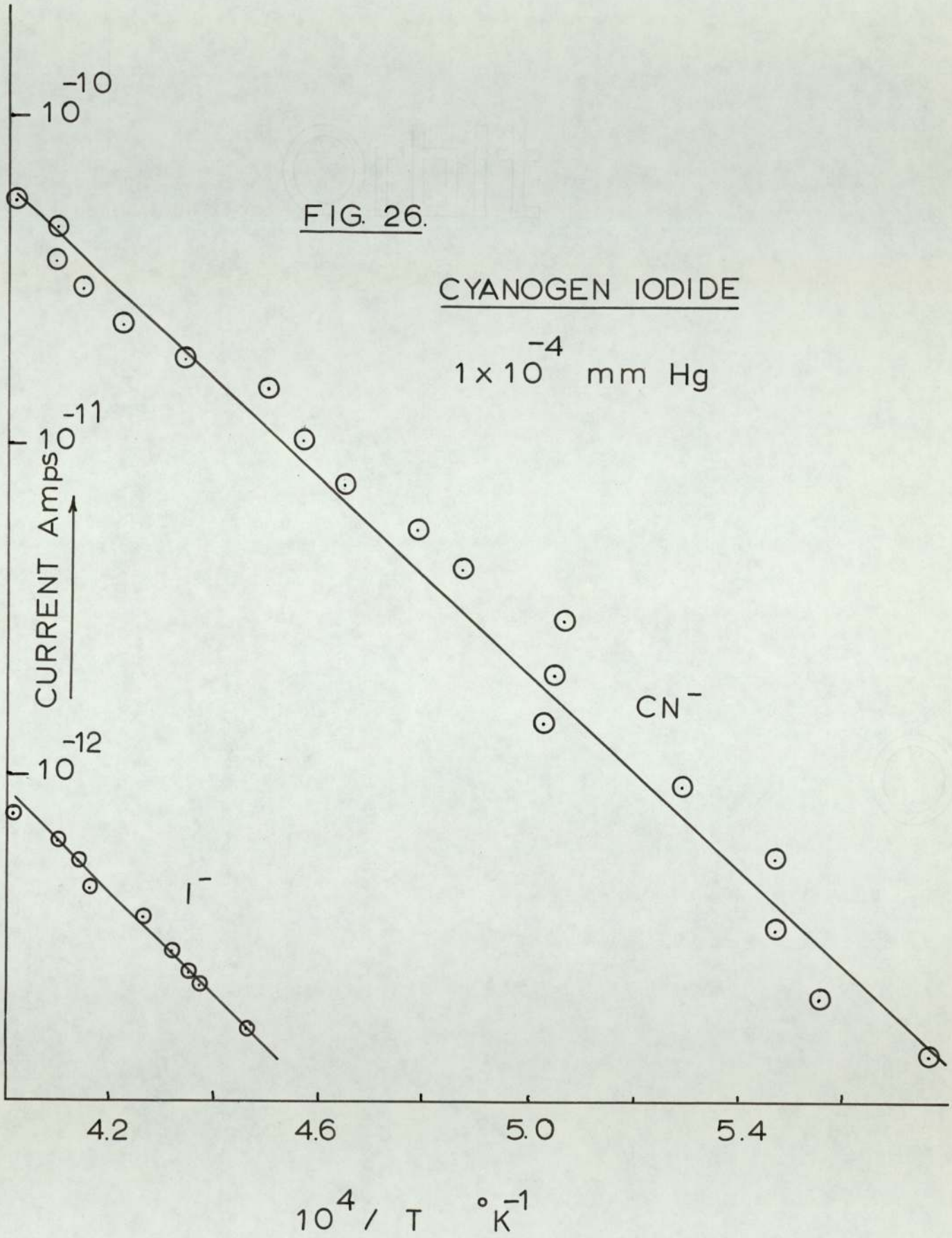
FIG. 26.
CYANOGEN IODIDE
1 x 10^-4 mm Hg
10^-10
10^-11
10^-12
CURRENT Amps
CN^-
I^-
4.2
4.6
5.0
5.4
10^4 / T °K^-1

FIG. 27.

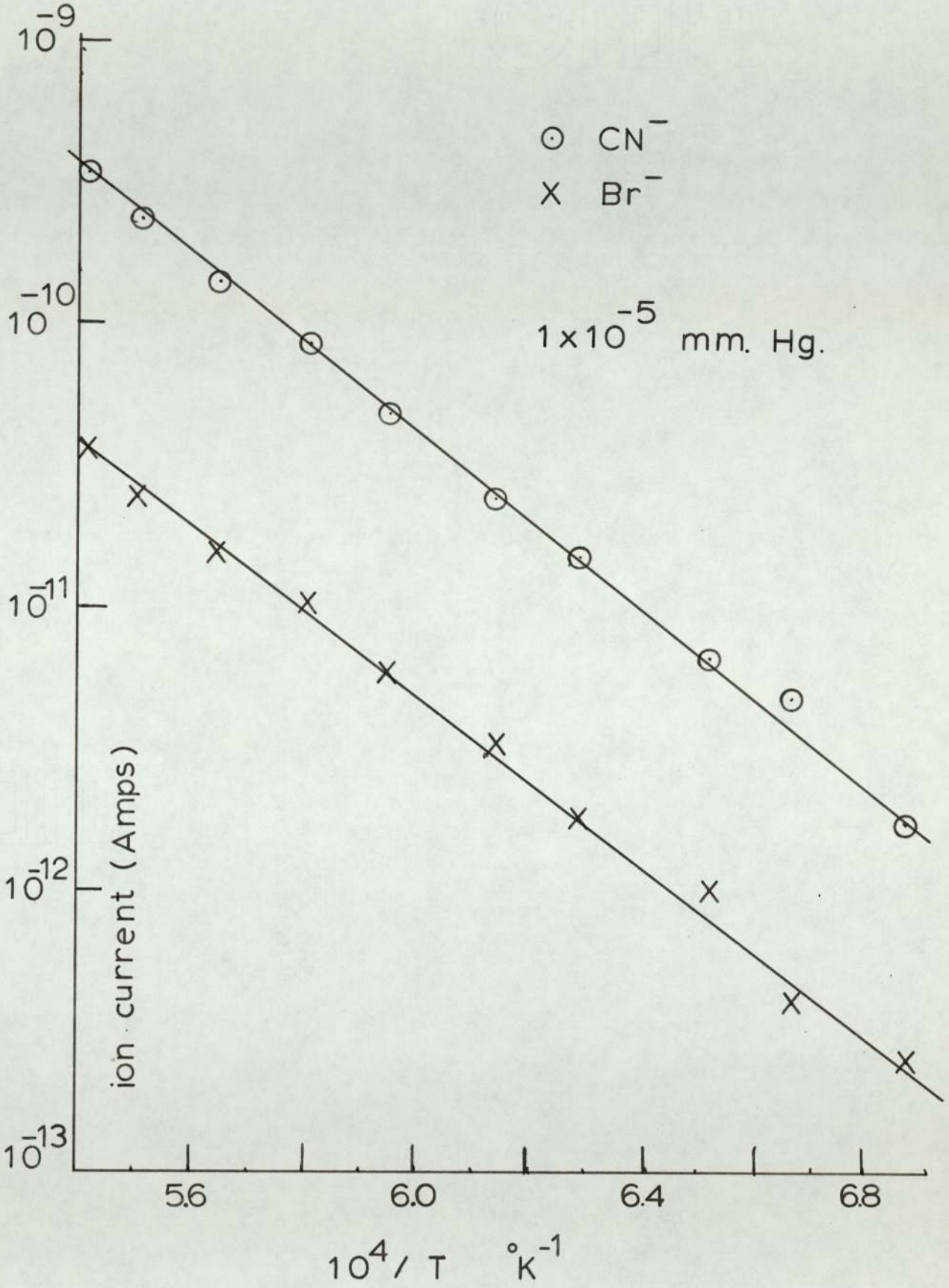

Variation of negative ion currents with 1/temp. for CYANOGEN BROMIDE.

FIG. 28.

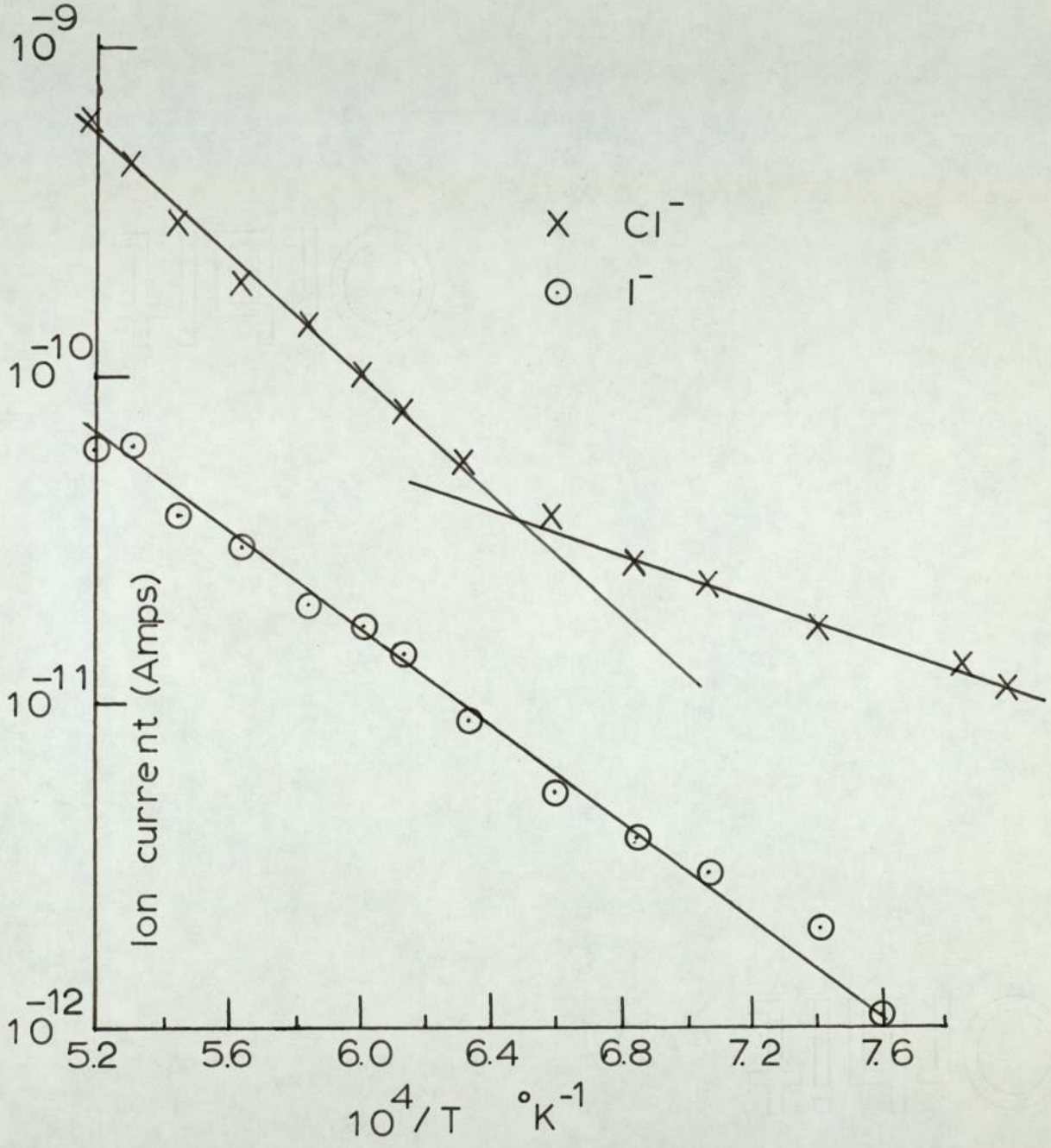

Variation of ion currents with 1/temp.
for IODINE CHLORIDE.
at 1×10^{-5} mm. Hg.

at about 1530°K. Values of $d \log j_i / d (1 / T)$ for each of these portions is shewn, together with those for the iodine negative ion currents, in table 5.

The values obtained for $E'_{Cl} - E'_I$ in the two temperature ranges may now be compared to the literature values. From Meyers results, $E_{Cl} - E_I$ was found to be $+ 56{\cdot}0 \pm 10{\cdot}5$ J mol^{-1} and from Berrys results, + 52·7 J mol^{-1}.

Clearly the value of $E'_{Cl} - E'_I$ obtained at low temperatures is the difference in the true electron affinities of chlorine and iodine. The bond energy of iodine chloride is 210·3 J mol^{-1}, at 298°K, and so a type ii process might be expected to occur, giving the apparent electron affinity difference equal to the true electron affinity difference.

It is clear that at high temperatures, some other process must be occuring. It had been found for iodine chloride that the cathode had to be "conditioned" by heating to very high temperatures (over 2400°K) for long periods, in order that reproducible results could be obtained. This suggested that adsorption might be important and as only the chlorine negative ion current was affected, the adsorption process might be occuring in the chlorine ion formation process.

TABLE 5

IODINE CHLORIDE

Number of runs = 6.

$d(\ln j_{I^-})/d(1/T)$	$d(\ln j_{Cl^-_{low}})/d(1/T)$	$E_{Cl_{low}} - E_I$	$d(\ln j_{Cl^-_{upp}})/d(1/T)$	$E_{Cl_{upp}} - E_I$
-121.2	-148.0	-26.8	-85.6	+35.6
-148.0	-186.4	-38.4	-64.4	+83.6
-150.4	-171.8	-21.4	-60.6	+89.8
-125.8	-161.0	-35.0	-68.6	+57.3
-113.4	-123.4	-10.0	-60.6	+52.6
-112.8	-171.4	-58.6	-59.0	+54.0
	MEAN =	-31.7	MEAN =	+62.2
	Std.Dev. =	15.0	Std. Dev. =	18.8

The values given in this Table are expressed in KJ mol^{-1}.

For a type iv process:

$$E' = E_{true} - D + Q$$

so that the difference in apparent electron affinities of chlorine and iodine, in the upper temperature range, derived from iodine chloride, may be given by:

$$(E_{Cl_{true}} - D_{I-Cl} + Q_{I/Ta}) - E_{I_{true}}$$

The value for the heat of adsorption of iodine on tantalum, $Q_{I/Ta}$, may be deduced by Eleys method (88).

$$Q_{I/Ta} = \tfrac{1}{2} (E_{Ta-Ta} + E_{I-I}) + 23{\cdot}06\ M^2$$

where: E_{Ta-Ta} is the tantalum-tantalum bond energy.
E_{I-I} is the dissociation energy of iodine.
M is the difference in the electronegativety of tantalum and iodine.

A value for E_{Ta-Ta} may be estimated from the heat of sublimation of tantalum. Tantalum has a body-centred-cubic lattice (89) and Eley suggests that:

$$E_{Ta-Ta} = E_{Ta_{vap}} / 6$$

Therefore,

$$E_{Ta-Ta} = 777{\cdot}6 / 6 \text{ kJ mol}^{-1}$$
$$= 129{\cdot}6 \text{ kJ mol}^{-1}.$$

The electronegativities of tantalum and iodine are 1·9 ± 0·4 and 2·5, respectively, according to Pauling (90). Thus M has the value 0·6. The bond energy of iodine is 150·9 kJ mol^{-1}.

Hence:

$$Q_{I/Ta} = \tfrac{1}{2} (129{\cdot}6 + 150{\cdot}9) + 23{\cdot}06 \times (0{\cdot}6)^2 \times 4{\cdot}18$$
$$= 175{\cdot}0 \text{ kJ mol}^{-1}.$$

This calculated value for $Q_{I/Ta}$ is refered to 298°K. Page (91) has shewn that a factor of at least $\frac{1}{2}$ R T must be deducted from this value, to give the value for $Q_{I/Ta}$ at the temperature of the measurement. Thus, at 1700°K, $Q_{I/Ta}$ is 169·2 kJ mol^{-1}.

Similarly, the value for the iodine chloride bond energy must be corrected to the temperature of the measurement. D_{I-Cl} is 210·3 kJ mol^{-1} at 298°K. At 1700°K at factor of at least 3/2· R T must be added to the value at 0°K. Therefore, D_{I-Cl} has a value of 227·7 kJ mol^{-1}.

Inserting these values into the equation:

$$E_{Cl} - D_{I-Cl} + Q_{I/Ta} - E_I = E'_{Cl} - E'_I$$

we obtain:

$$347{\cdot}7 - 227{\cdot}7 + 169{\cdot}2 - 295{\cdot}1$$

No correction was made for the electron affinities of chlorine and iodine as, by taking the difference, the correction factors will cancel out.

Thus, a value for the difference in the apparent electron affinities of chlorine and iodine, assuming that a type iv process was occuring in the formation of the chlorine ions, is deduced as $-5{\cdot}9$ kJ mol^{-1}.

This calculated value for the difference in the apparent electron affinities of chlorine and iodine, assuming a type iv process for chlorine ion formation, is in poor agreement with the observed value of $-31{\cdot}8$ kJ mol^{-1}. However, the estimated value of the heat of adsorption of iodine on tantalum is probabaly too high, due to uncertainty in the values of the electronegativeties used and also the E_{Ta-Ta} term. A reduction in the $Q_{I/Ta}$ term would give better agreement with the observed results.

Such agreement, however, may be fortuitous and further results, using different cathode materials, would be required before the assumption that adsorption was occuring, could be justified.

6. THE SURFACE IONISATION OF SOME SUBSTITUTED PYRIDINES ON POLYCRYSTALLINE TANTALUM.

Failes, Watton and Joyce (92,93) have recently studied, by means of the magnetron technique, the surface ionisation of various methyl substituted pyridines and have argued in favour of pyridinyl type radicals, methyl radicals, or a mixture of both, being formed on the filament surface. The object of this portion of the work was to obtain additional information on the surface ionisation of these heterocycles.

The following compounds were examined:

Pyridine ,
2-methyl-pyridine ,
3-methyl-pyridine,
4-methyl-pyridine,
2-6-dimethyl-pyridine,
2-4-6-trimethyl-pyridine,
and 4-isopropyl-pyridine.

These compounds were purified by a trap to trap distillation and degassed by the "freeze-thaw" technique. Negative ion mass spectra were obtained in the quadrupole system at about 5×10^{-5} mm Hg and about $1850^{\circ}K$ and are shewn in Figs. 30 - 36.

FIG. 29.

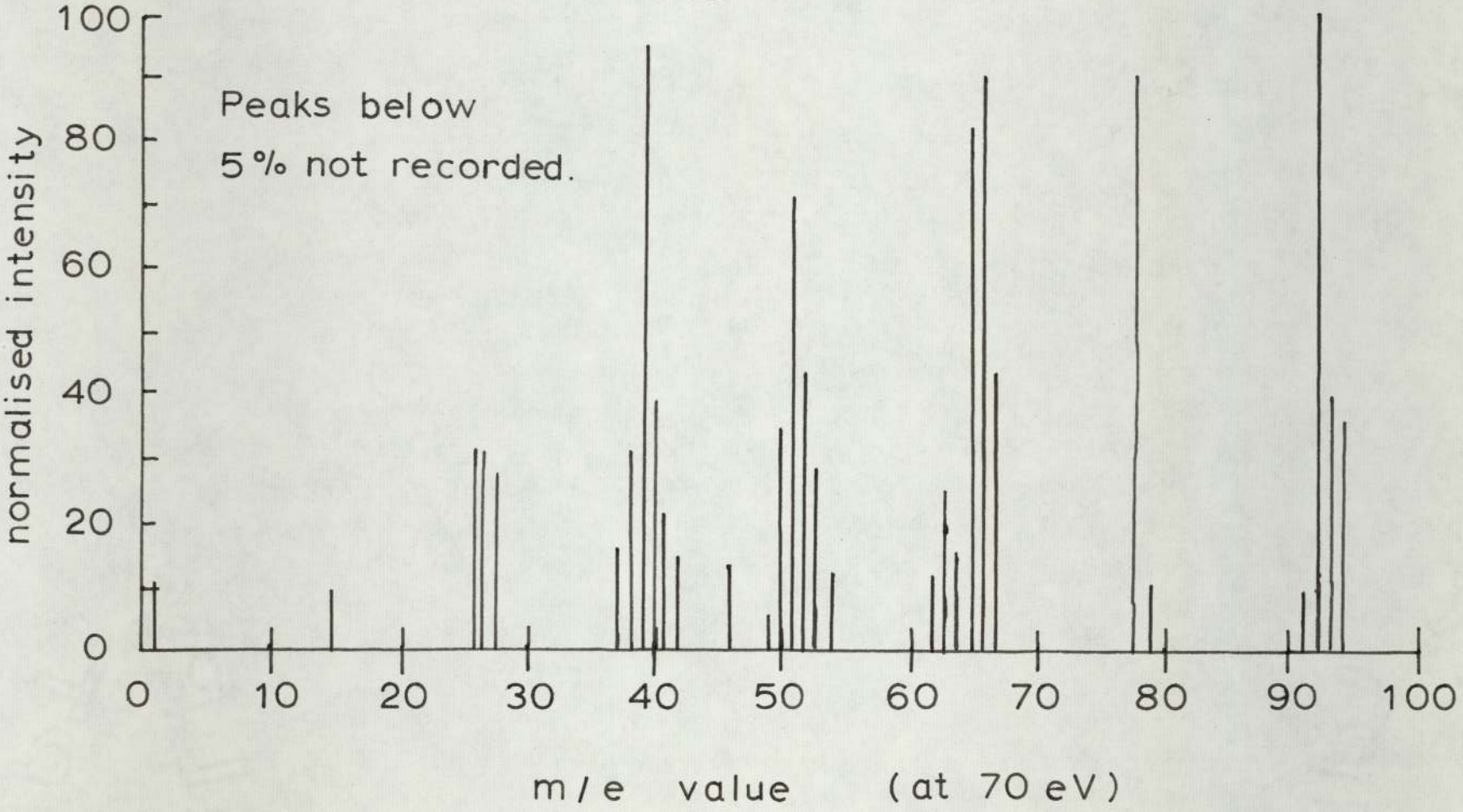

A.E.I. M.S.9. mass spectrum of 2-methyl-pyridine.

FIG 30

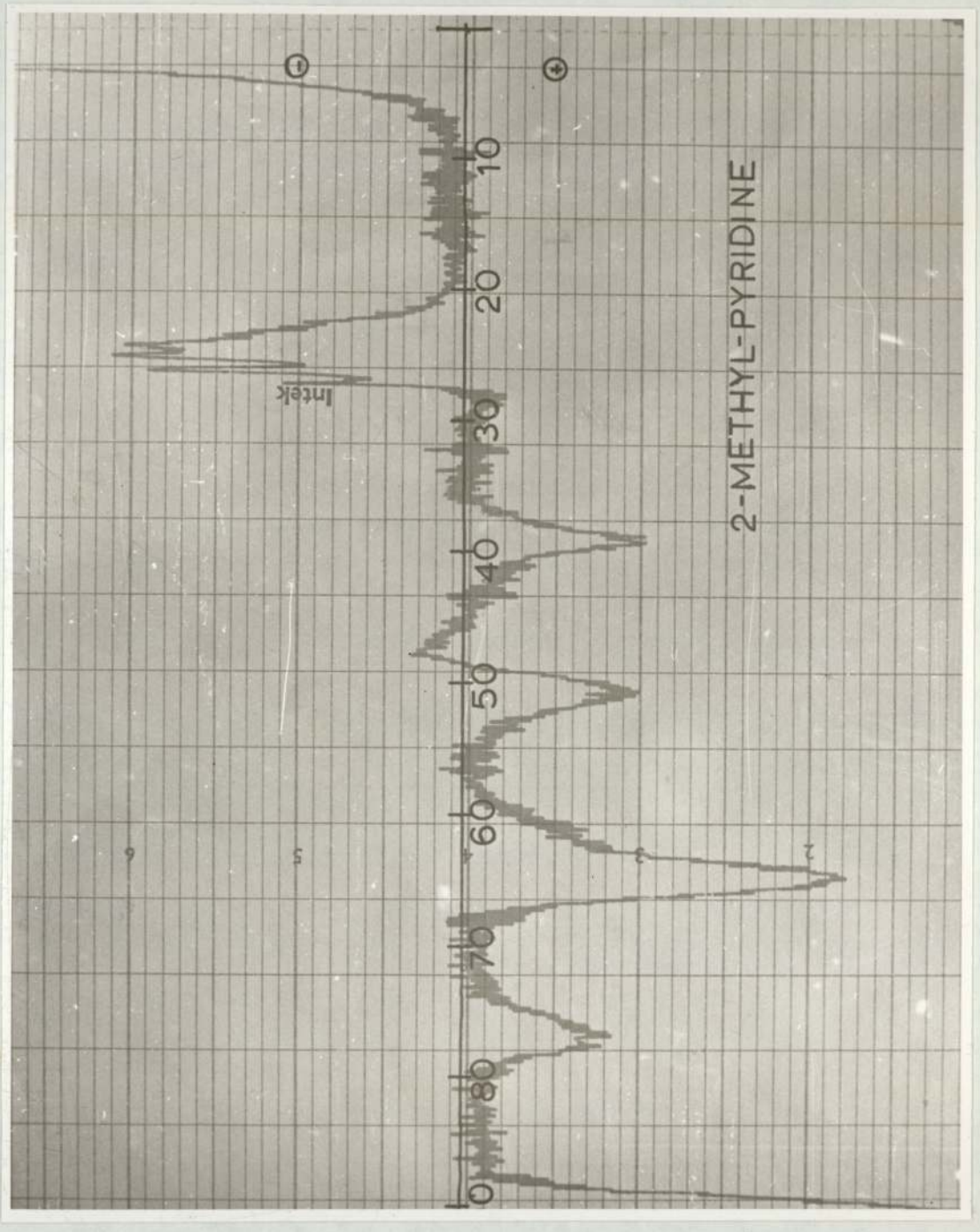

FIG 31

FIG 32

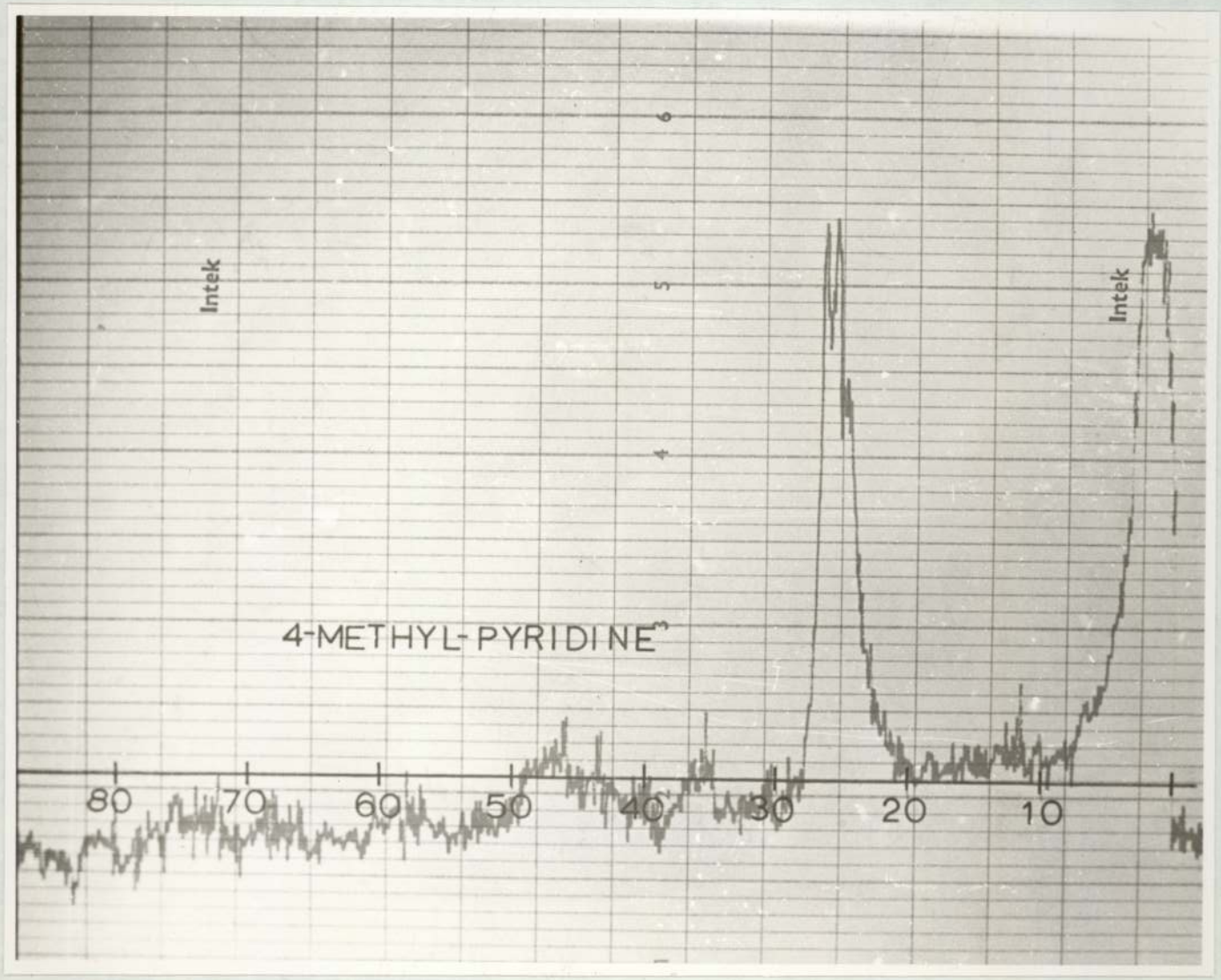

FIG 33

Intek
Intek
2-6-DI-METHYL-PYRIDINE.
6
5
4
3
10
20
30
40
50
60
70
80
90

FIG 34

Intek
Intek
5
4
3
2
2-4-6-TRI-METHYL-PYRIDINE"
90
80
70
60
50
40
30
20
10

FIG 35

FIG. 36.

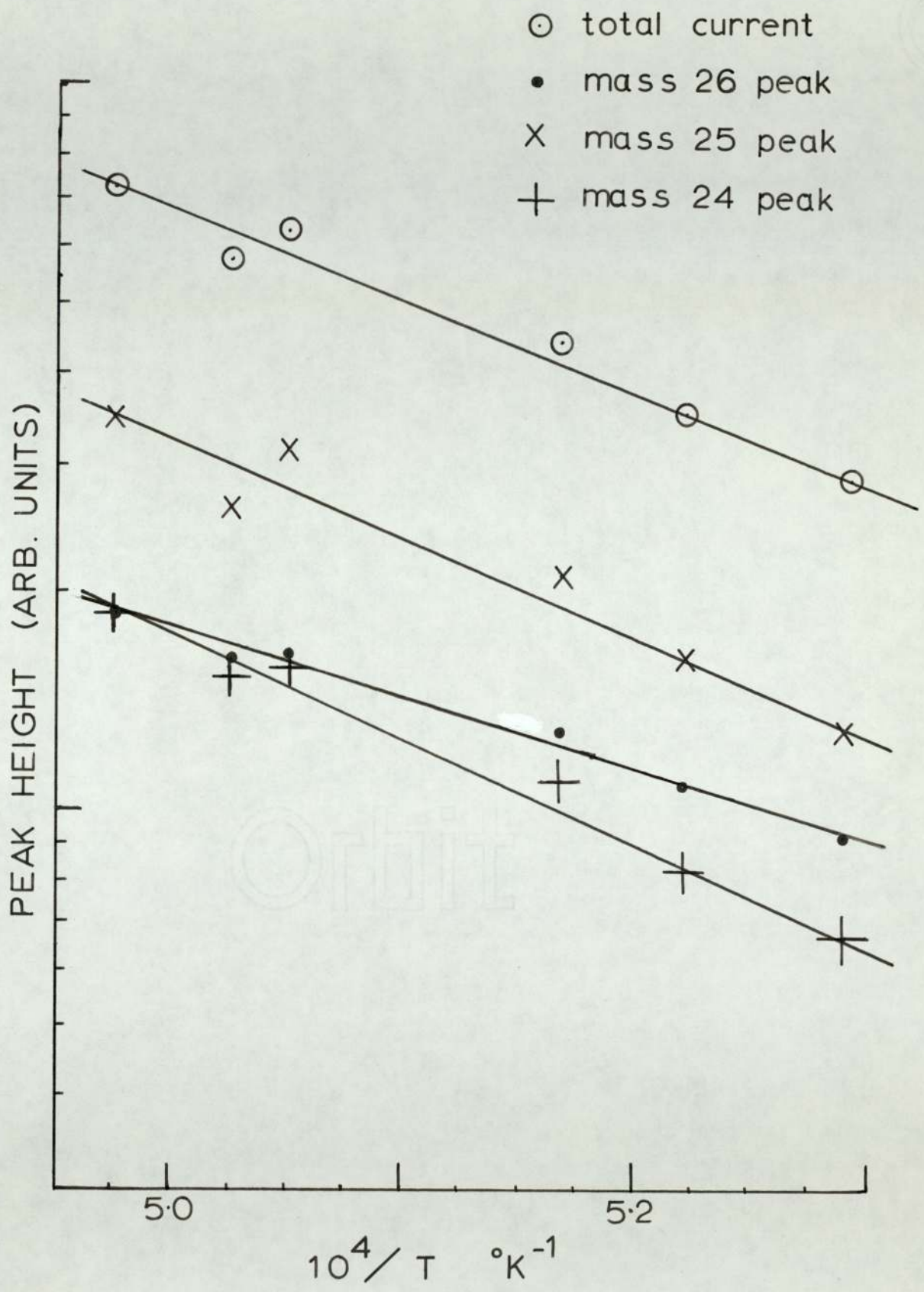

Variation of negative mass spec. peaks with 1/temperature for 2-6-dimethyl-pyridine.

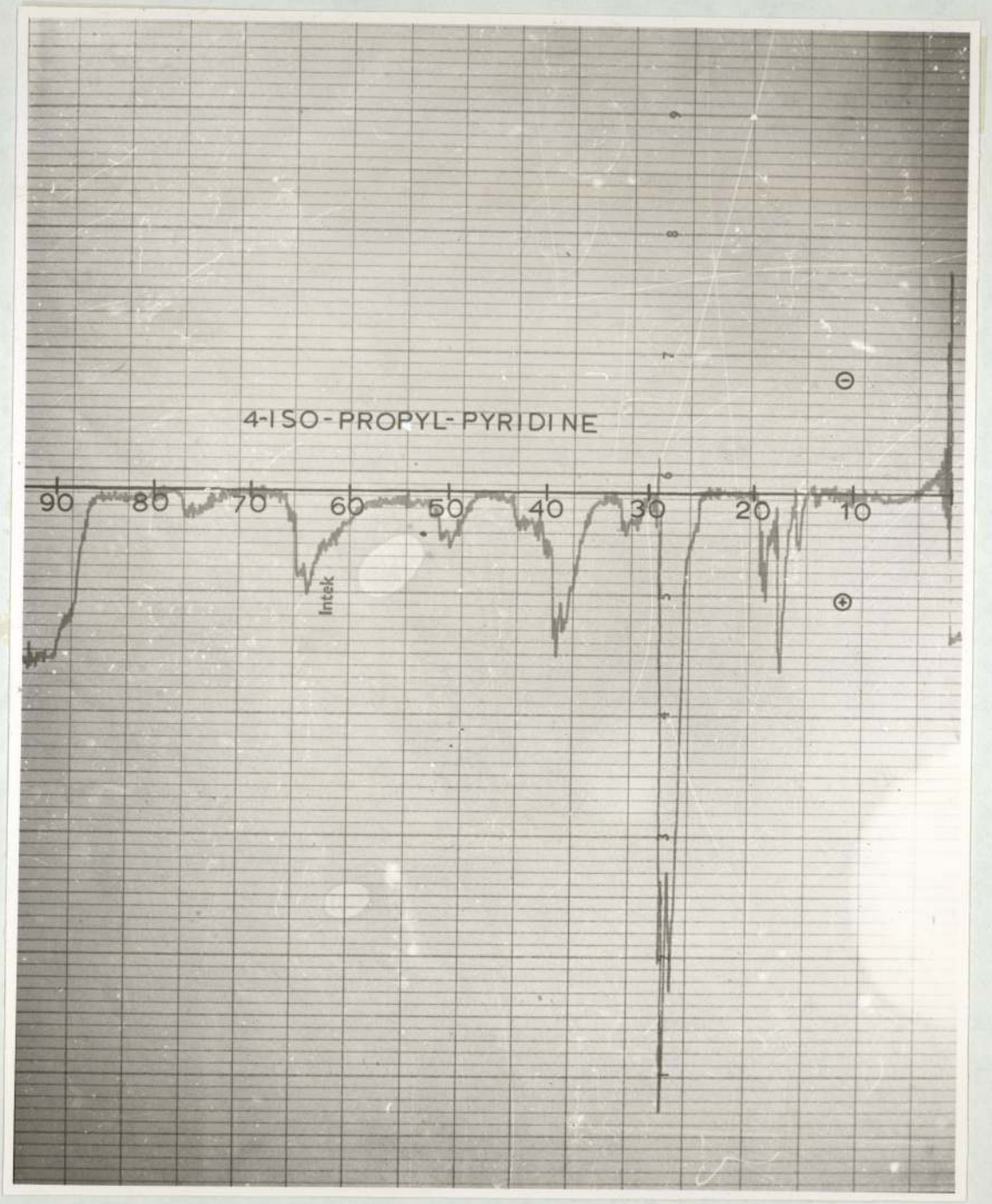

FIG 37

In the presence of these vapours, it was noticed that the tantalum cathode turned a lustrous golden colour in use and an X ray powder diffraction photograph shewed that the cathode had been converted to tantalum carbide.

Examination of the spectra revealed an interesting phenomenon, namely, both negative and positive currents were recorded in the same spectrum, whereas only negative ion currents were to be expected. The large electron peak always enabled the sign of the other peaks to be determined.

It was also noticed that all the positive peaks were much broader than the negative ion peaks, suggesting that these positive ions had not traversed the whole length of the quadrupole field, resulting in a lower resolution in the mass spectra. Increasing the pressure of the vapour slightly, served to increase the peak heights of both positive and negative spectra.

The insensitivity of quadrupole mass filters to axial velocity (60) makes improbable any phenomena resulting in a positive ion being formed and entering the mass filter at much higher velocities than the negative ions, and therefore, at lower resolution relative to the negative ions.

In the previous chapter, it was shewn that the path length of ions in the quadrupole field were such that above 5×10^{-4} mm Hg, of halogen vapours, the positive

ion current, obtained by collisional detachment processes occuring within the mass filter, were large enough to completely mask any negative ion current.

Thus, it is suggested that electron and negative ion collisions with the sample gas in the mass filter, results in the formation of positive ions, which are then detected, together with any negative ions produced in the source region, by the Faraday cylinder.

Support for this suggestion comes from a study of the usual positive ion mass spectra of these compounds, obtained using an AEI mass spectrometer (MS9). The spectrum obtained for 2-methyl-pyridine is given, as a bar chart, in Fig. 29.

Comparison of Fig. 29 with the spectrum shewn in Fig. 31, shews that the positive ion patterns are similar and this was also observed in all the compounds studied. This phenomenon observed as a useful check on the mass scale calibration.

The mass spectrum of 4-isopropyl-pyridine Fig. 37, shewed only positive ions; a group of intense positive peaks, presumably derived from the isopropyl group, completely obscuring any negative ion peak which may have been in the range 23 - 28 amu.

During the work with 4-methyl-pyridine, it was noticed initially, that a negative ion peak occured

at mass number 31. This peak gradually disappeared on heating the filament to over 2400°K for several hours, and did not reappear during the course of the experiments. It is suggested that the ion formed may have been CH_3O^-. Initially, some oxygen impurities may have been present on the cathode surface, which may then react with the 4-methyl-pyridine to give CH_3O^-. If this conclusion is correct, then this would support the idea that methyl fragments may be adsorbed onto the cathode under certain conditions (94).

It should be noted in passing that the use of in-line electron multipliers with grounded first dynode, to detect negative ions in quadrupole systems will enable any ion leaving the mass filter, be it charged negative or positive, to be detected. The spectrum produced in such a system will be, in fact, a mixture of positive and negative ion peaks, all extending along the same direction on the chart paper.

The negative ions detected are given in table 6. The negative ion peaks were well resolved relative to the positive ion peaks except the broad peak which occurred at about 47 amu. This peak was always less than about 5% that of the other negative ion peaks. The fact that the peak is broad argues in favour of gas phase formation in the mass filter.

TABLE 6

Compound:	Negative ion peaks observed at these mass numbers:
Pyridine	25 , 26 , 27 and 46-49
2-Methyl-pyridine	24 , 25 , 26 , 27 and 46-49
3-Methyl-pyridine	24 , 25 , 26 , 27 and 46-49
4-Methyl-pyridine	25 , 26 , 27 and 46-49
2-6-Dimethyl-pyridine	24 , 25 , 26 and 46-49
2-4-6-Trimethyl-pyridine	25 , 26 , 27 and 46-49
4-Iso-propyl-pyridine	no negative ions observed.

This negative ion may be C_4^-, however, this assignment is tentative.

There are several mechanisms for the formation of the negative ions produced in the source region.

i) The "parent" molecule was adsorbed onto the cathode, where electron attachment then occured, followed by a breakdown of the "parent" into "daughter" negative ions. In such a process, the observed energetics will depend on the primary ion formation, but the mass filter will record only the secondary ions.

ii) The "parent" molecule may be adsorbed onto the cathode and pyrolise to give various fragments, which may then attach electrons. These fragment negative ions may then be observed by the mass filter. The observed energetics of this type of process will be determined by the manner in which fragmentation and electron attachment occur.

iii) The parent molecule may capture an electron in the gas phase, near to the cathode surface, to produce the observed negative ions, especially if dissociation occurs, that is:

$$AB + e = A^* + B^-$$

iv) A combination of i, ii, and iii.

It is clear that mass spectrometric evidence alone, is insufficient to enable a choice to be made between the above processes.

However, a choice may be made if the energetics of the system are known. Page and Goode (7) have shewn that the diagnosis of reaction type in the magnetron may be based on the magnitude of the apparent electron affinity, the effect of varying the filament material and the calculation of the entropy of the reaction.

Processses which involve mechanism iii may be distinguished by plotting $\log (j_e/j_i)$ versus $1/T$. Zandberg and Paleev (95) have shewn that ions formed in the gas phase give zero slopes for this type of plot, whilst ions formed by a surface ionisation process give mainly non-zero slopes, as the currents of secondary ions, produced in the gas phase, are proportional to the electron current. Hence $\log(j_e/j_i)$ will be independent of cathode temperature for the gas phase process.

Using a magnetron, Failes et al have shewn, for the methyl substituted pyridines studied here, that a plot of $\log (j_e/j_i)$ versus $10^4/T$ was non zero in every case.

However, as the magnetron measures only the total ion current, it is possible that, of the observed ions, only one was produced by surface ionisation; the others being produced by a gas phase capture process.

The temperature dependence of the individual negative ion currents from 2-6-dimethyl-pyridine are shewn in Fig. 36, over the range 1890 - 2010°K. No measurement of the electron current was made in this range, however, the experimental work function may be deduced by use of Failes et al data (93).

It may be shewn that:

$$d\left(\ln\left(j_e/j_i\right)\right) / d\left(10^4/T\right) = d \ln j_e / d\left(10^4/T\right) - d \ln j_i / d\left(10^4/T\right)$$

The experimental work function is $d \ln j_e / d\left(10^4/T\right)$.

Failes et al shewed that for 2-6-dimethyl-pyridine, $d\left(\log j_e/j_i\right) / d\left(10^4/T\right)$ was - 0·599.

In this work it was found that $d\left(\log I\right) / d\left(10^4/T\right)$ where I is the total current, was found to be - 1·260. Inserting these values into the above equation and rearranging:

$$d(\log j_e) / d(10^4/T) = -0{\cdot}599 + (-1{\cdot}260)$$
$$= -1{\cdot}859$$

Thus the value for the experimental work function is 356 kJ mol^{-1}. This value falls mid-way in the range of work functions determined for tantalum carbide, namely, 380 to 302 kJ mol^{-1} (96).

It was found that $d(\log j_i) / d(10^4/T)$ for the individual negative ion currents were as follows:

CN^- = - 194 kJ mol^{-1}
C_2^- = - 273 kJ mol^{-1}
C_2H^- = - 265 kJ mol^{-1}

It may be seen that, if the work function was indeed 356 kJ mol^{-1}, as deduced above, the value of $d(\log j_e/j_i) / d(1/T)$ was not zero for each negative ion observed.

If we take the worst case, in that the work function was 302 kJ mol^{-1}, the lowest tabulated value, then $d(\log j_e/j_i) / d(1/T)$ will only be zero if we allow an error of 29 kJ mol^{-1} in the value of $d(\log j_i) / d(10^4/T)$ for C_2^- and 34 kJ mol^{-1} for C_2H^-.

It is unreasonable to suppose that the overall process incurs an error of at least 83 kJ mol^{-1}.

It may thus be stated that the three negative ions CN^-, C_2H^- and C_2^- appear to be derived from 2-6-dimethyl-pyridine by a surface ionisation process.

Failes et al have argued that the surface ionisation of the methyl substituted pyridines involves the formation of either pyridinyl type radicals, methyl radicals, or a mixture of both.

In the light of the results from this work, these radicals, if formed, must breakdown to the observed ions, indicating that the overall energetics are likely to be more complex than might otherwise be expected.

7. CONCLUSIONS.

This thesis has attempted to provide information on the production of negative ions from vapours passed over a hot polycrystalline tantalum surface.

In order that the identification of the negative ions formed at such a surface might bedirectly determined, a quadrupole mass filter system was constructed, using an AMP 3 residual gas analyser. The construction and operation of this system was described in detail. A planar diode was found to be the most suitable surface ionisation source system.

A study was made of the performance of a channel electron multiplier detector. This shewed that the use of a channel electron multiplier was impracticable when quantitative results were required, due to the "fatigue" of the multiplier at high count rates. In such work, a Faraday cylinder detector was found to be more suitable, provided that secondary electron emission was avoided.

The ionisation of some interhalogens and cyanogen halides was studied, using the mass filter system, as the thermodynamic properties of these compounds are known, thus enabling a clear interpretation of the results to be made.

An attempt was made to evaluate the stabilities of the observed negative ions, either halogen or cyanide, by applying the kinetic methods of Page to the measured electron and ion currents. Initially, the results obtained were at variance with the literature values. The reason for this was traced to a difference in the transmission of negative ions and electrons through the mass filter. A slight modification of the Page method allowed the evaluation of the difference in electron affinity of two radicals ionising simultaneously on the cathode.

The difference in electron affinity of the following pairs of radicals was determined:

I - CN

Br - CN

Br - I

and Cl - I

In the case of iodine chloride, the results indicated that an adsorption process might have occured in the formation of the chlorine negative ions.

At pressures higher than 5×10^{-5} mm Hg., positive currents were measured at the Faraday cylinder detector, using iodine chloride.

These results were explained quantitatively on the assumption that positive ions were formed in the mass filter section, by negative ion collisions with the sample vapour.

The ionisation of various substituted pyridines was also studied in the mass filter system. In general, the methyl substituted pyridines gave fragment negative ions, of m / e values, 24, 25, 26 and 27.

A broad negative ion peak at about m / e 48 was attributed to C_4^- , produced by a gas phase reaction. This peak, however, was always less than 5 per cent of the other negative ion peaks' intensity.

In particular, 2-6-dimethyl-pyridine was shewn, by comparison of the result obtained in this work with those obtained by Failes et al. , to give three negative ions, C_2^- , C_2H^- and CN^- , which were produced by some surface ionisation process.

An unusual feature of the mass spectra obtained with these compoundswas that both negative and positive ion peaks were observed, in the same spectrum. The positive peaks were deduced to be positive ion fragments of the sample compound, the expla nation for this phenomenon being based again on the assumption that negative ion collisions with the sample vapour, in the mass filter section, produced the observed positive ions.

The magnetron method, which has been, until recently, the major technique for studying negative surface ionisation, was reviewed from an experimental aspect. This study indicated that the major criticisms of the magnetron method were unfounded and that gas phase ion formation, as a primary process, was of no importance.

Provided that the magnetron method was supported by direct evidence of the charge carriers, the method appeared to be valid for the determination of the electron affinities of atoms, molecules or radicals.

# # #

BIBLIOGRAPHY.

1. S.C. Brown. Basic data of Plasma Physics, Wiley, 1969.
2. Knoff and Krafft. 6th. Int. Conf. Mass Spec. Edinburgh, 1973
3. J.J. Thompson. Phil. Mag. 47, 337, (1924)
4. G.C. Reid. J. Geophys.Rev. 66, 4071, (1961)
5. H.S.W. Massey and D.R. Bates. Astrophys. J. 91, 202, (1940)
6. S. Chandrasekher and R. Wildt. Astrophys, J. 100, 87, (1944).
7. G.C. Goode. Ph. D. thesis. Aston University. 1969.
8. J.E. Lovelock, A. Zlatkis and R.S. Becker. Nature 193, 540, (1962).
9. L.G. Christophorou. Rad. Chem. Conf. Notre Dame University, Indiana, 1972.
10. Reported in New Scientist, July, 1973.
11. L.M. Branscomb, M.L. Seman and B.J.Stiener. J. Chem. Phys. 37, 1200, (1962)
12. R.S. Berry, C.W. Reimann and G.N. Spokes. ibid. 37, 2278, (1962)
13. W.C. Lineberger and B.W. Woodward. Phys Rev. Lett. 25, 424, (1970)
14. Rolla and Picardi. Atti. Acad. Linei VL 2, 29, 128, 173, 334, (1925)

15. G. Glockler and M. Calvin.
J. Chem. Phys. 4, 492, (1936)

16. P.P. Sutton and J.E. Meyer.
ibid. 3, 20, (1935)

17. F.M. Page and G.C. Goode.
Negative ions and the magnetron, Wiley, 1969

18. V.M. Dukelskii and N.I. Ionov.
J.E.T.P. (USSR) 10, 1248, (1940)

19. N.I. Ionov.
Prog. Surf. Sci. 1, 237, (1972)

20. E. Ya. Zandberg and V.I. Paleev.
Sov. Phys. Dok. 190, 562, (1970)

21. M.D. Scheer and J. Fine.
J. Chem. Phys. 46, 3998, (1967)

22. M.D. Scheer and J. Fine.
ibid. 47, 4267, (1967)

23. I.N. Bakulina and N.I.Ionov.
Sov. Phys. Dok. 105, 680, (1955)

24. I.N. Bakulina and N.I. Ionov.
ibid. 155, 309, (1964)

25. T.R. Bailey.
J. Chem. Phys. 28, 792, (1958)

26. I.N. Bakulina and N.I. Ionov.
Sov. Phys. Dok. 116, 41, (1957)

27. I.N. Bakulina and N.I. Ionov.
ibid. 153, 309, (1964)

28. I.N. Bakulina and N.I. Ionov.
Sov. Phys. Dok. 99, 1023, (1954)

29. A.W. Hull. Phys. Rev. 18, 31, (1921)

30. P. Parker.
Electronics. p. 973. Arnold, London, 1963

31. E. Ya. Zandberg and V.I. Paleev.
Sov. Phys. T.P. 17, 665, (1972)

32. H.S.W. Massey.
Electron and ionic impact phenomena, Clarendon Press 1969.

33. F.M. Page. Trans. Far. Soc. 56, 1742, (1960)

34. Chaffee.
Theory of thermionic vacuum tubes, M^{c}Graw-Hill. 1933.

35. P. Parker.
Electronics. p 55, Arnold, London, 1963

36. Harvey.
Ultra high frequency Thermionic tubes,
Chapman and Hall, 1943.

37. F.M. Page. Private communication.

38. L.G. Christophorou and R.P. Blauenstein.
Rad. Reasearch. 37, 229, 1969

39. J.T. Herron, H.M. Rosenstock and W.R. Shields.
Nature. 206, 611, (1965)

40. A.L. Farragher, F.M. Page and J. Wheeler.
Disc. Far. Soc. 37, 203, (1964)

41. I.N. Bakulina, E.Ya. Zandberg and N.I.Ionov
Sov. Phys. T. P. 10, 437, (1965)

42. J. Kay and F.M. Page.
Trans Far. Soc. 60, 1042, (1964)

43. A. Gaines and F.M. Page.
ibid. 59, 1266, (1963)

44. H.A. Tasman, A. Boerboom and J. Kistemacker.
Vac. 13, 33, (1963)

45. F.T. Worrell. Vac. 13, 309,(1963)

46. J. Hengross and W.K. Huber.
Vac. 13, 1, (1963)

47. L. Holland. Vac. 21, 45, (1971)

48. M.J. Fulker, M.A.Baker and L. Laurenson.
Vac. 19, 555, (1969)

49. M.A. Baker, L. Holland and L. Laurenson.
Vac. 21, 479, (1971)

50. W.M. Langdon and E.G. Fochtman.
10th. Nat. Vac. Symp. p. 128, (1963)

51. M.A. Baker and G.H. Staniforth.
Vac. 18, 17, 1968.

52. M.A. Baker and L. Laurenson.
Vac. 19, 81,)1969)

53. R.D. Craig. J. Phys. E. 3, 338, (1970)

54. M.J. Fulker. Vac. 18, 445, (1968)

55. W.W. Roepke and K.G. Pung.
Vac. 18, 457, (1968)

56. K.R. James. J. Chem. Phys. 24, 1110, (1956)

57. A. Dudley, J. Homer and W.R. M^{c}Whinnie.
In the press. (Chemm. Comms of J.C.S. 1973)

58. T.R. Bailey. J. Chem. Phys. 28, 792, (1958)

59. L. Malter and D.B. Langmuir.
Phys. Rev. 55, 743, (1939)

60. P.H. Dawson and N.R. Whetten.
Adv. Elect. Electron Phys. 27, 59, (1969)

61. J.A. Richards. Private communication.

62. W.M. Brubaker and W.S. Chamberlin.
Proc. Int. Conf. Mass Spec. p. 98, (1969)

63. P.H. Dawson and N.R. Whetten.
I. J. M. S. and I. P. 3, 1, (1969)

64. W. Arnold. J. Vac. Sci. Tech. 7, 191, (1970)

65. D.R. Denison. ibid. 8, 266, (1971)

66. H.W. Werner, H. de Grefte and J.V. Berg.
I. J. M. S. and I. P. 8, 458, (1972)

67. C.H. Petley. Mullard Tech. Comm. 11, 218, (1971)

68. R.D. Reed, E.G. Shelley, J.C. Bakke, T. Sanders
and J. M^{c}Daniel. I.E.E.E. Trans. Nuc. Phys.
NS16, 359, (1969)

69. A. Egidi, R. Marconero, G. Pizzella and F. Sperli.
Rev. Sci. Inst. 40, 881, (1970)

70. M. van Gorkom, D.P.Beggs and R.E. Glick.
I. J. M. S. and I. P. 4, 441, (1971)

71. J.M. Goodings, J.M. Jones and D.A. Parkes.
I. J. M. S. and I. P. 9, 417, (1972)

72. E.S. Parilis and L.M. Kisinevskii.
Sov. Phys. S.S. 3, 885, (1966)

73. U.A. Arifov and V.M. Khashimov.
Radio. Eng. Elec. Phys(USSR) 8, 274, (1963)

74. PP. Sutton and J.E. Meyer.
J. Chem. Phys. 3, 20, (1935)

75. P.M. Doty and J.E. Meyer.
ibid. 12, 323, (1944)

76. K.J. M^{c}Callum and J.E. Meyer.
ibid. 11, 56, (1943)

77. Bernstein and Metlay.
ibid. 19, 1612, (1951)

78. Vier and J.E. Meyer.
ibid. 12, 28, (1944)

79. L.M. Branscombe, S Smith and Tisone.
ibid. 43, 2906, (1965)

80. C. Herring and M. Nichols.
Rev. Mod. Phys. 21, 185, (L949)

81. F.M. Page. Trans. Far. Soc. 56, 1764, (1960)

82. A.L. Farragher.
Ph. D. thesis. Aston University. 1966.

83. B.S. Thyagarajan.
Cyanogen Halides, Interscience reports 2, (1968)
D.D. Davies and H. Okabe. J. Chem. Soc 49, 5526, 1968

84. M. Mosharrafa and H.J. Oskam.
Physica. 32, 1759, (1966)

85. J. Yinon and F.S. Klein. Vac. 21, 379, (1971)

86. W.M. Brubaker and W.S. Chamberlin
Proc. Int. Conf. Mass Spec p. 98, (1969)

87. F.M. Page. J. Chem. Phys. 49, 2466, (1968)

88. D.D. Eley. Disc. Far. Soc. 8, 34, (1950)

89. W.E. Addison.
Structural principles in Inorganic compounds,
Longmans, 1961.

90. L. Pauling.
The nature of the chemical bond and the structure of molecules and crystals. Cornell Univ. Press. 1960

91. F.M. Page. Nature. 188, 1021, (1960)

92. R.B. Failes, J.T. Joyce and E.C. Watton.
J.C.S. Far Trans. I 69, 1487, (1973)

93. R.B. Failes. Private Communication.

94. M.R. Painter.
Ph.D Thesis Aston University, 1973

95. E. Ya. Zandberg and V.I. Paleev.
Sov. Phys. T.P. 17, 665, (1972)

96. V.S. Fomenko and G.V. Samsonov.
Handbook of thermodynamic properties, Plenum Press.